A Theoretical Study of the Generation of Squeezed-State Light via Degenerate Parametric Amplification

Thesis by

David Dale Crouch

In Partial Fulfillment of the Requirements

for the Degree of

Doctor of Philosophy

California Institute of Technology

Pasadena, California

1988

(Submitted May 16, 1988)

To Julie

Acknowledgements

I thank my thesis supervisor, Carl Caves, for his encouragement and his support of the work leading to this thesis, and my faculty advisor, Professor Kip Thorne, for the opportunity to work in the Theoretical Astrophysics Group. I am also grateful to Professor Amnon Yariv for allowing me to be his teaching assistant during the last three years.

The friendship and support of my friends, especially those at the West Covina Church of Christ, is gratefully acknowledged.

I thank my wife, Julie, for her love and understanding over the last 3 1/2 years, and my parents for their continued love and encouragement.

My years at Caltech have been funded by a Hughes Aircraft Masters Fellowship, Research and Teaching Assistantships, the Office of Naval Research, and Caltech's Program in Advanced Technologies, sponsored by Aerojet General, General Motors, and TRW. Their support is gratefully acknowledged.

Abstract

This thesis is primarily a theoretical study of degenerate parametric amplification as a means of generating squeezed-state light.

i) A wideband traveling-wave formalism is developed for analyzing quantum mechanically a degenerate parametric amplifier. The formalism is based on *spatial* differential equations—spatial Langevin equations—that propagate temporal Fourier components of the field through the nonlinear medium. In addition to the parametric nonlinearity, the Langevin equations include absorption and associated fluctuations, dispersion, and pump quantum fluctuations. The dominant effects of dispersion and pump quantum fluctuations on the squeezing produced by a degenerate parametric amplifier are analyzed.

ii) The wideband formalism of i) is used to carry out a more detailed analysis of the effects of phase mismatching. With the assumption of a lossless medium and a classical pump, we find that parametric amplification is capable of generating squeezed-state light over a wide band if materials with large $\chi^{(2)}$ nonlinearities can be found, and that the squeezing bandwidth can be enhanced by phase mismatching away from degeneracy.

iii) We consider again the effect of pump quantum fluctuations on the squeezing produced by parametric amplification. We perform discrete-mode calculations for a parametric amplifier with a quantum pump, and discuss some of the limitations of calculations of this sort in quantum optics. We derive stochastic differential equations (SDEs) for one- and two-mode parametric amplifiers, and from them obtain an iterative solution showing that pump quantum fluctuations impose a limitation on the degree of squeezing obtainable from a parametric amplifier.

iv) A possible application of squeezing is considered; in particular, we study the effects of squeezing the intracavity noise in a laser oscillator. We solve the classical noise problem of a realistic laser model by making a bold—and possibly unrealizable—assumption, that the in-phase and quadrature Langevin sources which are responsible for the "noisiness" of the laser can

be squeezed. We show that the effect of squeezing the in-phase quadrature is to reduce the phase noise, including the linewidth, of the laser but, due to amplitude-phase coupling, not to eliminate them altogether.

Table of Contents

Acknowledgements iii

Abstract iv

Chapter 1 1

Chapter 2 28

Chapter 3 67

Chapter 4 83

Chapter 5 129

CHAPTER 1

Introduction

This thesis is a theoretical investigation into (i), the use of traveling-wave parametric amplification for the generation of squeezed-state light, and (ii), the possibility of reducing the phase noise—and hence the linewidth—of laser oscillators by squeezing the intracavity noise. A recent experiment[1] has shown that *cavity* parametric amplification can produce significant squeezing over a fairly narrow spectral region, the bandwidth being limited by the cavity resonance width. Traveling-wave parametric amplification, on the other hand, is not so limited, being an inherently wide-band process. The only bandwidth limitation is due to phase-matching considerations. The work in this thesis includes the following topics: (i) a traveling-wave analysis of the effects of phase mismatching, linear loss, and pump quantum fluctuations on the squeezing produced by a parametric amplifier near degeneracy (Chapter 2); (ii) an investigation of the possibility of using degenerate parametric amplification to generate broadband squeezed-state light (Chapter 3); (iii) a quantum-mechanical analysis, using stochastic differential equations, of the limitations to squeezing in a parametric amplifier due to pump quantum fluctuations (Chapter 4); (iv) a study of the spectral consequences of squeezing the intracavity noise in a laser oscillator (Chapter 5).

The present chapter will serve as an introduction to squeezing and some of the theory behind it. Section 1.1 describes what squeezed-state light is, and how it is characterized by phase-dependent quantum noise. Section 1.2 gives a simple physical analogy from which we gain some insight into the processes capable of generating squeezed-state light, and describes some recent experiments in which squeezed-state light has been generated and detected. The important mathematical tools used to describe squeezed-state light, the quadrature phases and the quadrature-phase amplitudes, are discussed in Section 1.3, as is balanced homodyne detection, the preferred method used to detect squeezed-state light. Finally, a brief introduction to the rest of

this thesis is given in Section 1.4.

1.1 What is Squeezed-State Light?

In this section, we will consider a nearly monochromatic, nearly plane-wave electromagnetic field with a single polarization to illustrate the important ideas behind the theory of squeezed-state light. The electric field can by decomposed into two quadrature components with time dependence $\cos\Omega t$ and $\sin\Omega t$. The quantum-mechanical operators corresponding to the amplitudes of the two quadratures of the field, called quadrature phases, will be shown to be non-commuting Hermitian operators (see Section 1.3); the two quadratures thus obey an uncertainty principle. When the field is in a vacuum state or a coherent state, the uncertainty product for the two operators is a minimum, the uncertainties in the two quadratures being equal. When the field is in a squeezed state, the variance of one quadrature—the squeezed quadrature—is less than that of the vacuum, while the variance of the other quadrature is increased in accordance with the uncertainty principle.

The electric field, propagating in the z-direction, is given at a particular point in space $z=0$ by

$$E(t)=E_1(t)\cos\Omega t+E_2(t)\sin\Omega t\ , \tag{1.1}$$

where the operators $E_1(t)$ and $E_2(t)$ are the *quadrature phases* of the electric field. They are non-commuting Hermitian operators with the equal-time commutator

$$[E_1(t),E_2(t)]=i\frac{8\hbar\Omega}{c\sigma}\int_\beta\frac{1}{2}\,d\omega\ , \tag{1.2}$$

where σ is a cross-sectional area used to account crudely for the transverse structure of the field and β is an appropriate bandwidth. For non-commuting Hermitian operators A

and B,[2]

$$[A,B]=C \Longrightarrow \langle \Delta A^2 \rangle \langle \Delta B^2 \rangle \geq \frac{1}{4} |\langle C \rangle|^2 , \tag{1.3}$$

where, for any operator θ, $\Delta\theta=\theta-\langle\theta\rangle$. When applied to the quadrature phases, Eq. (1.3) yields the uncertainty principle

$$\langle \Delta E_1^2(t) \rangle \langle \Delta E_2^2(t) \rangle \geq \left[\frac{4\hbar\Omega}{c\sigma} \int_\beta \frac{1}{2} d\omega \right]^2 . \tag{1.4}$$

Equation (1.4), when the equality holds, represents the ultimate quantum-mechanical limit to the resolution of the quadrature phases after all other sources of noise have been eliminated. Although the uncertainty *product* is constrained by Eq. (1.4), the individual uncertainties $\langle \Delta E_1^2(t) \rangle$ and $\langle \Delta E_2^2(t) \rangle$ are *not* constrained; we might try to "beat" the uncertainty principle by producing light with $\langle \Delta E_1^2(t) \rangle \neq \langle \Delta E_2^2(t) \rangle$, but such that the equality in Eq. (1.4) is satisfied. Such is the nature of squeezed-state light.

Coherent-state light, i.e., light produced by an ideal laser over time scales short compared to the phase diffusion time, has equal fluctuations in the two quadratures, such that the equality holds in Eq. (1.4); that is,

$$\langle \Delta E_1^2(t) \rangle = \langle \Delta E_2^2(t) \rangle = \frac{4\hbar\Omega}{c\sigma} \int_\beta \frac{1}{2} d\omega . \tag{1.5}$$

Squeezed-state light, on the other hand, while satisfying the equality in Eq. (1.4), has unequal fluctuations in the two quadratures:

$$\langle \Delta E_1^2(t) \rangle = \frac{4\hbar\Omega}{c\sigma} \int_\beta \frac{G}{2} d\omega , \tag{1.6a}$$

$$\langle \Delta E_2^2(t) \rangle = \frac{4\hbar\Omega}{c\sigma} \int_\beta \frac{1}{2G} d\omega , \tag{1.6b}$$

where $G > 0$. To keep our largely heuristic argument simple, we will assume that G is a constant over the bandwidth β, considering the more general case in which G is a function of frequency in Section 1.3 and in later chapters of this thesis. If $G > 1$, fluctuation in the E_1 quadrature is increased, while fluctuation in the E_2 quadrature is decreased, or *squeezed*. The converse holds true when $G < 1$.

The fluctuation in the electric field itself is given by

$$<\Delta E^2(t)> = <\Delta E_1^2(t)> \cos^2\Omega t + <\Delta E_1(t)\Delta E_2(t)>_{sym} \sin 2\Omega t$$

$$+ <\Delta E_2^2(t)> \sin^2\Omega t \ , \tag{1.7}$$

where sym denotes a symmetrized product. If the fluctuations in the two quadratures are uncorrelated, then $<\Delta E_1(t)\Delta E_2(t)>_{sym} = 0$. If we take $(4\hbar\Omega/c\sigma)\int_\beta (1/2)\,d\omega = 1$ for simplicity (this simply means measuring the noise in vacuum units), then

$$<\Delta E^2(t)>^{1/2} = \left[G^2 \cos^2\Omega t + \frac{1}{G^2} \sin^2\Omega t \right]^{1/2} . \tag{1.8}$$

Figure 1 illustrates graphically the nature of the quantum fluctuations for coherent- and squeezed-state light. We assume in the figures that $<E_1(t)> = A$ and $<E_2(t)> = 0$. Figures 1a, 1c, and 1e are phasor diagrams for the electric field $E(t)$ in a rotating frame in which the optical frequency "rotation" at frequency Ω is removed. The quantum nature of coherent-state light, i.e., light with $G = 1$, is illustrated in Fig. 1a; a "quantum fuzzball," representing the quantum quadrature-phase fluctuations, is superimposed on the vector representing the mean electric field. It is obvious that the noise shows no preference for either quadrature, i.e., coherent-state light's quantum noise is *not* phase sensitive. The quantum nature of squeezed-state light is illustrated in the phasor diagrams of Figs. 1c and 1e. In Fig. 1c, the E_1 quadrature is squeezed; the amplitude

fluctuations are reduced and the phase fluctuations are increased in comparison to the coherent-state light in Fig. 1a. The converse is true in Fig. 1e. It is clear from Figs. 1c and 1e that squeezed-state light has *phase-dependent* noise. This is further borne out by the time variation of the electric field, illustrated in Figs. 1b, 1d, and 1f. In each graph, the dark line represents the mean electric field $\langle E(t)\rangle = A\cos\Omega t$, and the shaded region represents the uncertainty in the electric field, described by Eq. (1.8). Figure 1d shows the well-defined peaks characteristic of reduced amplitude fluctuations, and Fig. 1f shows the well-defined zero-crossings characteristic of reduced phase fluctuations.

1.2. Methods of Generating Squeezed-State Light

In the last section, we found that squeezed-state light is characterized by phase-dependent quantum noise. What is needed is a phase-sensitive amplifier to generate light with amplified quantum noise—amplified above the vacuum level—in one quadrature, and deamplified or ''squeezed'' quantum noise—deamplified below the vacuum level— in the other quadrature. What kind of physical process will accomplish such a phase-sensitive amplification?

A physical analogy will aid in answering this question. Suppose we have a variable length pendulum; that is, we can vary the length of the string to which the pendulum bob is attached by pulling on the string while the bob is in motion, keeping the pivot point fixed (by hanging the string over a pulley, for example). A simple experiment shows that by pulling up on the string (i.e., shortening the string) each time the bob is at its lowest point and returning the string to its original length when the bob is at its highest point, we can *amplify* the motion. In pulling up on the string when the bob is at its lowest point (when its velocity is a maximum), we give the velocity a ''kick'' for the same reason that a twirling figure skater with arms extended rotates faster as she

draws her arms in towards her. In one cycle of oscillation, we pull up on the string twice, once as the pendulum swings to the left, and again as it swings to the right; we "pump" the pendulum at twice its resonant frequency, and obtain an amplification of the motion.

Now suppose we change the phase of the "pump" by 180°, i.e., we *lower* the string each time the bob is at its lowest point, and pull up on the string when the bob is at its highest point. The previous argument showing that the bob, when at its lowest point, speeds up when the string is pulled up now shows that the opposite occurs when the bob is lowered; the bob slows down, resulting in a deamplified motion.

Relative to the phase of the "pump," there are two quadratures of the pendulum motion, one in which the bob is pulled up when at its lowest point, and the other in which the bob is lowered when at its lowest point. As we have seen, one quadrature is amplified and the other is deamplified. This is just the phase-sensitive physical process we need to generate squeezed-state light; devices implementing this process are known as *parametric amplifiers.*

Nonlinear susceptibilities provide the means of producing parametric amplification at optical frequencies. Three nonlinear-optical processes have been used recently to generate squeezed-state light in the laboratory. Squeezed-state light was successfully generated for the first time in the pioneering experiment of Slusher et al.[3] They used backward four-wave mixing in an optical cavity to produce squeezed-state light and balanced homodyne detection to detect it (see Section 1.3). Backward four-wave mixing makes use of two counter-propagating pump beams, each of frequency Ω, interacting with counter-propagating signal and idler beams, at frequencies $\Omega+\varepsilon$ and $\Omega-\varepsilon$, respectively, where the signal and idler are in separate cavity modes. The interaction is mediated by the $\chi^{(3)}$ nonlinearity provided by a beam of atomic sodium. The

weakness of the nonlinearity necessitates the use of an optical cavity, allowing the field to make many passes through the sodium beam. In their best effort, they observed a 17% reduction[4] of the quantum noise level below that of the vacuum. Squeezed-state light has also been generated by four-wave mixing in a forward geometry in the experiment of Shelby et al.[5] An optical fiber provided the $\chi^{(3)}$ nonlinearity in their experiment, the 114 meters of optical fiber obviating the need for an optical cavity. They obtained a noise reduction of 12.5% below the vacuum level. The best results to date were obtained by Wu et al.,[1] who used optical parametric down conversion to generate squeezed-state light with a noise reduction of greater than 50% relative to the vacuum level. Parametric down conversion uses a $\chi^{(2)}$ nonlinearity to mediate the interaction of a powerful pump beam at frequency 2Ω with a signal beam at frequency $\Omega+\varepsilon$ and an idler beam at frequency $\Omega-\varepsilon$. Here the signal and idler belong to the same cavity mode centered on $\varepsilon=0$ (degeneracy). A frequency-doubled laser provides the pump at frequency 2Ω, and a cavity, resonant at frequencies Ω and 2Ω, provides a long effective interaction length by allowing the photons to make many passes through the nonlinear medium.

The common link between parametric down conversion and four-wave mixing (whether backwards or forwards) is the reliance on a mechanism that couples a powerful pump component at frequency 2Ω to signal and idler components at frequencies $\Omega+\varepsilon$ and $\Omega-\varepsilon$, where in all cases $\varepsilon \ll \Omega$. For parametric down conversion, the pumping field itself oscillates at frequency 2Ω, and is coupled to the signal and idler fields through the $\chi^{(2)}$ nonlinearity. Four-wave mixing, on the other hand, uses the $\chi^{(3)}$ nonlinearity to couple the signal and idler fields to the *square* of the pump field oscillating at frequency Ω. The *squared* field contains the component at frequency 2Ω needed for parametric amplification to occur. Both processes can thus be understood in terms of our simple

pendulum analogy; the pumping at frequency 2Ω causes a phase-sensitive amplification to occur, resulting in the production of squeezed-state light.

1.3. Quadrature Phases, Quadrature-Phase Amplitudes, and Balanced Homodyne Detection

A plane-wave electromagnetic field traveling through free space in the positive-z direction can be described by the positive frequency part of the electric field

$$E^{(+)}=[E^{(-)}]^{\dagger}=\int_{\beta}\frac{d\omega}{2\pi}\left[\frac{2\pi\hbar\omega}{c\sigma}\right]^{1/2}a(\omega)\,e^{-i\omega(t-z/c)}, \tag{3.1}$$

where the integral runs over a bandwidth β symmetric about Ω that contains all relevant signal frequencies, and σ is an effective cross-sectional area that crudely accounts for the transverse structure of the field. The electric field operator is given by $E=E^{(+)}+E^{(-)}$. The operators $a(\omega)$ and $a^{\dagger}(\omega)$ are annihilation and creation operators for the field which satisfy the continuum commutation relation

$$[a(\omega),a^{\dagger}(\omega')]=2\pi\delta(\omega-\omega'). \tag{3.2}$$

The total energy (power integrated over all time) transported by the field through the surface $z=\text{constant}$ is

$$\int_{\beta}\frac{d\omega}{2\pi}\,\hbar\omega\,a^{\dagger}(\omega)a(\omega).$$

We let $\omega=\Omega\pm\varepsilon$, where ε is positive by definition and $\varepsilon\ll\Omega$ over the bandwidth β; we find that the electric field operator can be expressed in the form

$$E(z,t)=E_1(z,t)\cos\Omega(t-z/c)+E_2(z,t)\sin\Omega(t-z/c), \tag{3.3}$$

where $E_1(z,t)$ and $E_2(z,t)$ are known as the *quadrature phases* [6] of the electric field. The quadrature phases, in turn, are given by

$$E_1(z,t)=\left(\frac{8\pi\hbar\Omega}{c\sigma}\right)^{1/2}\int_0^{\Delta}\frac{d\varepsilon}{2\pi}\left[\alpha_1(\varepsilon)e^{-i\varepsilon(t-z/c)}+\alpha_1^{\dagger}(\varepsilon)^{i\varepsilon(t-z/c)}\right], \tag{3.4a}$$

$$E_2(z,t)=\left(\frac{8\pi\hbar\Omega}{c\sigma}\right)^{1/2}\int_0^{\Delta}\frac{d\varepsilon}{2\pi}\left[\alpha_2(\varepsilon)e^{-i\varepsilon(t-z/c)}+\alpha_2^{\dagger}(\varepsilon)^{i\varepsilon(t-z/c)}\right], \tag{3.4b}$$

where $\alpha_1(\varepsilon)$ and $\alpha_2(\varepsilon)$ are the *quadrature-phase amplitudes* [6,7]

$$\alpha_1(\varepsilon)=\frac{1}{2}\left[(1+\varepsilon/\Omega)^{1/2}a(\Omega+\varepsilon)+(1-\varepsilon/\Omega)^{1/2}a^{\dagger}(\Omega-\varepsilon)\right], \tag{3.5a}$$

$$\alpha_2(\varepsilon)=-\frac{i}{2}\left[(1+\varepsilon/\Omega)^{1/2}a(\Omega+\varepsilon)-(1-\varepsilon/\Omega)^{1/2}a^{\dagger}(\Omega-\varepsilon)\right]. \tag{3.5b}$$

Here $\Omega+\Delta$ is the upper limit of the band β. We see from Eqs. (3.4) that the quadrature-phase amplitudes are the Fourier components of the quadrature phases, and hence contain the spectral information about quantum fluctuations of the quadrature phases. The quadrature-phase amplitudes obey the following commutation relations:

$$[\alpha_1(\varepsilon),\alpha_1(\varepsilon')]=[\alpha_2(\varepsilon),\alpha_2(\varepsilon')]=[\alpha_1(\varepsilon),\alpha_2(\varepsilon')]=0, \tag{3.6a}$$

$$[\alpha_1(\varepsilon),\alpha_1^{\dagger}(\varepsilon')]=[\alpha_2(\varepsilon),\alpha_2^{\dagger}(\varepsilon')]=\frac{\varepsilon}{2\Omega}2\pi\delta(\varepsilon-\varepsilon'), \tag{3.6b}$$

$$[\alpha_1(\varepsilon),\alpha_2^{\dagger}(\varepsilon')]=[\alpha_1^{\dagger}(\varepsilon),\alpha_2(\varepsilon')]=\frac{i}{2}2\pi\delta(\varepsilon-\varepsilon'). \tag{3.6c}$$

Equations (3.6) imply the commutator Eq. (1.2) for the quadrature phases, and hence the uncertainty principle Eq. (1.4), as discussed earlier.

The real significance of the quadrature phases and the quadrature-phase amplitudes becomes clear in a discussion of the method used to detect squeezed-state light. A phase-sensitive detection scheme is needed to detect the phase dependence of squeezed-state light; a balanced homodyne detector,[8,9] shown in Fig. 2, is the preferred detector for this purpose. The signal beam $E_s(z,t)$ is mixed with a powerful local oscillator (LO) beam $E_{\rm LO}(z,t)$ by a 50-50 beam splitter. The LO can be expressed as the sum of a monochromatic field at frequency Ω plus a quantum fluctuation term

$$E_{\rm LO}(z,t)=A\cos[\Omega(t-z/c)-\phi_{\rm LO}]+\Delta E_{\rm LO}(z,t)\,, \tag{3.7}$$

where

$$<\Delta E_{\rm LO}(z,t)>=0\,. \tag{3.8}$$

The 50-50 beam splitter mixes the LO and the signal beams, producing the following linear superpositions of the two at its outputs:

$$E_H(z,t)=\frac{1}{\sqrt{2}}[E_{\rm LO}(z,t)+E_s(z,t)]=E_H^{(+)}(z,t)+E_H^{(-)}(z,t)\,, \tag{3.9a}$$

$$E_V(z,t)=\frac{1}{\sqrt{2}}[E_{\rm LO}(z,t)-E_s(z,t)]=E_V^{(+)}(z,t)+E_V^{(-)}(z,t)\,. \tag{3.9b}$$

The sign difference between Eqs. (3.9a) and (3.9b) is due to energy conservation; the field energy incident at the input ports of the beam splitter must be equal to the field energy leaving the output ports.[9] The electric fields $E_H(z,t)$ and $E_V(z,t)$ are incident on the photodetectors D_1 and D_2, respectively, which we will assume are located at $z=0$. The photodetectors respond to the normally ordered part of the incident power flux, $\propto E^{(-)}(t)E^{(+)}(t)$, since the remaining terms, containing terms like $E^{(+)2}(t)$ and $E^{(-)2}(t)$, oscillate at optical frequencies, far beyond the bandwidth of any photodetector. An ideal

photodetector emits one photoelectron for each incident photon, so the photocurrent operator is obtained by using the classical expression of the current but treating the fields as operators. Taking the electron charge as e and the area of the photodetector as σ_{det}, we find that the current operators are

$$I_1(t)=\frac{c\,\sigma_{det}}{2\pi\hbar\Omega}E_H^{(-)}(t)E_H^{(+)}(t)$$

$$=\frac{c\,\sigma_{det}}{4\pi\hbar\Omega}[E_{LO}^{(-)}(t)E_{LO}^{(+)}(t)+E_s^{(-)}(t)E_s^{(+)}(t)+E_{LO}^{(-)}(t)E_s^{(+)}(t)+E_s^{(-)}(t)E_{LO}^{(+)}(t)]\,, \qquad (3.10a)$$

$$I_2(t)=\frac{c\,\sigma_{det}}{2\pi\hbar\Omega}E_V^{(-)}(t)E_V^{(+)}(t)$$

$$=\frac{c\,\sigma_{det}}{4\pi\hbar\Omega}[E_{LO}^{(-)}(t)E_{LO}^{(+)}(t)+E_s^{(-)}(t)E_s^{(+)}(t)-E_{LO}^{(-)}(t)E_s^{(+)}(t)-E_s^{(-)}(t)E_{LO}^{(+)}(t)]\,. \qquad (3.10b)$$

A balanced homodyne detector takes the photocurrents from the two detectors and subtracts them coherently:

$$I_D(t)=I_1(t)-I_2(t)=\frac{c\,\sigma_{det}}{2\pi\hbar\Omega}[E_{LO}^{(-)}(t)E_s^{(+)}(t)+E_{LO}^{(+)}(t)E_s^{(-)}(t)]\,. \qquad (3.11)$$

Using Eq. (3.7), Eq. (3.11) can be written as

$$I_D(t)=\frac{c\,\sigma_{det}}{2\pi\hbar\Omega}\left\{\frac{A}{2}[E_s^{(+)}(t)e^{i(\Omega t-\phi_{LO})}+E_s^{(-)}(t)e^{-i(\Omega t-\phi_{LO})}]\right.$$

$$\left.+\Delta E_{LO}^{(-)}(t)E_s^{(+)}(t)+\Delta E_{LO}^{(+)}(t)E_s^{(-)}(t)\right\}\,. \qquad (3.12)$$

From Eq. (3.1), Eqs. (3.4) and Eqs. (3.5), we find the useful relations

$$E_1(z,t)=E_s^{(+)}(z,t)e^{i\Omega(t-z/c)}+E_s^{(-)}(z,t)e^{-i\Omega(t-z/c)}\,, \qquad (3.13a)$$

$$E_2(z,t) = -iE_s^{(+)}(z,t)e^{i\Omega(t-z/c)} + iE_s^{(-)}(z,t)e^{-i\Omega(t-z/c)} . \tag{3.13b}$$

Substituting Eqs. (3.13) into Eq. (3.12), we find

$$I_D(t) = \frac{c\,\sigma_{det}A}{4\pi\hbar\Omega}[E_1(t)\cos\phi_{LO} + E_2(t)\sin\phi_{LO}] , \tag{3.14}$$

where we have ignored the second term of Eq. (3.12) by assuming that A is very large. Notice that the fluctuations from the local oscillator cancel; the local oscillator fluctuations are correlated, or ''balanced'' in the two arms of the detector, and thus make no contribution to the photocurrent.

By changing the phase of the local oscillator ϕ_{LO}, we can, according to Eq. (3.14), make the photocurrent operator $I_D(t)$ proportional to any relative combination of $E_1(t)$ and $E_2(t)$. In particular, for $\phi_{LO}=0$, the current is proportional to $E_1(t)$; for $\phi_{LO}=\pi/2$, the current is proportional to $E_2(t)$. A more general argument makes this even clearer. We can re-express the signal field [Eq. (3.3)] so that it possesses the same argument as the local oscillator field:

$$\begin{aligned} E_s(z,t) &= E_1(\phi_{LO};z,t)\cos[\Omega(t-z/c)-\phi_{LO}] + E_2(\phi_{LO};z,t)\sin[\Omega(t-z/c)-\phi_{LO}] \\ &= [E_1(\phi_{LO};z,t)\cos\phi_{LO} - E_2(\phi_{LO};z,t)\sin\phi_{LO}]\cos\Omega(t-z/c) \\ &+ [E_1(\phi_{LO};z,t)\sin\phi_{LO} + E_2(\phi_{LO};z,t)\cos\phi_{LO}]\sin\Omega(t-z/c) . \end{aligned} \tag{3.15}$$

Equating Eqs. (3.3) and (3.15), we find

$$E_1(\phi_{LO};z,t) = E_1(z,t)\cos\phi_{LO} + E_2(z,t)\sin\phi_{LO} , \tag{3.16a}$$

$$E_2(\phi_{LO};z,t) = E_2(z,t)\cos\phi_{LO} - E_1(z,t)\sin\phi_{LO} . \tag{3.16b}$$

The $E_1(\phi_{LO};z,t)$ quadrature is in phase with the local oscillator. From Eqs. (3.14) and

(3.16a), we see that $I_D(t) \propto E_1(\phi_{LO};z,t)$; that is, at any phase ϕ_{LO}, the differenced photocurrent from a balanced homodyne detector is proportional to the quadrature *which is in phase with the local oscillator.*[10]

Experimentally, one is interested in the *spectrum* of the differenced photocurrent. Spectral information is obtained using a spectrum analyzer, which yields an output signal proportional to the mean spectral power in a bandwidth B centered on frequency ε as a function of ε. The relevant quantity here is the spectral density of $I_D(t)$, which by the Wiener-Khinchin theorem is the Fourier transform of the two-point correlation function

$$<\Delta I_D(t)\Delta I_D(t+\tau)>_{sym} = \left(\frac{c\,\sigma_{det}A}{4\pi\hbar\Omega}\right)^2 <\Delta E_1(\phi_{LO};0,t)\Delta E_1(\phi_{LO};0,t+\tau)>_{sym}$$

$$= \left(\frac{c\,\sigma_{det}A}{4\pi\hbar\Omega}\right)^2 \frac{8\pi\hbar\Omega}{c\,\sigma}\int_0^{\Delta}\frac{d\varepsilon}{2\pi}S_{11}(\phi_{LO},\varepsilon)\cos\varepsilon\tau\,, \qquad (3.17)$$

where

$$S_{11}(\phi_{LO},\varepsilon) = S_{11}(\varepsilon)\cos^2\phi_{LO} + [S_{12}(\varepsilon)+S_{21}(\varepsilon)]\cos\phi_{LO}\sin\phi_{LO} + S_{22}(\varepsilon)\sin^2\phi_{LO} \qquad (3.18)$$

is the spectral density of $E_1(\phi_{LO};0,t)$, normalized so that the vacuum has a value of 1/2. Here we have assumed

$$<\Delta\alpha_m(\varepsilon')\Delta\alpha_n(\varepsilon)>_{sym} = <\alpha_m^{\dagger}(\varepsilon')\Delta\alpha_n^{\dagger}(\varepsilon)>_{sym} = 0\,, \qquad (3.19a)$$

$$<\Delta\alpha_m^{\dagger}(\varepsilon')\Delta\alpha_n(\varepsilon)>_{sym} = \pi S_{mn}(\varepsilon)\delta(\varepsilon-\varepsilon')\,. \qquad (3.19b)$$

Equations (3.19) characterize what is known as *time-stationary quadrature-phase noise,* [6,10] i.e., the conditions set forth by Eqs. (3.19) guarantee that Eq. (3.17) is independent of the time t. The *spectral-density matrix* $S_{mn}(\varepsilon)$, [6,10] which contains all the spectral

information about the quadrature-phase noise, is due to beats between the local oscillator frequency Ω and the signal frequencies $\Omega \pm \varepsilon$. The photodetectors D_1 and D_2 (Fig. 2) are sensitive to such beats over a limited bandwidth only, their electronic bandwidth. We identify this electronic bandwidth with our bandwidth β of relevant frequencies; in other words, we identify Δ as roughly the highest beat frequency to which either photodetector can respond.

The time domain noise moments $<\Delta E_1^2(t)>$ and $<\Delta E_2^2(t)>$ can be recovered from Eq. (3.17). In particular, for $\tau=0$ and $\phi_{LO}=0$, we find

$$<\Delta E_1^2(t)> = \frac{4\hbar\Omega}{c\sigma}\int_0^{\Delta} d\varepsilon\, S_{11}(\varepsilon)\,, \tag{3.20a}$$

and for $\tau=0$ and $\phi_{LO}=\pi/2$,

$$<\Delta E_2^2(t)> = \frac{4\hbar\Omega}{c\sigma}\int_0^{\Delta} d\varepsilon\, S_{22}(\varepsilon)\,. \tag{3.20b}$$

Comparison with Eqs. (1.6) shows that $S_{11}(\varepsilon)=S_{22}(\varepsilon)=1/2$ for coherent- or vacuum-state light. To squeeze the fluctuations in E_1 or E_2, one must have $S_{11}(\varepsilon)<1/2$ or $S_{22}(\varepsilon)<1/2$, respectively, over a significant portion of the bandwidth Δ. Regardless of whether E_1 or E_2 are squeezed, one has squeezing over frequency bands of width less than Δ when $S_{mm}<1/2$ over said band, where $m=1$ or 2.

Rather than looking at the entire spectrum, one usually looks only at the spectrum in the bandwidth $B \ll \Delta$ about the analysis frequency ε and sweeps the local oscillator phase ϕ_{LO}, displaying the resulting trace on an oscilloscope. Assuming that the spectral density is nearly constant over the bandwidth B, one can assume that the mean spectral power over B is proportional to $BS_{11}(\phi_{LO},\varepsilon)$. Let us consider a specific example. Squeezed-state light in which the E_1 quadrature is squeezed, as in Figs. 1c and 1d, has

the spectral-density matrix elements [see Eq. (3.11) of Chapter 2]

$$S_{11}(\varepsilon)=\frac{1}{2}e^{-2u}\,, \tag{3.21a}$$

$$S_{22}(\varepsilon)=\frac{1}{2}e^{2u}\,, \tag{3.21b}$$

$$S_{12}(\varepsilon)=S_{21}(\varepsilon)=0\,, \tag{3.21c}$$

where u (assumed positive) is known as the squeezing parameter and we have assumed the spectrum to be constant over the bandwidth B about ε. Using Eq. (3.18) and Eqs. (3.21), we find for the rms spectral current (proportional to the square root of the mean spectral power)

$$I(\phi_{LO},\varepsilon)=[e^{-2u}\cos^2\phi_{LO}+e^{2u}\sin^2\phi_{LO}]^{1/2}\,, \tag{3.22}$$

where we have set the proportionality constant equal to one for convenience. Figure 3 is a plot of Eq. (3.22) as a function of ϕ_{LO}. The dashed circle of radius one in Fig. 3 shows the rms spectral current for $u=0$, corresponding to unsqueezed vacuum noise entering the signal port of the detector. The vacuum noise, which gives rise to shot noise in the differenced photocurrent, is clearly insensitive to the phase of the local oscillator. The same figure also shows the corresponding rms spectral current for a squeezed vacuum with $u=\ln 4$. We see clearly the reduced fluctuations for $\phi_{LO}=0$, and the increased fluctuations for $\phi_{LO}=\pi/2$. The phase sensitivity of the noise in a squeezed vacuum is obvious; any fluctuation in the phase of the local oscillator near $\phi_{LO}=0$ may degrade the observed squeezing by mixing part of the amplified quadrature E_2 with the squeezed quadrature E_1.

A typical experimental set-up, the one used by Wu et al.,[1] is shown in Fig. 4. Here

a degenerate parametric amplifier (in an oscillator configuration) is the source of squeezed-state light—squeezed vacuum in this case. The effective length of the nonlinear medium is increased by placing the crystal in an optical cavity, since it allows the light to make multiple passes through the crystal. Notice that the same laser that pumps the nonlinear crystal also acts as the source for the local oscillator. Figure 5 shows some of the results of this experiment. The rms noise voltage $V(\theta)$ is plotted as a function of the local oscillator phase θ. Here the noise voltage corresponds to our rms spectral current plotted in Fig. 3. For certain values of θ, the noise voltage dips below the vacuum level, given by the dotted line in Fig. 5.

1.4. Introduction to the Remaining Chapters

In Chapter 2, we develop a wideband traveling-wave formalism for analyzing quantum mechanically a degenerate parametric amplifier. The formalism is based on *spatial* differential equations—spatial Langevin equations—that propagate temporal Fourier components of the field operators through the nonlinear medium. In addition to the parametric nonlinearity, the Langevin equations include absorption and associated fluctuations, dispersion (phase mismatching), and pump quantum fluctuations. We analyze the dominant effects of phase mismatching and pump quantum fluctuations on the squeezing near degeneracy ($\varepsilon=0$) produced by a degenerate parametric amplifier.

We carry out a more detailed analysis of the effects of phase mismatching in Chapter 3. The spatial Langevin equations derived in Chapter 2 are easily solved with the assumption of a lossless medium and a classical pump. We find that parametric amplification is capable of generating squeezed-state light over a wide band if materials with large $\chi^{(2)}$ nonlinearities can be found, and that the squeezing bandwidth can be enhanced by phase matching away from degeneracy. We compare our results with

similar results recently found for four-wave mixing in an optical fiber.

Chapter 4 considers again the effect of pump quantum fluctuations on the squeezing produced by parametric amplification. We briefly describe a wave-packet approach that enables us to treat traveling-wave problems quantum-mechanically with discrete-mode calculations. The equations of motion resulting from such an approach are *spatial* differential equations—as in Chapter 2—for the wave packet amplitude operators. Under certain assumptions, we can replace the spatial variable z by the temporal variable ct/n_0, where n_0 is the index of refraction (assumed nondispersive). The resulting equations of motion are of the same form as those one would derive from a Hamiltonian using the standard approach to problems in quantum optics; one assumes the field can be described by a few discrete modes, and writes down an appropriate Hamiltonian for the process being considered. We justify our use of this Hamiltonian, and use it to derive Fokker-Planck equations for one- and two-mode parametric amplifiers. Standard methods of stochastic calculus[11] are then used to derive Ito stochastic differential equations (SDEs) from the Fokker-Planck equations. An approximate solution of the SDEs is obtained by iteration, and the full semiclassical correction (the correction to order $\bar{N}^{-1}$, where $\bar{N}$ is the initial number of pump photons) is then calculated analytically. The corrections obtained agree with the dominant correction calculated via spatial Langevin equations in Chapter 2.

A possible application of squeezing is considered in Chapter 5; in particular, we study the effects of squeezing the intracavity noise in a laser oscillator. We solve the classical noise problem of a realistic laser model by making a bold—and possibly unrealizable—assumption, that the in-phase and quadrature Langevin sources which are responsible for the "noisiness" of the laser can be squeezed. We show that the effect of squeezing the in-phase quadrature is to reduce the phase noise, including the

linewidth, of the laser but, due to amplitude-phase coupling, not to eliminate them altogether. Intensity fluctuations, on the other hand, are fully squeezed.

REFERENCES

1. L. -A. Wu, H. J. Kimble, J. L. Hall, and H. Wu, Phys. Rev. Lett. **57**, 2520 (1986).

2. E. Merzbacher, *Quantum Mechanics* (Wiley, New York, 1970).

3. R. E. Slusher, L. W. Hollberg, B. Yurke, J. C. Mertz, and J. F. Valley, Phys. Rev. Lett. **55**, 2409 (1985).

4. D. Walls, Nature **324**, 210 (1986).

5. R. M. Shelby, M. D. Levenson, S. H. Perlmutter, R. G. DeVoe, and D. F. Walls, Phys. Rev. Lett. **57**, 691 (1986).

6. C. M. Caves and B. L. Schumaker, Phys. Rev. A**31**, 3068 (1985).

7. B. Yurke, Phys. Rev. A**32**, 300 (1985).

8. H. P. Yuen and V. W. S. Chan, Opt. Lett. **8**;, 177 (1983).

9. B. L. Schumaker, Opt. Lett. **9**, 189 (1984).

10. C. M. Caves and B. L. Schumaker, in *Quantum Optics IV,* J. D. Harvey and D. F. Walls, eds. (Springer, Berlin, 1986), p. 20.

11. C. W. Gardiner, *Handbook of Stochastic Methods* (Springer-Verlag, Berlin, 1983); L. Arnold, *Stochastic Differential Equations* (Wiley, New York, 1973).

12. C. M. Caves, Phys. Rev. D**23**, 1693 (1981).

FIGURE CAPTIONS

Fig. 1. Graphs of the electric field versus time for three states of the electromagnetic field. The graph on the left represents the "error box" of the complex amplitude, while the graph on the right is the time variation of the electric field for the same state. The dark line is the expectation value of the electric field, and the shaded region represents the uncertainty in the electric field. (a),(b) Coherent-state light. (c), (d) Squeezed-state light with reduced amplitude fluctuations. (e),(f) Squeezed-state light with reduced phase fluctuations. Reproduced with permission from Caves.[12]

Fig. 2. A balanced homodyne detector. The 50-50 beam splitter mixes the incoming signal with a powerful local oscillator, with the output fields incident on the photodetectors D_1 and D_2. The output signal is obtained by coherently subtracting the photodetector currents I_1 and I_2.

Fig. 3. A plot of the rms current $I(\phi_{LO},\varepsilon)$ from a balanced homodyne detector as a function of local oscillator phase ϕ_{LO} for fixed analysis frequency ε. The dashed line is for a signal composed of un-squeezed vacuum noise, and the solid line is for a signal composed of squeezed vacuum noise.

Fig. 4. Diagram of the principal elements of the apparatus for squeezed-state generation by degenerate parametric down conversion. Reproduced with permission from Kimble.[1]

Fig. 5. Measurement of the phase dependence of the quantum fluctuations in a squeezed state produced by degenerate parametric down conversion. The phase dependence of the rms noise voltage $V(\theta)$ from a balanced homodyne detector is displayed as a function of local oscillator phase θ at fixed analysis frequency (1.8 MHz) and bandwidth (100 kHz) in the spectral distribution of photocurrent fluctuations. With the OPO input blocked, the vacuum field entering the signal port of the detector

produces the noise voltage given by the dashed line with no sensitivity on θ. With the OPO input present, the dips below the vacuum level represent a 50% reduction in noise power relative to the vacuum noise level. Note that the ordinate is a linear scale in noise voltage. The dotted line is the amplifier noise level. Reproduced with permission from Kimble.[1]

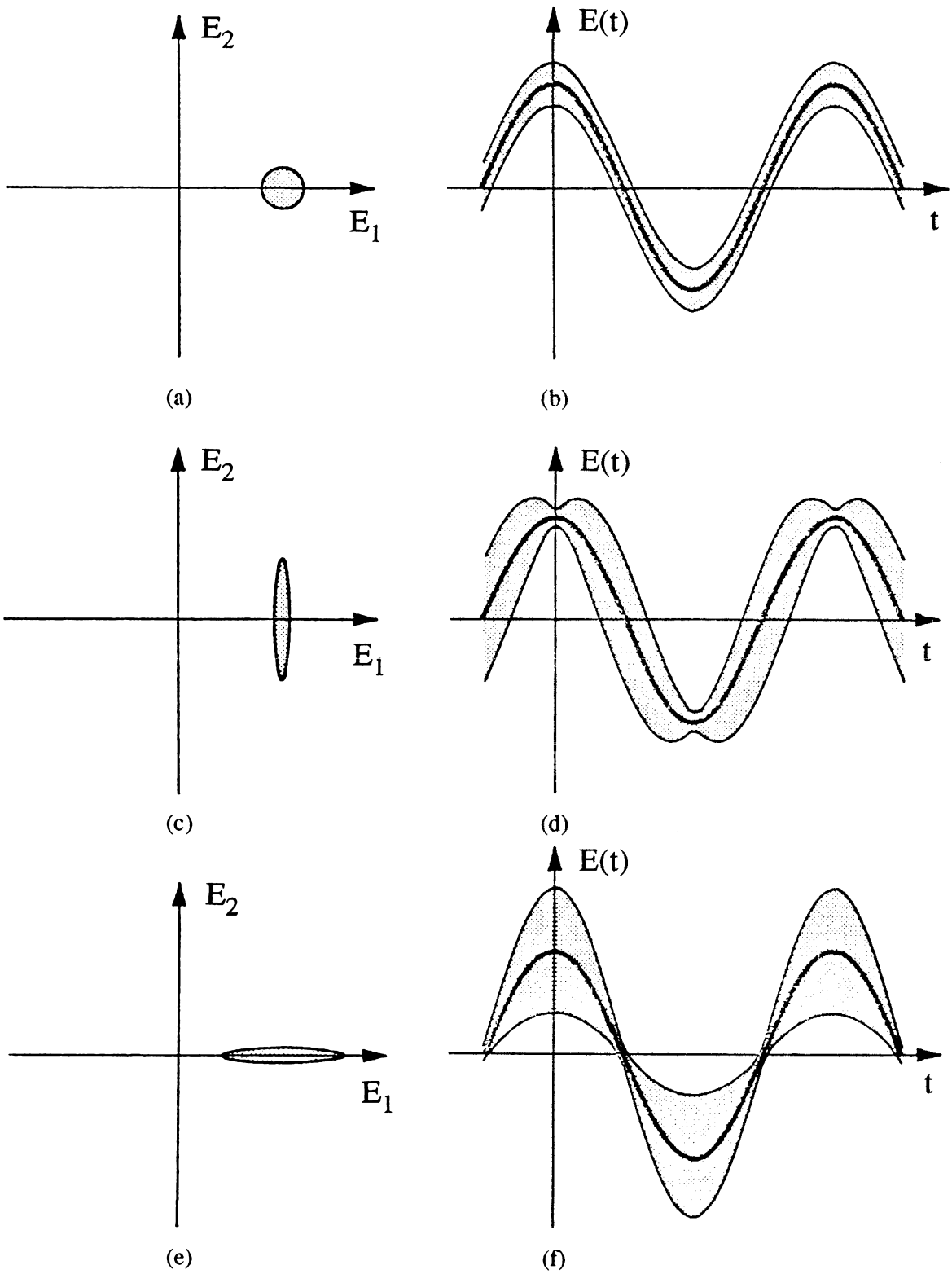

Figure 1

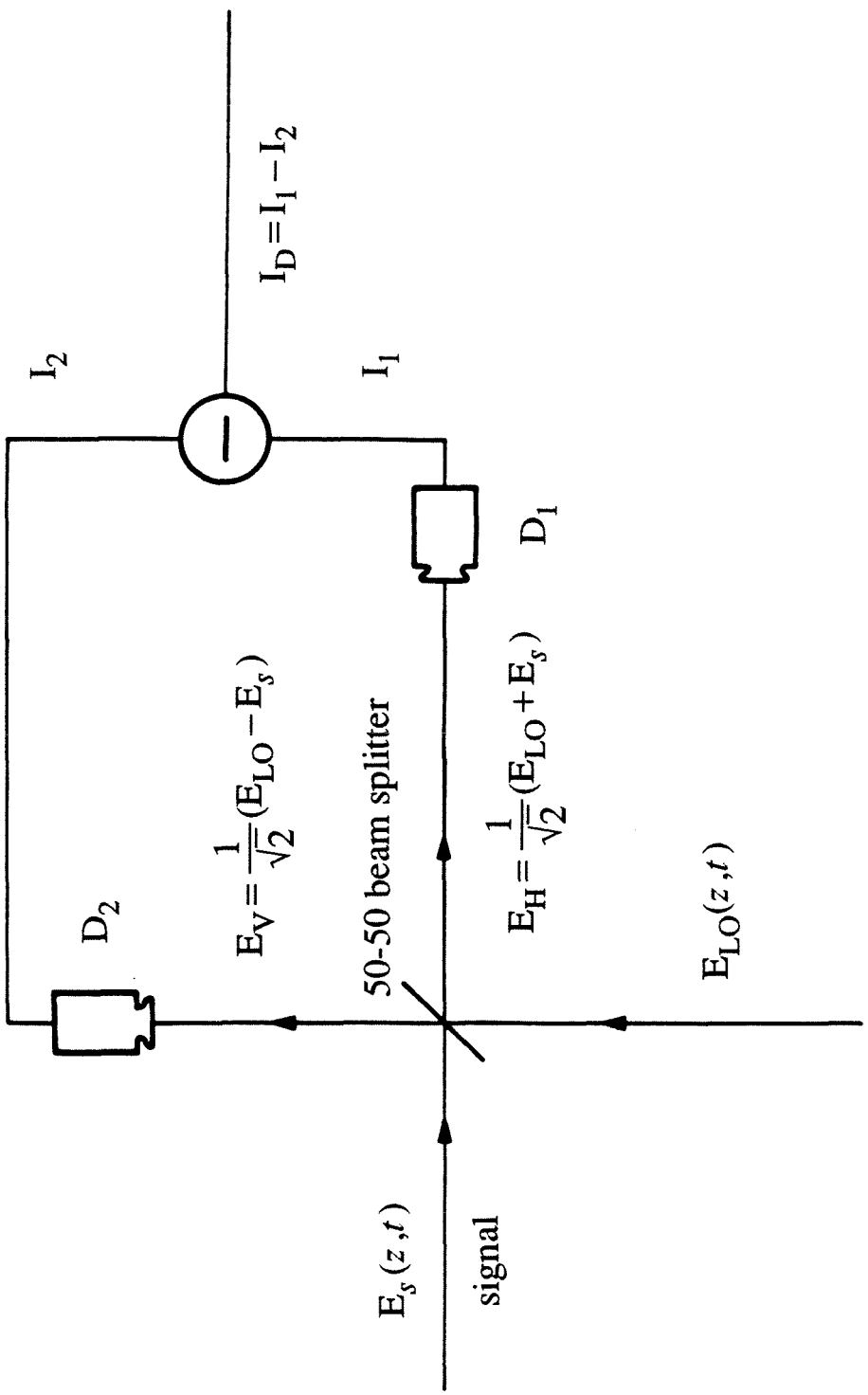
I_2
$I_D = I_1 - I_2$
I_1
D_2
D_1
$E_V = \frac{1}{\sqrt{2}}(E_{LO} - E_s)$
50-50 beam splitter
$E_H = \frac{1}{\sqrt{2}}(E_{LO} + E_s)$
$E_{LO}(z,t)$
$E_s(z,t)$
signal
local oscillator (LO)

Figure 2

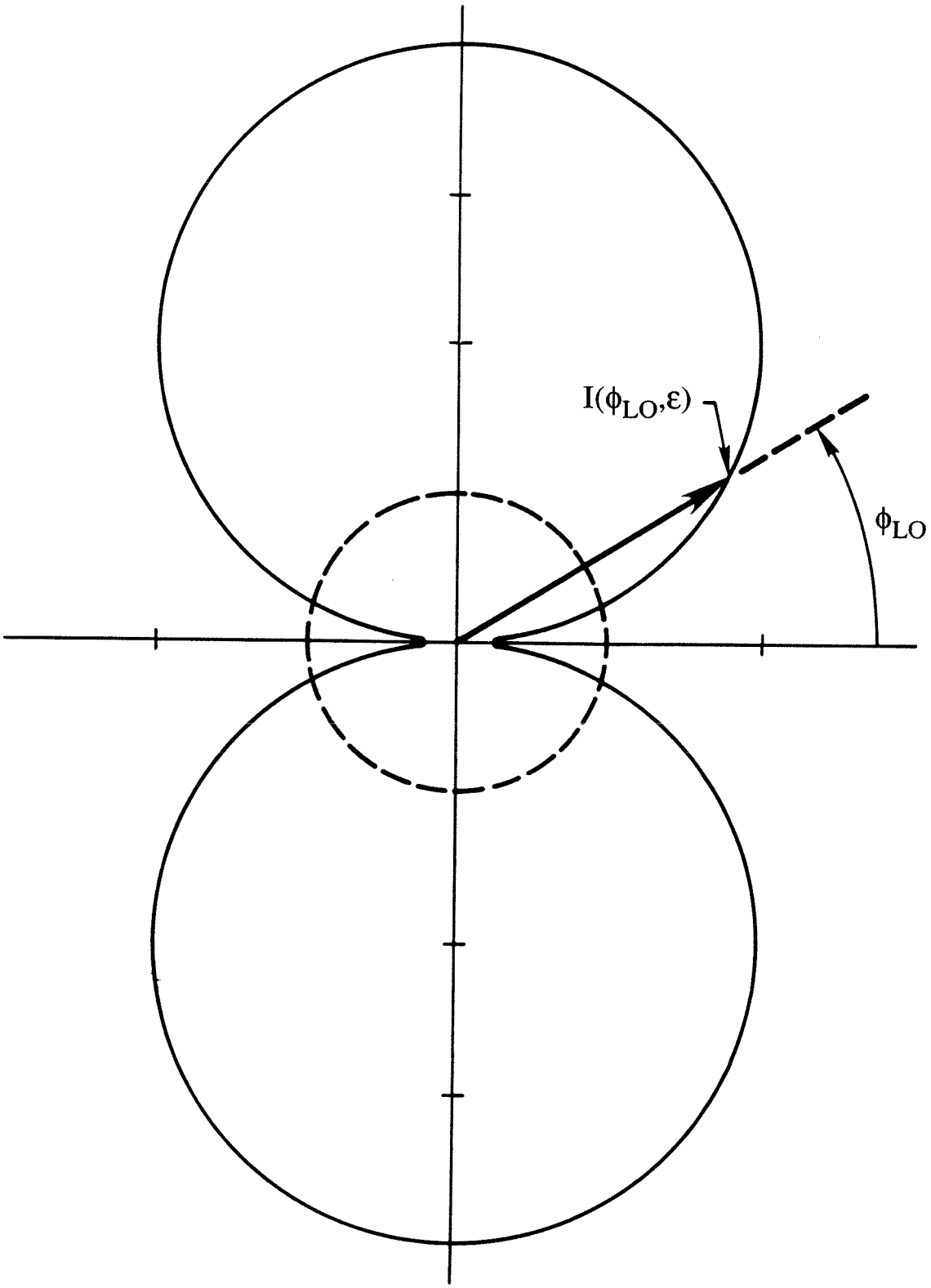

Figure 3

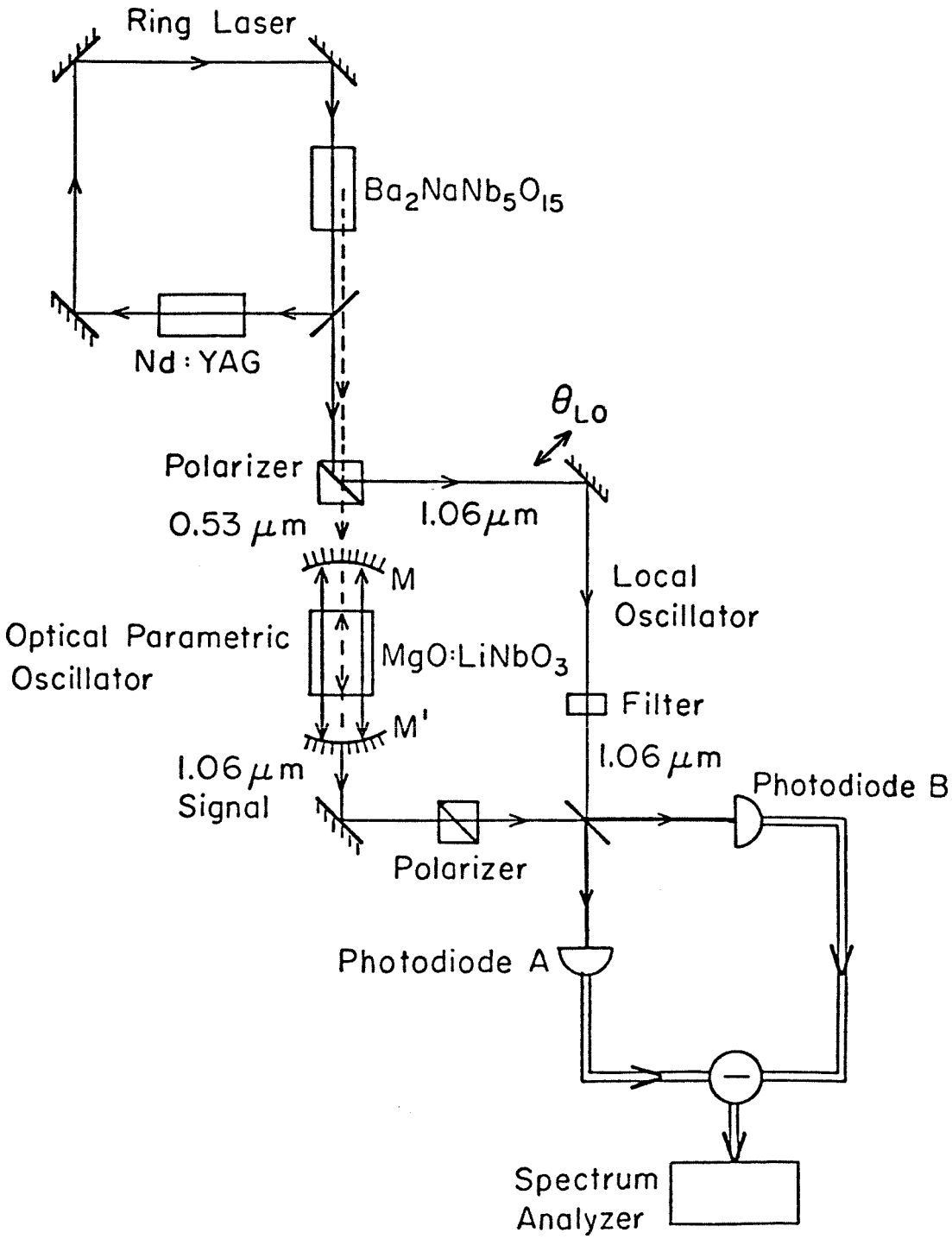
Ring Laser
$Ba_2NaNb_5O_{15}$
Nd : YAG
θ_{LO}
Polarizer
0.53 μm
1.06μm
M
Local
Oscillator
Optical Parametric
Oscillator
MgO:$LiNbO_3$
Filter
M'
1.06 μm
1.06 μm
Signal
Photodiode B
Polarizer
Photodiode A
Spectrum
Analyzer

Figure 4

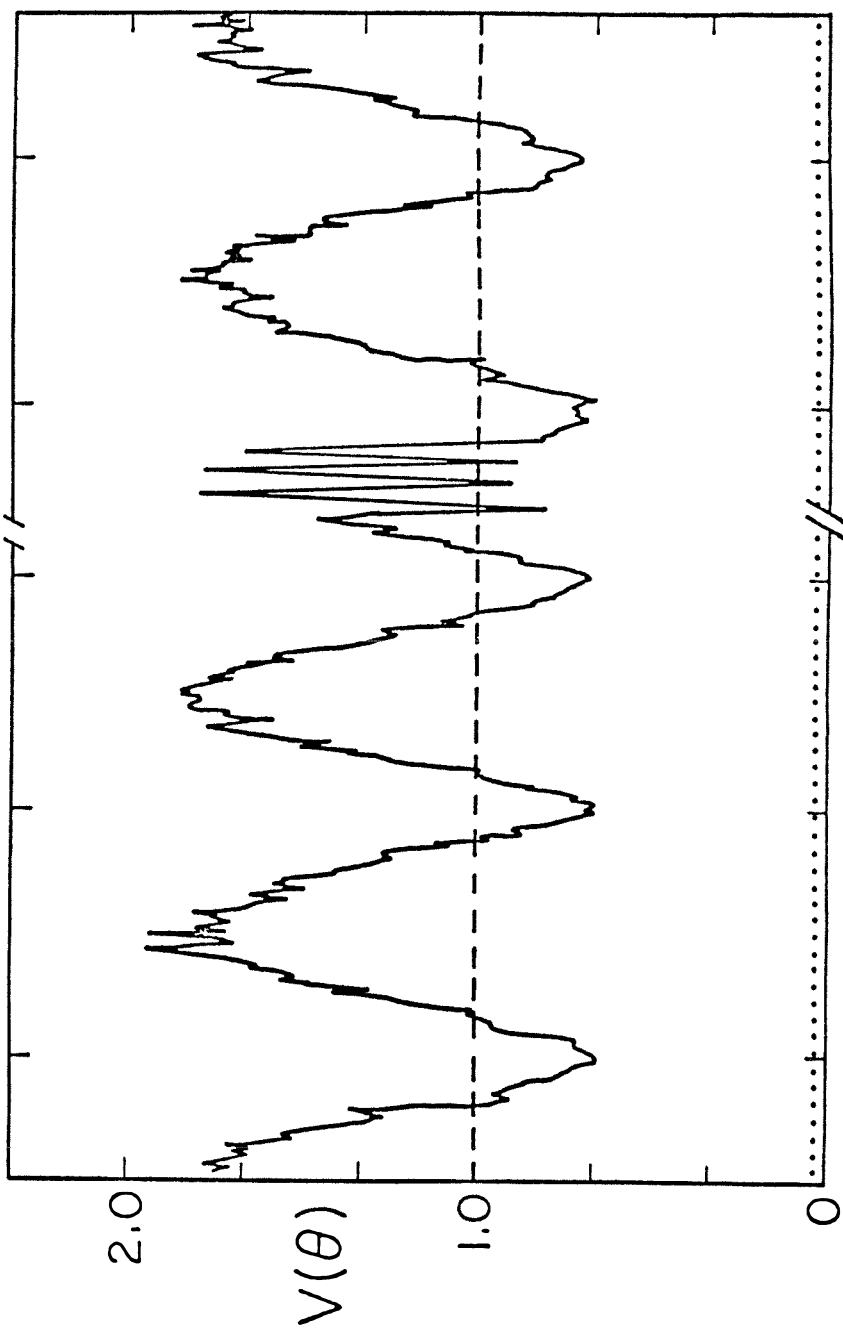

Figure 5

CHAPTER 2

Quantum Wideband Traveling-Wave Analysis of a Degenerate Parametric Amplifier

by Carlton M. Caves and David D. Crouch

Published in the Journal of the Optical Society of America B4, 1535 (1987).

ABSTRACT

We develop a wideband traveling-wave formalism for analyzing quantum mechanically a degenerate parametric amplifier. The formalism is based on *spatial* differential equations—spatial Langevin equations—that propagate temporal Fourier components of the field operators through the nonlinear medium. In addition to the parametric nonlinearity, the Langevin equations include absorption and associated fluctuations, dispersion (phase mismatching), and pump quantum fluctuations. We analyze the dominant effects of phase mismatching and pump quantum fluctuations on the squeezing produced by a degenerate parametric amplifier.

1. INTRODUCTION

A degenerate parametric amplifier (DPA) is the prototypic device for generating squeezed-state light.[1–3] A DPA runs on the nonlinear interaction between a signal field near frequency Ω and a pump field at frequency $\Omega_p = 2\Omega$.[4] This parametric interaction has been exploited to generate squeezed-state light[5]—but in an oscillator, rather than an amplifier configuration. In the oscillator configuration the nonlinear medium is enclosed in an optical cavity, in which multiple passes through the medium increase the effective nonlinearity.[6–10] If one could find materials with larger $\chi^{(2)}$ nonlinearities, however, one might prefer an amplifier configuration because of its intrinsically wider bandwidth.

The conventional approach to quantum problems in nonlinear optics is to specialize to a few interacting modes of the electromagnetic field. All the spatial dependence is contained in the spatial mode functions. The basic equations are *temporal* differential equations that describe the evolution of the modes. In one realization these equations are temporal operator Langevin equations for the evolution of the creation and annihilation operators of the modes.

This conventional approach is well-suited to analyzing a parametric oscillator, in which the appropriate modes are modes of the optical cavity, but it is ill-suited to analyzing a DPA, which is a traveling-wave device not easily thought of in terms of a few discrete modes. To analyze a DPA, one would like a set of *spatial* differential equations for the propagation of the fields through the nonlinear medium. One way to get such spatial differential equations is to take the temporal differential equations for discrete modes interacting parametrically and to replace t with $z/v_{\rm ph}$, where $v_{\rm ph}$ is the phase velocity in the medium.[11] Aside from its questionable validity, this procedure runs into trouble when there is dispersion, and it does not address questions about

bandwidths. These problems with the conventional approach have been stressed by Tucker and Walls,[12] who developed a wave-packet formalism in an attempt to deal with them.

In this chapter we model a DPA in a different way. Our approach is patterned after the approach used in classical nonlinear optics, which is formulated in terms of spatial differential equations for coupled Fourier components of the fields. We start with an ideal, lossless, dispersionless medium with a nonlinear susceptibility $\chi^{(2)}$. In such a medium the Heisenberg equations for the field operators are an operator version of the macroscopic Maxwell equations, together with a constitutive relation that includes the nonlinearity.[13] A temporal Fourier transform then yields spatial differential equations for propagation of the Fourier components of the field operators through the medium. These equations describe a parametric interaction between signal frequencies $\Omega \pm \varepsilon$ and the pump at frequency Ω_p. Because there is no dispersion, the parametric interaction is perfectly phase matched.

Our next step is to include absorption and dispersion phenomenologically. We replace the actual nonlinear medium by a sequence of slabs of ideal medium separated by beam splitters. Reflection at the beam splitters models a linear loss mechanism, and frequency-dependent phase shifts at the beam splitters introduce dispersion. The final result is a set of spatial propagation equations that include absorption and phase mismatching. These equations might well be called spatial operator Langevin equations for the propagation of the field through the nonlinear medium.

Throughout our analysis we are interested in the dominant effect of quantum fluctuations in the pump field, our goal being to investigate the conditions under which the pump can be treated classically. The dominant effect arises from quantum phase fluctuations in the pump, which feed noise from the amplified signal quadrature into the

squeezed signal quadrature. The quantum phase fluctuations in the pump can be viewed as due to vacuum fluctuations at unexcited frequencies near Ω_p, which couple to signal frequencies through the parametric nonlinearity. The bandwidth over which such vacuum fluctuations are important, which can be thought of as the pump bandwidth, determines the size of the quantum phase fluctuations in the pump. This pump bandwidth is limited by phase mismatching, which renders frequencies sufficiently far removed from Ω_p effectively uncoupled from the signal frequencies. We evaluate this pump bandwidth within our model. Perhaps surprisingly, it is smaller than the bandwidth over which the DPA is phase matched.

In Section 2 we describe our model of a DPA, present a simple heuristic argument for the conditions necessary for a classical pump, and then derive the spatial Langevin equations for the model. In Section 3 we use the spatial Langevin equations to investigate the effects of phase mismatching and pump quantum fluctuations on the squeezing spectrum.

2. MODEL FOR DEGENERATE PARAMETRIC AMPLIFIER

A. Description of model

Consider a nonlinear medium of length L, which lies between $z=0$ and $z=L$. The nonlinearity is described by a nonlinear susceptibility $\chi^{(2)}$. Propagating through the medium in the $+z$ direction is a strong pump wave at frequency Ω_p and a signal wave at frequencies near the degeneracy frequency $\Omega=\Omega_p/2$. The parametric nonlinearity couples the pump to signal frequencies $\Omega\pm\varepsilon$. We idealize all the waves as plane waves with a single polarization in which the electric (magnetic) field lies along the x-axis (y-axis). Specializing to a single polarization ignores the details of how phase matching is

achieved in many real DPAs, but these details are not important for our quantum analysis. Specializing to plane waves ignores the transverse structure of the waves, which we, nonetheless, take into account crudely by introducing an effective cross-sectional area σ for the waves.

We assume, for simplicity, that the index of refraction for frequencies near Ω_p is uniform with value $n_p = n_0$; hence the pump wave number is $K_p = \Omega_p n_0/c$. The index of refraction for frequencies $\omega = \Omega \pm \varepsilon$ near Ω is allowed to be dispersive with value $n(\omega) = n_0 + \Delta n(\omega)$; the corresponding wave number is denoted $k(\omega) = \omega n(\omega)/c$. We assume perfect phase matching at degeneracy—i.e., $\Delta n(\Omega) = 0$—so that the wave number at degeneracy is $K = \Omega n_0/c = K_p/2$.

We assume for convenience that the medium is lossless for frequencies near Ω_p, but we allow for absorption at frequencies ω near Ω. The absorption is characterized by an absorption coefficient $\gamma(\omega)$, which gives the loss per unit length in photon units.

The pump's magnetic field has complex amplitude $iA_p e^{i\phi_p} = iA_p e^{2i\phi}$, where A_p is the pump amplitude and $\phi_p = 2\phi$ is the pump phase. The corresponding pump power is $P_p = (c\sigma/8\pi n_0)A_p^2$.

It is useful to introduce a dimensionless measure of the nonlinearity,

$$\alpha_0 \equiv \frac{2\pi\chi^{(2)}A_p}{n_0^2} = 2\pi\frac{\chi^{(2)}}{n_0^{3/2}}\left[\frac{8\pi P_p}{c\sigma}\right]^{1/2}, \tag{2.1}$$

in terms of which the nonlinear gain coefficient of the medium is

$$g_0 \equiv \alpha_0(\Omega/c) = \alpha_0(K/n_0). \tag{2.2}$$

There are three important spatial rates in our model: (i) the rate of accumulation of phase K, (ii) the nonlinear gain coefficient g_0, and (iii) the absorption coefficient γ. The

fundamental assumption of our analysis—just as it is the fundamental assumption of a classical analysis of a DPA[4]—is that these spatial rates satisfy

$$g_0, \gamma \ll K \ . \tag{2.3}$$

That $g_0 \ll K$ is equivalent to saying that the dimensionless nonlinearity $\alpha_0 \ll 1$.

The nonlinear gain is effective only over the bandwidth for which the medium is phase matched. The extent of phase mismatching at frequencies $\Omega \pm \varepsilon$ is characterized by

$$\Delta k(\varepsilon) \equiv K_p - k(\Omega+\varepsilon) - k(\Omega-\varepsilon) = -\frac{(\Omega+\varepsilon)\Delta n(\Omega+\varepsilon)}{c} - \frac{(\Omega-\varepsilon)\Delta n(\Omega-\varepsilon)}{c} \ . \tag{2.4}$$

The index of refraction varies only a small amount over the phase-matched bandwidth, so we can expand it as

$$\Delta n(\Omega \pm \varepsilon) = \pm n'\varepsilon + \frac{1}{2} n''\varepsilon^2 \ , \tag{2.5}$$

where the derivatives of $n(\omega)$ are evaluated at Ω. One then finds that

$$\Delta k(\varepsilon) = -p\,\varepsilon^2/\Omega c \ , \quad p \equiv 2\Omega n' + \Omega^2 n'' \ , \tag{2.6}$$

where p is a dimensionless factor for which a typical value might be $|p| \sim 0.1$. One can now introduce frequencies ε_1 and ε_2 at which the medium begins to be badly mismatched:

$$|\Delta k(\varepsilon_1) L| = 1 \implies \varepsilon_1 = |p|^{-1/2} (\Omega c/L)^{1/2} \ , \tag{2.7a}$$

$$|\Delta k(\varepsilon_2)/2g_0| = 1 \implies \varepsilon_2 = |p|^{-1/2} (2\Omega c g_0)^{1/2} \ . \tag{2.7b}$$

The bandwidth $\Delta/2\pi$ over which the DPA is phase matched can be defined as

$$\Delta/2\pi \equiv \pi^{-1}\min(\varepsilon_1,\varepsilon_2) \ll \Omega/2\pi\,. \tag{2.8}$$

B. Conditions for classical pump

The pump wave is, of course, not completely classical. Its monochromatic excitation at frequency Ω_p is inevitably accompanied by quantum fluctuations, which lead to fluctuations in the pump amplitude and phase. The limit in which the quantum fluctuations can be totally ignored and the pump is strictly classical is not just the limit of a very strong pump; rather, it is that the pump amplitude $A_p \to \infty$, while the nonlinear susceptibility $\chi^{(2)} \to 0$, in such a way that the dimensionless nonlinearity $\alpha_0 \propto \chi^{(2)} A_p$ (or the nonlinear gain g_0) is held constant. Knowing this limit, however, does not tell one whether the pump in a given DPA can be treated classically to a good approximation. Indeed, the important practical question concerns a given nonlinear medium with a fixed value of $\chi^{(2)}$—not a fixed value of α_0. One would like to know, given $\chi^{(2)}$, the range of pump powers P_p for which the pump is approximately classical.

There is a simple heuristic argument[14] for the dominant effect of pump quantum fluctuations. If the DPA were powered by a classical pump, it would produce ideal squeezed light at phase-matched signal frequencies. Such ideal squeezed light can be represented in a complex-amplitude diagram by an ellipse[15,16] with radius $e^{-g_0 L}$ for the squeezed quadrature and radius $e^{g_0 L}$ for the amplified quadrature (ellipse with solid lines in Fig. 1). The orientation of the ellipse is determined by the phase of the pump; in Fig. 1 the pump phase is chosen so that the ellipse with solid lines is oriented along the real and imaginary axes.

The dominant effect of pump quantum fluctuations arises from the phase fluctuations, which have characteristic size $\Delta\phi_p = 1/2N_p^{1/2} = 1/2\mathcal{A}_p$. Here N_p is the number of pump

photons, and $\mathcal{A}_p$ is a dimensionless pump amplitude in photon units. The pump phase fluctuations cause the orientation of the ellipse in Fig. 1 to fluctuate, as indicated schematically by the dotted ellipse. The characteristic angle through which the ellipse turns is $\Delta\phi = \Delta\phi_p/2 = 1/4\mathcal{A}_p$. These orientation fluctuations feed noise from the amplified signal quadrature into the squeezed signal quadrature, thereby degrading the squeezing. The characteristic size of the noise added to the squeezed quadrature is $\Delta\phi e^{g_0 L}$. Thus the condition for a classical pump is

$$\Delta\phi e^{g_0 L} = e^{g_0 L}/4\mathcal{A}_p \ll e^{-g_0 L} \implies \mathcal{A}_p \gg \frac{1}{4}e^{2g_0 L} = \frac{1}{4}e^{2\alpha_0(\Omega L/c)}. \tag{2.9}$$

One sees in this condition the limit for a strictly classical pump: $\alpha_0 = \text{constant}$, $\mathcal{A}_p \to \infty$.

Missing from the preceding argument is any hint of how to relate the physical pump amplitude A_p to the dimensionless amplitude $\mathcal{A}_p$. That relation requires identifying an appropriate bandwidth. The pump quantum fluctuations can be regarded as arising from vacuum fluctuations in unexcited frequencies near Ω_p, which are coupled to signal frequencies by the parametric nonlinearity. The size of the phase fluctuations—and, hence, the effective number of pump photons—depends on the bandwidth of nearby frequencies that must be considered. Clearly this pump bandwidth $\Delta_p/2\pi$ is limited by phase mismatching, which means that frequencies sufficiently far removed from Ω_p are not effectively coupled to frequencies in the signal field.

Given a pump bandwidth $\Delta_p/2\pi$, one can identify the number of pump photons as

$$N_p \equiv \frac{P_p}{\hbar\Omega_p\Delta_p/2\pi} = \frac{c\sigma}{4n_0\hbar\Omega_p\Delta_p}A_p^2 = \left[\frac{A_p}{A_{\text{vac}}}\right]^2 \equiv \mathcal{A}_p^2. \tag{2.10}$$

Here

$$A_{\text{vac}} \equiv (4n_0\hbar\Omega_p\Delta_p/c\sigma)^{1/2} \tag{2.11}$$

is an effective amplitude for the pump quantum fluctuations; it corresponds to a vacuum power $P_{vac}=(c\sigma/8\pi n_0)A_{vac}^2=\hbar\Omega_p\Delta_p/2\pi$. Notice that the variance in the pump phase is

$$(\Delta\phi_p)^2=1/4N_p=(\hbar\Omega_p/4P_p)(\Delta_p/2\pi)\,. \tag{2.12}$$

It is useful to introduce a dimensionless nonlinear susceptibility

$$\alpha_{vac}\equiv\frac{\alpha_0}{\mathcal{A}_p}=\frac{2\pi\chi^{(2)}A_{vac}}{n_0^2}\,, \tag{2.13}$$

which measures the intrinsic nonlinearity of the medium in units of the pump vacuum amplitude.

Now write the condition (2.9) for a classical pump as

$$\mathcal{A}_p\gg\frac{1}{4}\exp[2\alpha_{vac}(\Omega L/c)\mathcal{A}_p]\,. \tag{2.14}$$

For a given nonlinear medium with a fixed value of $\alpha_{vac}(\Omega L/c)$, there is a restricted range of pump amplitudes for which the pump is approximately classical. The upper end of the range is determined by the solution of

$$\mathcal{A}_{max}=\frac{1}{4}\exp[2\alpha_{vac}(\Omega L/c)\mathcal{A}_{max}]\,; \tag{2.15}$$

to be approximately classical, the pump must have dimensionless amplitude $\mathcal{A}_p$ much bigger than 1, but somewhat smaller than $\mathcal{A}_{max}$. Rewritten in terms of physical parameters, the condition for a classical pump becomes

$$P_p\gg\frac{1}{16}\hbar\Omega_p\frac{\Delta_p}{2\pi}\exp\left[8\pi\frac{\chi^{(2)}}{n_0^{3/2}}\left(\frac{\Omega L}{c}\right)\left(\frac{8\pi P_p}{c\sigma}\right)^{1/2}\right]\,. \tag{2.16}$$

These considerations hinge on knowing the pump bandwidth $\Delta_p/2\pi$. One's first guess might be that $\Delta_p/2\pi$ is about the same size as the phase-matched bandwidth $\Delta/2\pi$, but our detailed calculation in Section 3D confirms the preceding argument and shows that within our model

$$\Delta_p/2\pi = cg_0/\Omega|n'| , \tag{2.17}$$

which is typically smaller than $\Delta/2\pi$.

Previous analyses of pump fluctuations in a DPA have idealized to a few discrete modes; thus they do not address bandwidth questions. Wodkiewicz and Zubairy[17] specialized to a single-mode pump and a single-mode signal, and they analyzed classical fluctuations in the pump amplitude and phase. Their result is consistent with the above argument, with $\Delta\phi_p$ given by classical phase diffusion instead of quantum fluctuations. Hillery and Zubairy[14] considered a single-mode pump and a single-mode signal, and they evaluated the effect of pump quantum fluctuations by using a path-integral analysis. Their result is consistent with the preceding argument. Scharf and Walls[18] specialized to a single-mode pump and a two-mode signal (signal and idler modes), and they did a detailed asymptotic analysis of pump quantum fluctuations. In their analysis the dominant effect of pump quantum fluctuations is an error term $e^{3g_0L}/\sqrt{480}A_p$ (in our notation), a bigger effect than the dominant effect $e^{g_0L}/4A_p$ suggested by the above argument. If the Scharf-Walls result is correct, then pump quantum fluctuations are more serious than our analysis indicates.

C. Spatial Langevin equations

We are primarily interested in the behavior of the signal field. Propagating toward the nonlinear medium from the vacuum region $z<0$ is the input signal field, a free field whose positive-frequency field operators can be written as

$$B_{\text{in}}^{(+)} = D_{\text{in}}^{(+)} = E_{\text{in}}^{(+)} = \int_{\beta_s} \frac{d\omega}{2\pi} \left[\frac{2\pi\hbar\omega}{c\sigma} \right]^{1/2} a_{\text{in}}(\omega) e^{i\omega(z/c - t)}, \quad z \leq 0, \tag{2.18}$$

where the integral runs over a bandwidth β_s about Ω, which contains all relevant signal frequencies. The operators $a_{\text{in}}(\omega)$ and $a_{\text{in}}^{\dagger}(\omega)$ are annihilation and creation operators for the input signal field; they satisfy continuum commutation relations

$$[a_{\text{in}}(\omega), a_{\text{in}}^{\dagger}(\omega')] = 2\pi\delta(\omega - \omega'). \tag{2.19}$$

The total energy (power integrated over all time) transported by the input signal field through a surface $z = \text{constant}$ is

$$\int_{\beta_s} \frac{d\omega}{2\pi} \hbar\omega a_{\text{in}}^{\dagger}(\omega) a_{\text{in}}(\omega).$$

Similar considerations apply to the output signal field, which propagates away from the nonlinear medium into the vacuum region $z>L$. We denote it in the same way as the input signal field, but with "in" replaced by "out."

Inside the nonlinear medium we write the signal field in terms of a temporal Fourier expansion. The positive-frequency part of the magnetic field operator is given by

$$B_s^{(+)} = \int_{\beta_s} \frac{d\omega}{2\pi} B_s(\omega, z) e^{i(kz - \omega t)}, \quad k = \omega n(\omega)/c, \quad 0 \leq z \leq L, \tag{2.20a}$$

$$B_s(\omega, z) = \left[\frac{c}{n(\omega) v_g(\omega)} \right]^{1/2} \left[\frac{2\pi n(\omega)\hbar\omega}{c\sigma} \right]^{1/2} a_s(\omega, z). \tag{2.20b}$$

Here $v_g(\omega) \equiv (dk/d\omega)^{-1}$ is the group velocity in the medium.

If there were no nonlinearity, the Fourier components $B_s(\omega,z)$ would have no z dependence, and the displacement field operator $D_s^{(+)}$ and the electric field operator $E_s^{(+)}$ would have Fourier expansions similar to Eq. (2.20a), with $D_s(\omega) = [n(\omega)]^2 E_s(\omega) = n(\omega) B_s(\omega)$. In addition, the energy transported by the signal field through a surface $z = \text{constant}$ would be

$$\int_{\beta_s} \frac{d\omega}{2\pi} \hbar\omega a_s^\dagger(\omega) a_s(\omega)$$

[the group-velocity factor in Eq (2.20b) is included to ensure this form]. Since the nonlinearity is small, we ignore the energy stored in the nonlinear polarization; hence we can write the total energy transported by the signal field through a surface $z = \text{constant}$ in the nonlinear medium as

$$\int_{\beta_s} \frac{d\omega}{2\pi} \hbar\omega a_s^\dagger(\omega,z) a_s(\omega,z) .$$

Thus the operators $a_s(\omega,z)$ are Fourier components normalized to be in photon units.

These considerations show that if there are no reflections at the input and output surfaces (perfect antireflection coatings), then appropriate boundary conditions are

$$a_s(\omega,0) = a_{\text{in}}(\omega) , \quad a_{\text{out}}(\omega) = a_s(\omega,L) . \tag{2.21}$$

A priori one does not know the commutators of the Fourier components $a_s(\omega,z)$, because knowing them would require knowing the nonequal-time field commutators. Nonetheless, in this simple case of plane waves propagating in one direction with no reflections, the above boundary conditions specify the commutators for $a_s(\omega,0)$ and $a_s^\dagger(\omega',0)$ and also the commutators for $a_s(\omega,L)$ and $a_s^\dagger(\omega',L)$. Further, since the output boundary could be

put at any value of z, one in fact knows the equal-position commutators for any value of z:

$$[a_s(\omega,z),a_s^{\dagger}(\omega',z)]=2\pi\delta(\omega-\omega') . \tag{2.22}$$

Besides the signal field one also needs the pump field. Inside the medium we expand the pump's magnetic field operator as

$$B_p^{(+)}=\int_{\beta_p}\frac{d\omega}{2\pi}B_p(\omega,z)e^{i(k_\omega z-\omega t)} , \quad k_0=\omega n_0/c , \quad 0\le z\le L , \tag{2.23a}$$

$$B_p(\omega,z)=\frac{1}{2}iA_p e^{i\phi_p}2\pi\delta(\omega-\Omega_p)+\left[\frac{2\pi n_0\hbar\omega}{c\sigma}\right]^{1/2}a_p(\omega,z) . \tag{2.23b}$$

Here the integral runs over a bandwidth β_p about Ω_p, which contains all relevant pump frequencies. The first term in $B_p(\omega,z)$ is the strong mean pump field, and the second term represents fluctuations about the mean. Considerations identical to those for the signal field show that $a_p(\omega,0)$ and $a_p(\omega,L)$ are input and output annihilation operators at frequency ω. Throughout our analysis we assume that, aside from the strong excitation at frequency Ω_p, the input pump field is in the vacuum state.

We would like to include in our description absorption and dispersion in the signal field, but there is a difficulty in doing so. The equations that we use to describe the nonlinearity are an operator version of the macroscopic Maxwell equations, which are the Heisenberg equations derived from an appropriate Hamiltonian. It is difficult to include losses and dispersion in such a Hamiltonian formalism.[13] Therefore, we separate the losses and dispersion from the nonlinearity by using a trick (Fig. 2). Suppose that we have managed to propagate the signal and pump fields to position z in the medium and we wish to propagate them a further small distance Δz. We replace the actual medium between z and $z+\Delta z$ by a beam splitter followed by a slab of *ideal*

nonlinear medium, which has no absorption and no dispersion. The reflectivity of the beam splitter accounts for losses, and frequency-dependent phase shifts at the beam splitter introduce dispersion. The ideal nonlinear medium has uniform index of refraction n_0 and nonlinear susceptibility $\chi^{(2)}$.

The problem that must be solved is to relate the fields entering the actual medium at $z+\Delta z$, i.e., the Fourier components $a_s(\omega,z+\Delta z)e^{ik(z+\Delta z)}$ and $a_p(\omega,z+\Delta z)e^{ik_0(z+\Delta z)}$, to the fields leaving the actual medium at z, i.e., the Fourier components $a_s(\omega,z)e^{ikz}$ and $a_p(\omega,z)e^{ik_0z}$ (Fig. 2). To do this we need to know how to propagate the fields through the beam splitter and the ideal nonlinear medium.

As a first step we need to describe the fields within the ideal nonlinear medium. We denote these fields by a subscript 0, and we write each field operator as a sum of a signal field and a pump field. For example, the positive-frequency part of the magnetic field operator within the ideal nonlinear medium is

$$B_0^{(+)} = B_{0s}^{(+)} + B_{0p}^{(+)} . \tag{2.24}$$

The signal and pump fields are written in terms of temporal Fourier transforms:

$$B_{0s}^{(+)} = \int_{\beta_s} \frac{d\omega}{2\pi} B_{0s}(\omega,\xi) e^{i(k_0\xi-\omega t)} , \quad k_0 = \omega n_0/c , \tag{2.25a}$$

$$B_{0s}(\omega,\xi) = \left[\frac{2\pi n_0 \hbar\omega}{c\sigma}\right]^{1/2} a_{0s}(\omega,\xi) , \tag{2.25b}$$

$$B_{0p}^{(+)} = \int_{\beta_p} \frac{d\omega}{2\pi} B_{0p}(\omega,\xi) e^{i(k_0\xi-\omega t)} , \tag{2.26a}$$

$$B_{0p}(\omega,\xi) = \frac{1}{2} iA_p e^{i\phi_p} 2\pi\delta(\omega-\Omega_p) + \left[\frac{2\pi n_0 \hbar\omega}{c\sigma}\right]^{1/2} a_{0p}(\omega,\xi) \tag{2.26b}$$

($z \le \xi \le z+\Delta z$). Just as before, the operators $a_{0s}(\omega,\xi)$ and $a_{0p}(\omega,\xi)$ give the energy

transported in photon units, so it is appropriate to impose boundary conditions in terms of them.

The beam splitter transforms the fields that leave the actual medium at z before they reach the slab of ideal medium. Since the beam splitter has no effect on the pump field, the appropriate transformation at pump frequencies is

$$a_{0p}(\omega,z)=a_p(\omega,z)\,. \tag{2.27}$$

At signal frequencies the beam splitter has frequency-dependent reflectivity $\gamma(\omega)\Delta z$, which thus becomes the loss in photon units at frequency ω within the slab Δz. In other words, $\gamma(\omega)$ is the absorption coefficient (loss per unit length) of the actual medium. To conserve energy (or to preserve unitarity), the beam splitter must have a second input port, into which propagates a free field with annihilation operators $b_s(\omega)$, satisfying continuum commutation relations

$$[b_s(\omega),b_s^{\dagger}(\omega')]=2\pi\delta(\omega-\omega')\,. \tag{2.28}$$

This auxiliary signal field accounts for fluctuations associated with absorption; it is assumed to be in the vacuum state. The transformation law for the beam splitter at signal frequencies is

$$a_{0s}(\omega,z)e^{ik_0z}=e^{i\omega\Delta n(\omega)\Delta z/c}\{[1-\gamma(\omega)\Delta z]^{1/2}a_s(\omega,z)e^{ikz}+[\gamma(\omega)\Delta z]^{1/2}b_s(\omega)e^{ikz}\}\,. \tag{2.29}$$

The phase factors e^{ikz} and e^{ik_0z} are included so as to match the phase of the field leaving the actual medium to the phase of the field entering the ideal medium. The frequency-dependent phase shift at the beam splitter, $\omega\Delta n(\omega)\Delta z/c$, where $\Delta n(\omega)\equiv n(\omega)-n_0$, is simply the additional phase shift required to account for dispersion in the actual medium within the slab Δz.

It is useful in what follows to write $b_s(\omega)$ as an integral over a continuum of contributions within the slab Δz:

$$b_s(\omega)=(\Delta z)^{-1/2}\int_z^{z+\Delta z} d\xi\, b_s(\omega,\xi)\,. \tag{2.30}$$

The operators $b_s(\omega,\xi)$ obey the commutation relations

$$[b_s(\omega,\xi),b_s^{\dagger}(\omega',\xi')]=2\pi\delta(\omega-\omega')\delta(\xi-\xi')\,. \tag{2.31}$$

At the far end of the slab, the appropriate boundary conditions to get back into the actual medium are

$$a_p(\omega,z+\Delta z)=a_{0p}(\omega,z+\Delta z)\,, \tag{2.32}$$

$$a_s(\omega,z+\Delta z)e^{ik(z+\Delta z)}=a_{0s}(\omega,z+\Delta z)e^{ik_0(z+\Delta z)}\,. \tag{2.33}$$

Just as above, the phase factors in Eq. (2.33) match the phase of the field leaving the ideal medium to the phase of the field entering the actual medium.

What remains now is to propagate the field through the slab of ideal nonlinear medium. If we describe the nonlinearity by a susceptibility $\chi^{(2)}$, then the Heisenberg equations for a lossless, dispersionless nonlinear medium are simply an operator version of the macroscopic Maxwell equations, supplemented by a constitutive relation.[13] The two important Maxwell equations are $c^{-1}\partial D_{0q}^{(+)}/\partial t=-\partial B_{0q}^{(+)}/\partial\xi$ and $\partial E_{0q}^{(+)}/\partial\xi=-c^{-1}\partial B_{0q}^{(+)}/\partial t$, where q can stand for either s or p. We choose to write a constitutive relation for the electric field in terms of the displacement field,[13] rather than the usual relation for the displacement field in terms of the electric field. Thus we use a nonlinear susceptibility $\eta^{(2)}=n_0^{-6}\chi^{(2)}$. Decomposed in terms of signal and pump fields, the constitutive relation becomes

$$E_{0s}^{(+)} = n_0^{-2} D_{0s}^{(+)} - 8\pi\eta^{(2)} D_{0p}^{(+)} D_{0s}^{(-)}, \tag{2.34a}$$

$$E_{0p}^{(+)} = n_0^{-2} D_{0p}^{(+)} - 4\pi\eta^{(2)} [D_{0s}^{(+)}]^2 . \tag{2.34b}$$

By plugging the Fourier expansions [Eqs. (2.25) and (2.26)] into the Maxwell equations and the constitutive relation and by keeping only the highest-order terms in $\alpha_0 \ll 1$ and $\alpha_0 / \mathcal{A}_p \ll \alpha_0$, we find the following two spatial propagation equations: (i) a signal equation,

$$\frac{da_{0s}(\omega,\xi)}{d\xi} = -g_0 \left[\frac{\omega(\Omega_p - \omega)}{\Omega^2} \right]^{1/2} e^{2i\phi} a_{0s}^{\dagger}(\Omega_p - \omega, \xi)$$

$$+ i \frac{g_0}{\mathcal{A}_p} \int_{\beta_p} \frac{d\omega'}{2\pi} \left[\frac{\omega\omega'(\omega' - \omega)}{\Omega^2 \Omega_p} \right]^{1/2} \frac{a_{0p}(\omega', \xi)}{(\Delta_p / 2\pi)^{1/2}} a_{0s}^{\dagger}(\omega' - \omega, \xi), \tag{2.35a}$$

and (ii) a pump equation,

$$\frac{da_{0p}(\omega,\xi)}{d\xi} = \frac{i}{2} \frac{g_0}{\mathcal{A}_p} \int_{\beta_p} \frac{d\omega'}{2\pi} \left[\frac{\omega\omega'(\omega - \omega')}{\Omega^2 \Omega_p} \right]^{1/2} \frac{a_{0s}(\omega', \xi) a_{0s}(\omega - \omega', \xi)}{(\Delta_p / 2\pi)^{1/2}} . \tag{2.35b}$$

The first term in the signal equation is the primary effect of the parametric nonlinearity. It is the standard nonlinear coupling, mediated by the pump at frequency Ω_p, between signal frequencies $\omega = \Omega + \varepsilon$ and $\Omega_p - \omega = \Omega - \varepsilon$. The second term is an integral over equivalent couplings mediated by initially unexcited pump frequencies ω' within the bandwidth β_p; it includes the effects of pump quantum fluctuations. The pump equation describes an integral over nonlinear couplings between a pump frequency ω and signal frequencies ω' and $\omega - \omega'$; it includes, for example, the effects of pump depletion.

Equations (2.35) are the desired equations for propagation through the slab of ideal nonlinear medium. If we assume that the slab is sufficiently thin that $g_0 \Delta z \ll 1$, then we can approximate the solutions of Eqs. (2.35) as

$$a_{0s}(\omega,z+\Delta z)=a_{0s}(\omega,z)+\left[\frac{da_{0s}(\omega,\xi)}{d\xi}\right]_{\xi=z}\Delta z\ , \tag{2.36a}$$

$$a_{0p}(\omega,z+\Delta z)=a_{0p}(\omega,z)+\left[\frac{da_{0p}(\omega,\xi)}{d\xi}\right]_{\xi=z}\Delta z\ . \tag{2.36b}$$

If we further assume that $\gamma(\omega)\Delta z \ll 1$ and $\omega\Delta n(\omega)\Delta z/c \ll 1$ and linearize in these quantities, we can combine Eqs. (2.27), (2.29), (2.32), (2.33), (2.35), and (2.36) to relate the fields entering the actual medium at $z+\Delta z$ to the fields leaving the actual medium at z. By taking the limit $\Delta z \to 0$ and simultaneously introducing the operators $b_s(\omega,\xi)$ of Eq. (2.30), we can rewrite these relations as two spatial differential equations: (i) a signal equation,

$$\begin{aligned}\frac{da_s(\omega,z)}{dz} &= -\frac{1}{2}\gamma(\omega)a_s(\omega,z)\\ &\quad -g_0\left[\frac{\omega(\Omega_p-\omega)}{\Omega^2}\right]^{1/2} e^{2i\phi}e^{i\Delta K(\Omega_p,\omega)z}a_s^{\dagger}(\Omega_p-\omega,z)\\ &\quad +[\gamma(\omega)]^{1/2}b_s(\omega,z)\\ &\quad +i\frac{g_0}{A_p}\int_{\beta_p}\frac{d\omega'}{2\pi}\left[\frac{\omega\omega'(\omega'-\omega)}{\Omega^2\Omega_p}\right]^{1/2} e^{i\Delta K(\omega',\omega)z}\frac{a_p(\omega',z)}{(\Delta_p/2\pi)^{1/2}}a_s^{\dagger}(\omega'-\omega,z)\ ,\end{aligned} \tag{2.37a}$$

and (ii) a pump equation,

$$\frac{da_p(\omega,z)}{dz}=\frac{i}{2}\frac{g_0}{A_p}\int_{\beta_s}\frac{d\omega'}{2\pi}\left[\frac{\omega\omega'(\omega-\omega')}{\Omega^2\Omega_p}\right]^{1/2} e^{-i\Delta K(\omega,\omega')z}\frac{a_s(\omega',z)a_s(\omega-\omega',z)}{(\Delta_p/2\pi)^{1/2}}\ . \tag{2.37b}$$

These two equations are the spatial Langevin equations for our model of a DPA. The quantity

$$\Delta K(\omega',\omega) \equiv \frac{\omega' n_0}{c} - k(\omega) - k(\omega'-\omega) = -\frac{\omega \Delta n(\omega)}{c} - \frac{(\omega'-\omega)\Delta n(\omega'-\omega)}{c} \tag{2.38}$$

characterizes the phase mismatching between a pump frequency ω' and signal frequencies ω and $\omega'-\omega$.

The first term in the signal equation (2.37a) describes attenuation that is due to absorption, and the third term represents the fluctuations associated with absorption. The second and fourth terms are a consequence of the parametric nonlinearity; they are the same as the equivalent terms in the signal equation (2.35a) for an ideal medium, except for the presence of phase-mismatching factors. The characteristic size of the pump-fluctuation term is $1/\mathcal{A}_p$ times the size of the primary nonlinear term. The pump equation (2.37b) differs from the pump equation (2.35b) for an ideal medium because of a phase mismatching-factor.

The spatial Langevin equations (2.37) display clearly the classical-pump limit: $g_0 = \text{constant}$, $\mathcal{A}_p \to \infty$. In this limit the pump-fluctuation term in the signal equation goes away, and the pump is decoupled from the signal field.

It is instructive at this point to contrast our approach with the wave-packet formalism developed by Tucker and Walls,[12] which has been applied to a DPA by Lane *et al.*[19] In our approach, because we work in the temporal Fourier domain, frequency matching is enforced exactly. Just as in the usual classical analysis, phase mismatching appears as a mismatch $\Delta K(\omega',\omega)$ between wave numbers whose corresponding frequencies match exactly. Tucker and Walls idealize to an infinitely long medium so that wave-number matching is enforced exactly. In their formalism phase mismatching appears as a mismatch between frequencies whose corresponding wave numbers match exactly.

Before going further, we make a series of simplifications. We assume that the absorption coefficient is constant over the signal bandwidth, i.e., $\gamma(\omega) = \gamma$; we ignore the

variation of the square-root-of-frequency factors in Eqs. (2.37); and we choose the pump phase to be $\phi_p = 2\phi = 0$. With these assumptions it is convenient to rewrite Eqs. (2.37) in terms of deviations of signal and pump frequencies from Ω and Ω_p:

$$\frac{da_s(\Omega+\varepsilon,z)}{dz} = -\frac{1}{2}\gamma a_s(\Omega+\varepsilon,z) - g_0 e^{i\Delta k(\varepsilon)z} a_s^{\dagger}(\Omega-\varepsilon,z) + \gamma^{1/2} b_s(\Omega+\varepsilon,z) + P(\varepsilon,z), \quad (2.39a)$$

$$\frac{da_p(\Omega_p+\varepsilon,z)}{dz} = \frac{i}{2}\frac{g_0}{\mathcal{A}_p}\int_{-\infty}^{\infty}\frac{d\varepsilon'}{2\pi} e^{-i\Delta k(\varepsilon',\varepsilon'-\varepsilon)z}\frac{a_s(\Omega+\varepsilon',z)a_s(\Omega+\varepsilon-\varepsilon',z)}{(\Delta_p/2\pi)^{1/2}}. \quad (2.39b)$$

Here the pump-fluctuation term is given by

$$P(\varepsilon,z) \equiv i\frac{g_0}{\mathcal{A}_p}\int_{-\infty}^{\infty}\frac{d\varepsilon'}{2\pi} e^{i\Delta k(\varepsilon,\varepsilon')z}\frac{a_p(\Omega_p+\varepsilon-\varepsilon',z)}{(\Delta_p/2\pi)^{1/2}} a_s^{\dagger}(\Omega-\varepsilon',z), \quad (2.39c)$$

and the phase mismatching has been redefined in terms of

$$\Delta k(\varepsilon,\varepsilon') \equiv \Delta K(\Omega_p+\varepsilon-\varepsilon',\Omega+\varepsilon) = -\frac{(\Omega+\varepsilon)\Delta n(\Omega+\varepsilon)}{c} - \frac{(\Omega-\varepsilon')\Delta n(\Omega-\varepsilon')}{c}, \quad (2.40a)$$

$$\Delta k(\varepsilon) \equiv \Delta k(\varepsilon,\varepsilon) = -\frac{(\Omega+\varepsilon)\Delta n(\Omega+\varepsilon)}{c} - \frac{(\Omega-\varepsilon)\Delta n(\Omega-\varepsilon)}{c} \quad (2.40b)$$

[cf. Eq. (2.4)]. In Eqs. (2.39) we formally extend the integration limits to $\pm\infty$, anticipating that in the calculations of Section 3D, the phase-mismatching factors provide a natural cutoff for the integrals.

We now introduce quadrature-phase amplitudes[7,16,20] for the signal field, defined by

$$\alpha_1(\varepsilon,z) \equiv \frac{1}{2}[a_s(\Omega+\varepsilon,z) + a_s^{\dagger}(\Omega-\varepsilon,z)], \quad (2.41a)$$

$$\alpha_2(\varepsilon,z) \equiv -\frac{i}{2}[a_s(\Omega+\varepsilon,z) - a_s^{\dagger}(\Omega-\varepsilon,z)]. \quad (2.41b)$$

The quadrature-phase amplitudes are the Fourier components of the quadrature phases of the signal field, defined with respect to frequency Ω. Evaluated at $z = L$, they contain the spectral information about the squeezing produced by the DPA. They are defined here with respect to a phase such that when $\phi_p = 0$, the α_1 quadrature shows maximum squeezing near degeneracy. The frequency argument ε of a quadrature-phase amplitude is always assumed to be nonnegative.

Suppose that the output of the DPA is detected by a balanced homodyne detector.[21,22] If the detector is ideal, the quadrature-phase amplitudes (multiplied by an appropriate factor) give the Fourier components of the differenced photocurrent at the output of the detector.[7,23] Hence they provide the spectrum of the differenced photocurrent. Specifically, if the phase of the local oscillator powering the homodyne detector is chosen so as to display maximum squeezing for the phase-matched frequencies near degeneracy, then $\alpha_1(\varepsilon)$ gives the Fourier component at rf frequency ε of the differenced photocurrent.

We find it useful to introduce another set of quadrature-phase amplitudes,

$$\bar{\alpha}_1(\varepsilon,z) \equiv \frac{1}{2}[e^{-i\Delta k(\varepsilon)z/2} a_s(\Omega+\varepsilon,z) + e^{i\Delta k(\varepsilon)z/2} a_s^\dagger(\Omega-\varepsilon,z)] , \tag{2.42a}$$

$$\bar{\alpha}_2(\varepsilon,z) \equiv -\frac{i}{2}[e^{-i\Delta k(\varepsilon)z/2} a_s(\Omega+\varepsilon,z) - e^{i\Delta k(\varepsilon)z/2} a_s^\dagger(\Omega-\varepsilon,z)] , \tag{2.42b}$$

which are related to the original quadrature-phase amplitudes by a frequency- and position-dependent rotation:

$$\bar{\alpha}_1(\varepsilon,z) = \alpha_1(\varepsilon,z)\cos[\Delta k(\varepsilon)z/2] + \alpha_2(\varepsilon,z)\sin[\Delta k(\varepsilon)z/2] , \tag{2.43a}$$

$$\bar{\alpha}_2(\varepsilon,z) = -\alpha_1(\varepsilon,z)\sin[\Delta k(\varepsilon)z/2] + \alpha_2(\varepsilon,z)\cos[\Delta k(\varepsilon)z/2] . \tag{2.43b}$$

Evaluated at $z=L$, these barred quadrature-phase amplitudes also contain the spectral information about the squeezing produced by the DPA, but with some of the effects of phase mismatching removed. To detect these barred quadrature-phase amplitudes, one would have to vary the phase of the local oscillator in a homodyne detector as a function of rf frequency ε.

We now put the signal equation (2.39a) into the form that we use in Section 3 by writing it in terms of the barred quadrature-phase amplitudes:

$$\frac{d\bar{\alpha}_1(\varepsilon,z)}{dz} = -(g_0+\frac{1}{2}\gamma)\bar{\alpha}_1(\varepsilon,z)+\frac{1}{2}\Delta k(\varepsilon)\bar{\alpha}_2(\varepsilon,z)+\gamma^{1/2}\bar{\beta}_1(\varepsilon,z)+\bar{P}_1(\varepsilon,z)\,, \tag{2.44a}$$

$$\frac{d\bar{\alpha}_2(\varepsilon,z)}{dz} = +(g_0-\frac{1}{2}\gamma)\bar{\alpha}_2(\varepsilon,z)-\frac{1}{2}\Delta k(\varepsilon)\bar{\alpha}_1(\varepsilon,z)+\gamma^{1/2}\bar{\beta}_2(\varepsilon,z)+\bar{P}_2(\varepsilon,z)\,. \tag{2.44b}$$

Here

$$\bar{\beta}_1(\varepsilon,z)\equiv\frac{1}{2}[e^{-i\Delta k(\varepsilon)z/2}b_s(\Omega+\varepsilon,z)+e^{i\Delta k(\varepsilon)z/2}b_s^{\dagger}(\Omega-\varepsilon,z)]\,, \tag{2.45a}$$

$$\bar{\beta}_2(\varepsilon,z)\equiv-\frac{i}{2}[e^{-i\Delta k(\varepsilon)z/2}b_s(\Omega+\varepsilon,z)-e^{i\Delta k(\varepsilon)z/2}b_s^{\dagger}(\Omega-\varepsilon,z)] \tag{2.45b}$$

are quadrature-phase amplitudes for the fluctuations associated with absorption, and the pump-fluctuation terms are defined by

$$\bar{P}_1(\varepsilon,z)\equiv\frac{1}{2}[e^{-i\Delta k(\varepsilon)z/2}P(+\varepsilon,z)+e^{i\Delta k(\varepsilon)z/2}P^{\dagger}(-\varepsilon,z)]\,, \tag{2.46a}$$

$$\bar{P}_2(\varepsilon,z)\equiv-\frac{i}{2}[e^{-i\Delta k(\varepsilon)z/2}P(+\varepsilon,z)-e^{i\Delta k(\varepsilon)z/2}P^{\dagger}(-\varepsilon,z)]\,. \tag{2.46b}$$

Equations (2.44) show that the primary effect of the parametric interaction is to deamplify (squeeze) the $\bar{\alpha}_1$ quadrature and to amplify the $\bar{\alpha}_2$ quadrature. This primary effect

is degraded by absorption and phase mismatching.

3. MODEL PREDICTIONS FOR SQUEEZING SPECTRA

A. Solution of signal equations

We can write a formal Green function solution of the signal equations (2.44) for the barred quadrature-phase amplitudes:

$$\bar{\alpha}_m(\varepsilon,z)=\sum_{n=1,2}\left\{\bar{G}_{mn}(\varepsilon,z)\bar{\alpha}_n(\varepsilon,0)\right.$$

$$\left.+\int_0^z dz'\,\bar{G}_{mn}(\varepsilon,z-z')[\gamma^{1/2}\bar{\beta}_n(\varepsilon,z')+\bar{P}_n(\varepsilon,z')]\right\},\quad m=1,2\,. \tag{3.1}$$

Here the Green function matrix is given by

$$\bar{G}_{11}(\varepsilon,z)\equiv e^{-\gamma z/2}\frac{e-gz-\mu^2e^{gz}}{1-\mu^2}\,, \tag{3.2a}$$

$$\bar{G}_{22}(\varepsilon,z)\equiv e^{-\gamma z/2}\frac{e^{gz}-\mu^2e^{-gz}}{1-\mu^2}\,, \tag{3.2b}$$

$$\bar{G}_{12}(\varepsilon,z)=-\bar{G}_{21}(\varepsilon,z)=\mu e^{-\gamma z/2}\frac{e^{gz}-e^{-gz}}{1-\mu^2}\,, \tag{3.2c}$$

where

$$g=g(\varepsilon)\equiv\{g_0^2-[\Delta k(\varepsilon)/2]^2\}^{1/2}\,, \tag{3.3a}$$

$$\mu=\mu(\varepsilon)\equiv\frac{\Delta k(\varepsilon)/2}{g_0+g(\varepsilon)}\,. \tag{3.3b}$$

The Green function matrix represents the familiar classical solution for a DPA with

phase mismatching and absorption. Of course, only in the classical-pump limit, where the pump-fluctuation terms $\bar{P}_n$ vanish, does Eq. (3.1) give an actual solution of the signal equations. In the presence of pump fluctuations, Eq. (3.1) is an integral equation, which can be used as the starting point for an iterative solution procedure.

If ε lies well within the phase-matched bandwidth $\Delta/2\pi$ [Eq. (2.8)], then $\Delta k(\varepsilon) \to 0$. Thus the barred quadrature-phase amplitudes become the same as the unbarred quadrature-phase amplitudes and, in addition, $g(\varepsilon) \to g_0$ and $\mu(\varepsilon) \to 0$, so that the Green function matrix becomes diagonal, with the diagonal elements given by

$$\bar{G}_{11}(\varepsilon,z) = e^{-\gamma z/2} e^{-g_0 z} , \quad \bar{G}_{22}(\varepsilon,z) = e^{-\gamma z/2} e^{g_0 z} . \tag{3.4}$$

This is the classical solution for a phase-matched DPA with absorption; the parametric interaction deamplifies (squeezes) the α_1 quadrature and amplifies the α_2 quadrature.

B. Squeezing spectrum

Our goal is to calculate squeezing spectra for the light generated by our model DPA. Spectral information about the squeezing produced by the DPA is contained in the spectral-density matrix[7,16,20,23] $S_{mn}(\varepsilon)$ of the output quadrature-phase amplitudes $\alpha_m(\varepsilon,L)$. The spectral-density matrix arises from second-order noise moments of the quadrature-phase amplitudes:

$$<\Delta\alpha_m^\dagger(\varepsilon',L)\Delta\alpha_n(\varepsilon,L)>_{\text{sym}} = \pi S_{mn}(\varepsilon)\delta(\varepsilon-\varepsilon') , \quad m,n = 1,2 . \tag{3.5}$$

Here, for any operator O, $\Delta O \equiv O - <O>$, and sym denotes a symmetrized product. A similar spectral-density matrix can be defined for the barred quadrature-phase amplitudes:

$$<\Delta\bar{\alpha}_m^\dagger(\varepsilon',L)\Delta\bar{\alpha}_n(\varepsilon,L)>_{\text{sym}} = \pi\bar{S}_{mn}(\varepsilon)\delta(\varepsilon-\varepsilon') . \tag{3.6}$$

These two spectral-density matrices are related by

$$S_{11}=\bar{S}_{11}\cos^2(\Delta kL/2)+\bar{S}_{22}\sin^2(\Delta kL/2)$$

$$-(\bar{S}_{12}+\bar{S}_{21})\cos(\Delta kL/2)\sin(\Delta kL/2)\,, \tag{3.7a}$$

$$S_{22}=\bar{S}_{11}\sin^2(\Delta kL/2)+\bar{S}_{22}\cos^2(\Delta kL/2)$$

$$+(\bar{S}_{12}+\bar{S}_{21})\cos(\Delta kL/2)\sin(\Delta kL/2)\,, \tag{3.7b}$$

$$S_{12}=S_{21}^{*}=(\bar{S}_{11}-\bar{S}_{22})\cos(\Delta kL/2)\sin(\Delta kL/2)$$

$$+\bar{S}_{12}\cos^2(\Delta kL/2)-\bar{S}_{21}\sin^2(\Delta kL/2)\,, \tag{3.7c}$$

where $\Delta k=\Delta k(\varepsilon)$.

We are primarily interested in the spectrum of the squeezed quadrature, i.e., S_{11} or $\bar{S}_{11}$. As noted in Section 2C, $S_{11}(\varepsilon)$ gives the spectrum of the differenced photocurrent in an ideal balanced homodyne detector, when the phase of the local oscillator is chosen so as to display maximum squeezing for the phase-matched frequencies near degeneracy. The spectrum $\bar{S}_{11}(\varepsilon)$ would apply if one suitably varied the phase of the local oscillator as a function of rf frequency ε.

We must also specify the spectra of the input signal field and the auxiliary field associated with absorption. We assume that both are in the vacuum state, which means that their first moments vanish and that their second moments are given by

$$<\alpha_m^{\dagger}(\varepsilon',0)\alpha_n(\varepsilon,0)>_{\mathrm{sym}}=<\bar{\alpha}_m^{\dagger}(\varepsilon',0)\bar{\alpha}_n(\varepsilon,0)>_{\mathrm{sym}}=\frac{1}{2}\pi\delta_{mn}\,\delta(\varepsilon-\varepsilon')\,, \tag{3.8a}$$

$$<\bar{\beta}_m^{\dagger}(\varepsilon',z')\bar{\beta}_n(\varepsilon,z)>_{\mathrm{sym}}=\frac{1}{2}\pi\delta_{mn}\,\delta(\varepsilon-\varepsilon')\delta(z-z')\,. \tag{3.8b}$$

Recall also that we assume that the input pump field is in the vacuum state, aside from the strong excitation at frequency Ω_p.

In the classical-pump limit ($\bar{P}_m = 0$), it is straightforward to calculate the output spectral density matrix $\bar{S}_{mn}(\varepsilon)$ in terms of the Green function matrix:

$$\bar{S}_{mn}(\varepsilon) = \frac{1}{2} \sum_{p=1,2} \left\{ \bar{G}^*_{mp}(\varepsilon, L) \bar{G}_{np}(\varepsilon, L) + \gamma \int_0^L dz \, \bar{G}^*_{mp}(\varepsilon, L-z) \bar{G}_{np}(\varepsilon, L-z) \right\} . \tag{3.9}$$

The first term in this spectral-density matrix comes from the vacuum fluctuations in the input signal field, processed through the parametric interaction; this first term includes phase mismatching and attenuation that is due to absorption. The second term arises from the fluctuations associated with absorption. It is an integral over fluctuations injected at positions z within the medium; after a fluctuation is injected at z, it is processed through the remainder of the nonlinear medium between z and L.

If we assume further that ε lies well within the phase-matched bandwidth $\Delta/2\pi$, then $\bar{S}_{mn}(\varepsilon) = S_{mn}(\varepsilon)$ becomes diagonal, with the diagonal elements given by

$$\bar{S}_{11}(\varepsilon) = S_{11}(\varepsilon) = \frac{1}{2} \frac{\gamma + 2g_0 e^{-(\gamma + 2g_0)L}}{\gamma + 2g_0} , \tag{3.10a}$$

$$\bar{S}_{22}(\varepsilon) = S_{22}(\varepsilon) = \frac{1}{2} \frac{\gamma - 2g_0 e^{-(\gamma - 2g_0)L}}{\gamma - 2g_0} . \tag{3.10b}$$

This is the familiar situation of squeezing competing with losses. In the absence of absorption, Eqs. (3.10) reduce further to the spectra for ideal squeezing:

$$S_{11}(\varepsilon) = \frac{1}{2} e^{-2g_0 L} , \quad S_{22}(\varepsilon) = \frac{1}{2} e^{2g_0 L} . \tag{3.11}$$

C. Phase mismatching

The preceding analysis can be applied immediately to investigate the effect of phase mismatching on the squeezing spectrum. To isolate the phase-mismatching effect, we assume that there is no absorption ($\gamma=0$) and that the pump is classical ($\bar{P}_m=0$). Then the spectrum of the $\bar{\alpha}_1$ quadrature becomes

$$\bar{S}_{11}(\varepsilon)=\frac{1}{2}[|\bar{G}_{11}(\varepsilon,L)|^2+|\bar{G}_{12}(\varepsilon,L)|^2]\,. \tag{3.12}$$

The significance of phase mismatching for $\bar{S}_{11}(\varepsilon)$ is quantified by the dimensionless parameter

$$\Delta k(\varepsilon)/2g_0=-(p/|p|)(\varepsilon/\varepsilon_2)^2 \tag{3.13}$$

[cf. Eq. (2.7b)]. We assume that $|\Delta k(\varepsilon)/2g_0|\ll 1$, i.e., $\varepsilon\ll\varepsilon_2$, and we then expand in $|\Delta k(\varepsilon)/2g_0|$, keeping only the largest corrections to ideal squeezing. Under these circumstances, one sees that $g=g_0$ and

$$\mu(\varepsilon)=\Delta k(\varepsilon)/4g_0=-\frac{1}{2}(p/|p|)(\varepsilon/\varepsilon_2)^2\,. \tag{3.14}$$

When there is at least a moderate amount of squeezing, i.e., g_0L is somewhat larger than 1, the largest correction to ideal squeezing is the one that grows fastest with g_0L. This means that we can approximate

$$\bar{G}_{11}(\varepsilon,L)=e^{-g_0L}\,,\quad \bar{G}_{12}(\varepsilon,L)=\mu(\varepsilon)e^{g_0L}\,, \tag{3.15}$$

which leads to a squeezing spectrum

$$\bar{S}_{11}(\varepsilon)=\frac{1}{2}\left\{e^{-2g_0L}+[\mu(\varepsilon)]^2e^{2g_0L}\right\}=\frac{1}{2}\left[e^{-2g_0L}+\frac{1}{4}(\varepsilon/\varepsilon_2)^4e^{2g_0L}\right]\,. \tag{3.16}$$

The dominant correction to ideal squeezing arises because phase mismatching feeds a fraction $|\mu(\varepsilon)|$ of the amplified quadrature into the squeezed quadrature. In order to neglect phase mismatching and have ideal squeezing in the spectrum $\bar{S}_{11}(\varepsilon)$, one requires

$$|\mu(\varepsilon)|e^{g_0L} \ll e^{-g_0L} \implies \varepsilon \ll 2^{1/2}\varepsilon_2 e^{-g_0L} . \tag{3.17}$$

To explore the effect of phase mismatching on the squeezing spectrum $S_{11}(\varepsilon)$, one needs to consider an additional dimensionless parameter

$$\Delta k(\varepsilon)L = -(p/|p|)(\varepsilon/\varepsilon_1)^2 \tag{3.18}$$

[cf. Eq. (2.7a)]. Assuming that $|\Delta k(\varepsilon)L| \ll 1$ and performing a similar analysis to find the largest correction to ideal squeezing, one finds

$$S_{11}(\varepsilon) = \frac{1}{2}\left\{ e^{-2g_0L} + \left[\mu(\varepsilon) - \frac{1}{2}\Delta k(\varepsilon)L \right]^2 e^{2g_0L} \right\} . \tag{3.19}$$

Equations (3.16) and (3.19) somewhat overstate the deleterious effects of phase mismatching.[24] A frequency-dependent rotation of the barred quadrature-phase amplitudes $\bar{\alpha}_1(\varepsilon,L)$ and $\bar{\alpha}_2(\varepsilon,L)$ [similar to the rotation of $\alpha_1(\varepsilon,L)$ and $\alpha_2(\varepsilon,L)$ in Eqs. (2.43)] by an appropriate angle $\theta(\varepsilon,L)$ diagonalizes the resulting spectral-density matrix $\tilde{S}_{mn}(\varepsilon)$. This choice of $\theta(\varepsilon,L)$ minimizes (maximizes) $\tilde{S}_{11}(\varepsilon)$ [$\tilde{S}_{22}(\varepsilon)$]. Keeping only the dominant correction to ideal squeezing for g_0L somewhat larger than 1 and for $\varepsilon \ll \varepsilon_2$, one finds that

$$\tilde{S}_{11}(\varepsilon) = \frac{1}{2}e^{-2g_0L}\{1 + 4[\mu(\varepsilon)]^2 g_0L\} = \frac{1}{2}e^{-2g_0L}[1 + (\varepsilon/\varepsilon_2)^4 g_0L] . \tag{3.20}$$

The dominant correction arises from the reduction in the nonlinear gain due to phase

mismatching [Eq. (3.3a)]. In order to ignore phase mismatching and achieve ideal squeezing in the spectrum $\tilde{S}_{11}(\varepsilon)$, one requires that

$$2|\mu(\varepsilon)|(g_0L)^{1/2} \ll 1 \implies \varepsilon \ll \varepsilon_2(g_0L)^{-1/4} . \tag{3.21}$$

Relation (3.21) imposes a much less stringent restriction on the radio frequency ε than does expression (3.17).

D. Pump quantum fluctuations

We turn now to an analysis of quantum fluctuations in the pump field. The starting point is the formal solution [Eq. (3.1)] for the squeezed quadrature $\bar{\alpha}_1(\varepsilon,L)$. To simplify the analysis and to highlight the effect of pump fluctuations, we assume there is no absorption ($\gamma=0$), and we assume that ε lies well within the region of perfect phase matching ($\varepsilon \ll \varepsilon_2 e^{-g_0 L}$). With these simplifications, we can write

$$\bar{G}_{1n}(\varepsilon,z) = \delta_{1n} e^{-g_0 z} , \tag{3.22}$$

and the formal solution becomes

$$\bar{\alpha}_1(\varepsilon,L) = e^{-g_0 L}\bar{\alpha}_1(\varepsilon,0) + \int_0^L dz\, e^{-g_0(L-z)}\bar{P}_1(\varepsilon,z) . \tag{3.23}$$

One can solve Eq. (3.23) by an iterative procedure in which the fundamental expansion parameter is $1/\mathcal{A}_p \ll 1$. The procedure is to evaluate $\bar{P}_1(\varepsilon,z)$ to progressively higher orders in $1/\mathcal{A}_p$ by plugging in progressively higher-order approximations to the signal and pump fields. Here we are interested only in the first-order correction to $\bar{\alpha}_1(\varepsilon,L)$, so we can evaluate $\bar{P}_1(\varepsilon,z)$ using the zero-order solutions for the signal and pump fields.

Furthermore, we are interested in the dominant effect of pump fluctuations when there is at least a moderate amount of squeezing, i.e., $g_0 L$ is somewhat larger than 1. In this case the dominant contribution to $\bar{P}_1$ comes from the amplified $\bar{\alpha}_2$ quadrature, so we can neglect the contribution to $\bar{P}_1$ from $\bar{\alpha}_1$.

With this final assumption in mind, we use Eqs. (2.46a), (2.39c), (2.40), and (2.42) to put $\bar{P}_1$ in the form

$$\bar{P}_1(\varepsilon,z)=\frac{1}{2}\frac{g_0}{\mathcal{A}_p}\int_0^\infty \frac{d\varepsilon'}{2\pi}\left[e^{i\Omega n'(\varepsilon'-\varepsilon)z/c}\,\frac{a_p(\Omega_p+\varepsilon-\varepsilon',z)+a_p^\dagger(\Omega_p-\varepsilon+\varepsilon',z)}{(\Delta_p/2\pi)^{1/2}}-\bar{\alpha}_2(\varepsilon',z)\right.$$

$$\left. +e^{-i\Omega n'(\varepsilon'+\varepsilon)z/c}\,\frac{a_p(\Omega_p+\varepsilon+\varepsilon',z)+a_p^\dagger(\Omega_p-\varepsilon-\varepsilon',z)}{(\Delta_p/2\pi)^{1/2}}-\bar{\alpha}_2^\dagger(\varepsilon',z)\right], \tag{3.24}$$

where we make explicit use of the Taylor expansion (2.5) for the index of refraction.

The next step is to substitute the zero-order solutions into Eq. (3.24). The zero-order solution for the pump is that the operators $a_p(\omega,z)=a_p(\omega)$ have no z dependence (decoupling from the signal), and the zero-order solution for $\bar{\alpha}_2(\varepsilon',z)$ is given by the first term in Eq. (3.1) with $\gamma=0$. This step taken, one then performs the integral over z in Eq. (3.23). Before proceeding, however, the form [Eq. (3.24)] for $\bar{P}_1(\varepsilon,z)$ permits a further dramatic simplification.

The phase mismatching factors conspire in Eq. (3.22) to introduce new oscillating phase factors $\exp[i\Omega n'(\varepsilon'-\varepsilon)z/c]$ and $\exp[-i\Omega n'(\varepsilon'+\varepsilon)z/c]$. Once the integral over z in Eq. (3.23) is done, these phase factors cut off the ε' integral in Eq. (3.24). The first phase factor cuts off the integral when ε' is sufficiently far from ε that the phase factor oscillates rapidly on the scale g_0^{-1} set by the nonlinear gain. Similarly, the second phase factor cuts off the integral when ε' is sufficiently far from $-\varepsilon$. The frequency scale of these

cutoffs is characterized by a frequency ε_3, defined by

$$\frac{\Omega|n'|\varepsilon_3/c}{2g_0}=1 \implies \varepsilon_3=2cg_0/\Omega|n'|\,. \tag{3.25}$$

Notice that ε_3 is typically somewhat smaller than ε_2 [Eq. (2.7b)]; indeed we assume that $\varepsilon_3 \ll \varepsilon_2 e^{-g_0 L}$.

Since by assumption ε lies well within the region of perfect phase matching, and since ε' in Eq. (3.24) is restricted to be within about a distance ε_3 of ε, we are entitled to use in Eq. (3.24) the perfectly phase-matched zero-order solution for $\bar{\alpha}_2(\varepsilon',z)$, i.e., $\bar{\alpha}_2(\varepsilon',z)=e^{g\alpha z}\bar{\alpha}_2(\varepsilon',0)$. Substituting the zero-order solutions into Eq. (3.24) and performing the integral over z in Eq. (3.23), one finds

$$\begin{aligned}\bar{\alpha}_1(\varepsilon,L)=&e^{-g_0 L}\bar{\alpha}_1(\varepsilon,0)\\ &+\frac{e^{g_0 L}}{4\mathcal{A}_p}\int_0^\infty\frac{d\varepsilon'}{2\pi}\left[\frac{e^{i\Omega n'(\varepsilon'-\varepsilon)L/c}}{1+i\dfrac{\Omega n'}{2cg_0}(\varepsilon'-\varepsilon)}\,\frac{a_p(\Omega_p+\varepsilon-\varepsilon')+a_p^\dagger(\Omega_p-\varepsilon+\varepsilon')}{(\Delta_p/2\pi)^{1/2}}-\bar{\alpha}_2(\varepsilon',0)\right.\\ &\left.+\frac{e^{-i\Omega n'(\varepsilon'+\varepsilon)L/c}}{1-i\dfrac{\Omega n'}{2cg_0}(\varepsilon'+\varepsilon)}\,\frac{a_p(\Omega_p+\varepsilon+\varepsilon')+a_p^\dagger(\Omega_p-\varepsilon-\varepsilon')}{(\Delta_p/2\pi)^{1/2}}-\bar{\alpha}_2^\dagger(\varepsilon',0)\right]\,.\end{aligned} \tag{3.26}$$

This equation is the basic result for the dominant effect of pump quantum fluctuations on the squeezed quadrature.

The form of Eq. (3.26) [or of Eq. (3.24)] confirms the heuristic argument given in Section 2B. The pump field can be decomposed into quadrature phases whose quadrature-phase amplitudes are

$$\alpha_{p1}(\varepsilon,z)\equiv\frac{1}{2}[a_p(\Omega_p+\varepsilon,z)+a_p^{\dagger}(\Omega_p-\varepsilon,z)]\,, \tag{3.27a}$$

$$\alpha_{p2}(\varepsilon,z)\equiv-\frac{i}{2}[a_p(\Omega_p+\varepsilon,z)-a_p^{\dagger}(\Omega_p-\varepsilon,z)]\,. \tag{3.27b}$$

When $\phi_p=0$, the strong mean pump field at frequency Ω_p has complex amplitude iA_p. Thus the α_{p2} quadrature represents fluctuations that are in phase with the strong mean field, i.e., pump amplitude fluctuations, and the α_{p1} quadrature represents fluctuations that are 90° out of phase with strong mean field, i.e., pump phase fluctuations. A glance at Eq. (3.26) shows that the dominant effect of pump quantum fluctuations comes from fluctuations in the α_{p1} quadrature—phase fluctuations—which feed noise from the amplified signal quadrature into the squeezed signal quadrature. The characteristic size of this effect is given by the factor $e^{g_0L}/4\mathcal{A}_p$ in front of the integral in Eq. (3.26) [cf. Eq. (2.9)]. All that remains now is to use the integral to determine the pump bandwidth $\Delta_p/2\pi$.

Substituting Eq. (3.26) into the expression (3.6), one finds a flat squeezing spectrum

$$\bar{S}_{11}(\varepsilon)=\frac{1}{2}\left[e^{-2g_0L}+\frac{e^{2g_0L}}{16\mathcal{A}_p^2}\right]\,,\quad \varepsilon\ll\varepsilon_2 e^{-g_0L}\,, \tag{3.28}$$

where the pump bandwidth is defined by

$$\frac{\Delta_p}{2\pi}\equiv\int_{-\infty}^{\infty}\frac{d\varepsilon}{2\pi}\,\frac{1}{1+(\varepsilon/\varepsilon_3)^2}=\frac{1}{2}\varepsilon_3=\frac{cg_0}{\Omega|n'|} \tag{3.29}$$

[cf. Eq. (2.17)]. As expected, the frequency ε_3, which comes ultimately from phase mismatching, provides a cutoff for the pump bandwidth.

One further point deserves mention. We have calculated the first-order correction to $\bar{\alpha}_1(\varepsilon,L)$ resulting from pump quantum fluctuations; this first-order correction goes as $1/\mathcal{A}_p$. Squared in calculating the spectral density, it produces a correction to the spectrum that goes as $1/\mathcal{A}_p^2$. The second-order term in $\bar{\alpha}_1(\varepsilon,L)$ due to pump fluctuations goes as $1/\mathcal{A}_p^2$. Multiplied by the zero-order solution $e^{-g_0 L}\bar{\alpha}_1(\varepsilon,0)$ in forming the spectral density, this second-order term also yields a correction to the spectrum that goes as $1/\mathcal{A}_p^2$. Why have we ignored this correction when it is formally of the same size as the effect we have calculated? Because one can convince oneself, either by tedious analysis or by clever insight, that the correction to the spectrum due to the second-order term does not grow as fast as $e^{2g_0 L}$. Hence, the correction we have calculated is the dominant effect when there is at least a moderate amount of squeezing.

REFERENCES

1. H. Takahasi, Adv. Commun. Syst. **1**, 227 (1965), especially Section XI.
2. E. Y. C. Lu, Lett. Nuovo Cimento **3**, 585 (1972).
3. D. Stoler, Phys. Rev. Lett. **33**, 1397 (1974).
4. R. G. Smith, in *Laser Handbook,* edited by F. T. Arecchi and E. O. Schulz-Dubois (North-Holland, Amsterdam, 1972), Vol. I, p. 837.
5. L.-A. Wu, H. J. Kimble, J. L. Hall, and H. Wu, Phys. Rev. Lett. **57**, 2520 (1986).
6. B. Yurke, Phys. Rev. A **29**, 408 (1984).
7. B. Yurke, Phys. Rev. A **32**, 300 (1985).
8. M. J. Collett and C. W. Gardiner, Phys. Rev. A **30**, 1386 (1984).
9. C. W. Gardiner and C. M. Savage, Opt. Commun. **50**, 173 (1984).
10. M. J. Collett and D. F. Walls, Phys. Rev. A **32**, 2887 (1985).
11. Y. R. Shen, Phys. Rev. **155**, 921 (1967).
12. J. Tucker and D. F. Walls, Phys. Rev. **178**, 2036 (1969).
13. M. Hillery and L. D. Mlodinow, Phys. Rev. A **30**, 1860 (1984).
14. M. Hillery and M. S. Zubairy, Phys. Rev. A **29**, 1275 (1984).
15. C. M. Caves, Phys. Rev. D **23**, 1693 (1981).
16. C. M. Caves and B. L. Schumaker, Phys. Rev. A **31**, 3068 (1985).
17. K. Wodkiewicz and M. S. Zubairy, Phys. Rev. A **27**, 2003 (1983).
18. G. Scharf and D. F. Walls, Opt. Commun. **50**, 245 (1984).

19. A. Lane, P. Tombesi, H. J. Carmichael, and D. F. Walls, Opt. Commun. **48**, 155 (1983).

20. C. M. Caves, Phys. Rev. D **26**, 1817 (1982).

21. H. P. Yuen and V. W. S. Chan, Opt. Lett. **8**, 177 (1983).

22. B. L. Schumaker, Opt. Lett. **9**, 189 (1984).

23. C. M. Caves and B. L. Schumaker, in *Quantum Optics IV,* edited by J. D. Harvey and D. F. Walls (Springer, Berlin, 1986), p. 20.

24. M. J. Potasek and B. Yurke, Phys. Rev. A **35**, 3974 (1987).

FIGURE CAPTIONS

Fig. 1. Effect of pump quantum fluctuations on squeezing. Ideal squeezing is represented by the ellipse with solid lines. Pump phase fluctuations cause the orientation of the ellipse to fluctuate through a characteristic angle $\Delta\phi = 1/4\mathcal{A}_p$, as indicated schematically by the dotted ellipse. These fluctuations feed noise from the amplified signal quadrature into the squeezed signal quadrature.

Fig. 2. Trick for introducing absorption and dispersion (phase mismatching). The actual nonlinear medium between z and $z + \Delta z$ is replaced by a slab of ideal (lossless, dispersionless) nonlinear medium preceded by a beam splitter. Reflection at the beam splitter accounts for losses, and frequency-dependent phase shifts at the beam splitter introduce dispersion.

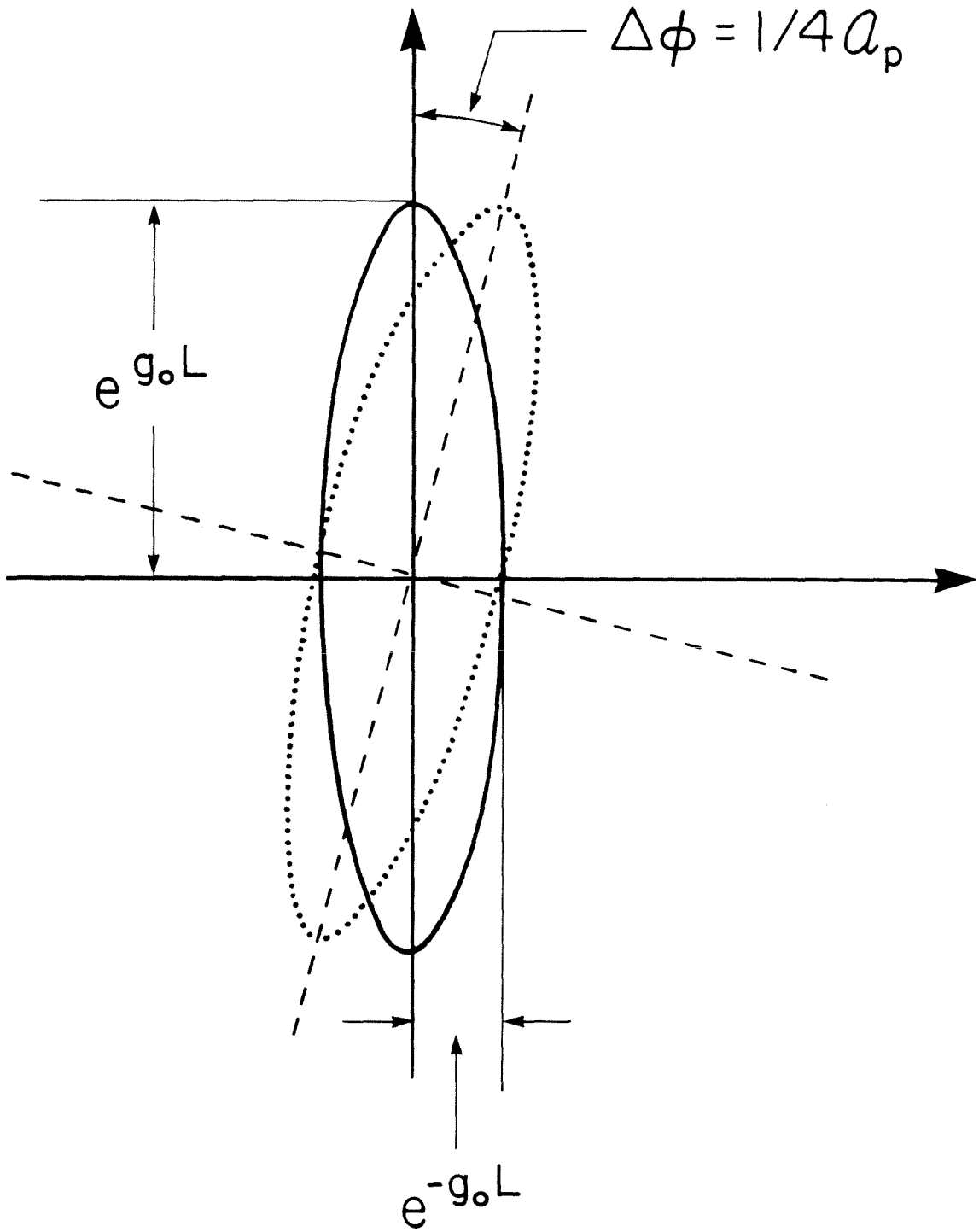

Figure 1

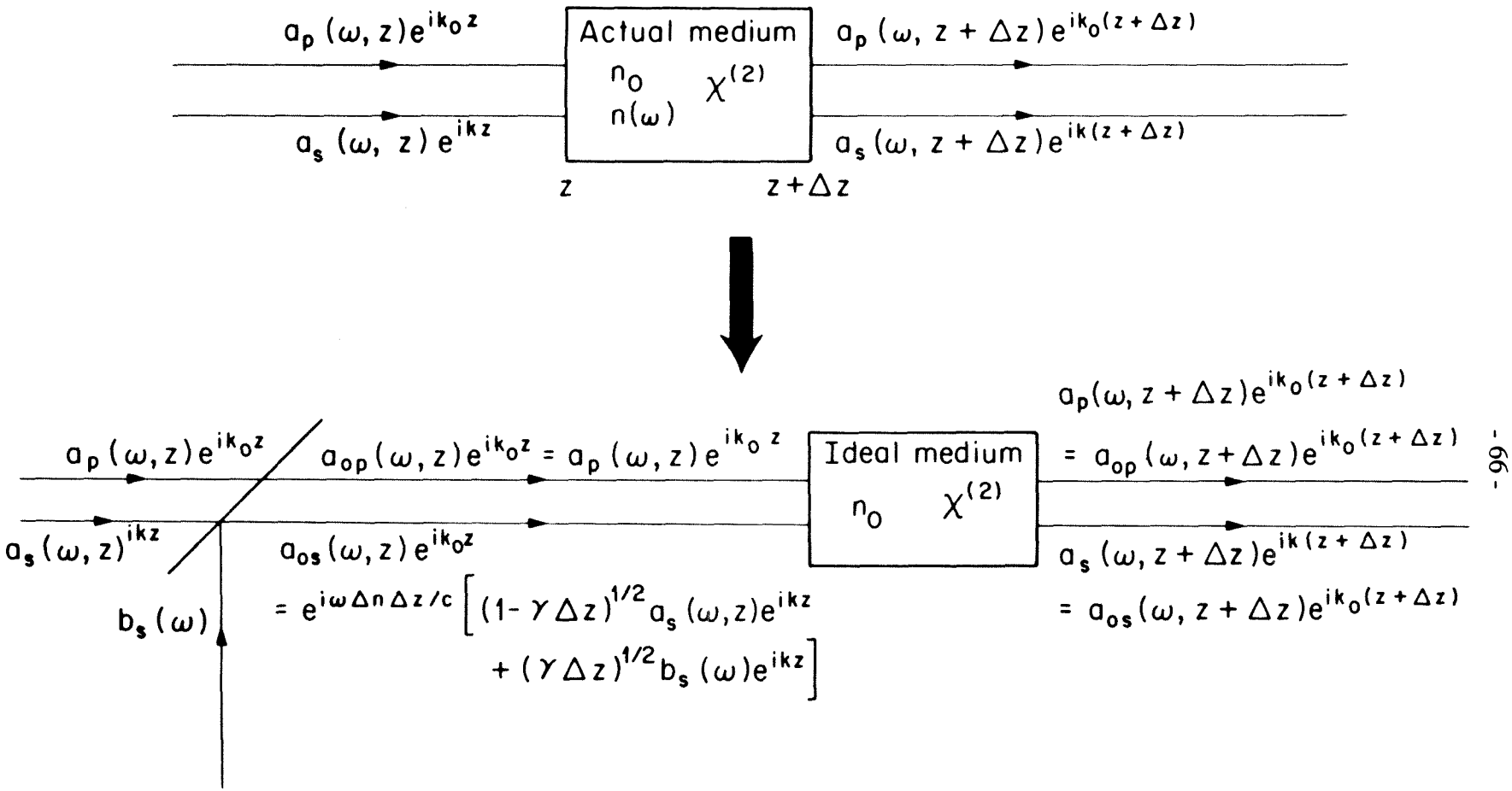
$a_p(\omega, z)e^{ik_0 z}$
$a_s(\omega, z)e^{ikz}$
Actual medium
n_0
$n(\omega)$
$\chi^{(2)}$
$a_p(\omega, z+\Delta z)e^{ik_0(z+\Delta z)}$
$a_s(\omega, z+\Delta z)e^{ik(z+\Delta z)}$
z
$z+\Delta z$
$a_p(\omega, z)e^{ik_0 z}$
$a_{op}(\omega, z)e^{ik_0 z} = a_p(\omega, z)e^{ik_0 z}$
$a_s(\omega, z)^{ikz}$
$a_{os}(\omega, z)e^{ik_0 z}$
$= e^{i\omega\Delta n\Delta z/c}\left[(1-\gamma\Delta z)^{1/2}a_s(\omega, z)e^{ikz} + (\gamma\Delta z)^{1/2}b_s(\omega)e^{ikz}\right]$
$b_s(\omega)$
Ideal medium
n_0
$\chi^{(2)}$
$a_p(\omega, z+\Delta z)e^{ik_0(z+\Delta z)}$
$= a_{op}(\omega, z+\Delta z)e^{ik_0(z+\Delta z)}$
$a_s(\omega, z+\Delta z)e^{ik(z+\Delta z)}$
$= a_{os}(\omega, z+\Delta z)e^{ik_0(z+\Delta z)}$

Figure 2

CHAPTER 3

Broadband Squeezing via Degenerate Parametric Amplification

by David D. Crouch

A condensed version of this chapter will be published in Physical Review A.

ABSTRACT

We show that parametric amplification is capable of generating squeezed-state light over a wide band if materials with large $\chi^{(2)}$ nonlinearities can be found, and that the squeezing bandwidth can be enhanced considerably by phase matching away from degeneracy. We compare our results with similar results recently found for four-wave mixing in an optical fiber.

Squeezed-state light has been generated recently using degenerate parametric amplification in both oscillator[1] and traveling-wave[2] configurations. In the experiment of Slusher *et al.*, [2] pulsed squeezed-state light was generated in a traveling-wave degenerate parametric amplifier (DPA), using a pulsed pump to increase the effective nonlinearity. If materials with larger $\chi^{(2)}$ nonlinearities can be found, one could generate squeezed-state light over a wide band using a continuous pump. Here we present a first-order analysis of a DPA with a cw (monochromatic) pump; we ignore losses and pump quantum fluctuations, which have been studied previously,[3] but we include dispersion.

The spatial differential equation describing the DPA is given by[3]

$$\frac{da_s(\Omega+\varepsilon,z)}{dz} = -g_0 e^{i[\Delta k(\varepsilon)z + 2\phi]} a_s^{\dagger}(\Omega-\varepsilon,z)\,, \tag{1}$$

where the parametric gain g_0 is given by

$$g_0 = \frac{2\pi\chi^{(2)}\Omega}{n_0^{3/2}}\left[\frac{8\pi P_p}{c^3\sigma}\right]^{1/2}, \tag{2}$$

and the phase mismatch $\Delta k(\varepsilon)$ by

$$\Delta k(\varepsilon) \equiv K_p(2\Omega) - k(\Omega+\varepsilon) - k(\Omega-\varepsilon) = \frac{1}{c}[2\Omega n(2\Omega) - (\Omega+\varepsilon)n(\Omega+\varepsilon) - (\Omega-\varepsilon)n(\Omega-\varepsilon)]\,. \tag{3}$$

Here $\phi_p = 2\phi$ is the pump phase, P_p the pump power, $\Omega_p = 2\Omega$ the pump frequency, $n(\omega)$ the index of refraction, $\chi^{(2)}$ the nonlinear susceptibility (assumed nondispersive over the frequencies of interest), and σ an effective cross-sectional area used to account crudely for the transverse structure of the waves. The operators $a_s(\omega,z)$ are Fourier components of the magnetic field operator

$$B_s^{(+)}(z,t)=\int_{\beta_s}\frac{d\omega}{2\pi}\left[\frac{c}{n(\omega)v_g(\omega)}\right]^{1/2}\left[\frac{2\pi n(\omega)\hbar\omega}{c\sigma}\right]^{1/2}a_s(\omega,z)\,e^{-i\omega[t-n(\omega)z/c]}\,. \tag{4}$$

Here β_s is the signal bandwidth, and $v_g(\omega)$ the group velocity.

We introduce a set of quadrature-phase amplitudes,[3–5] defined by

$$\bar{\alpha}_1(\varepsilon,z)=\frac{1}{2}[e^{-i[\Delta k(\varepsilon)z/2+\phi]}a_s(\Omega+\varepsilon,z)+e^{i[\Delta k(\varepsilon)z/2+\phi]}a_s^{\dagger}(\Omega-\varepsilon,z)]\,, \tag{5a}$$

$$\bar{\alpha}_2(\varepsilon,z)=-\frac{i}{2}[e^{-i[\Delta k(\varepsilon)z/2+\phi]}a_s(\Omega+\varepsilon,z)-e^{i[\Delta k(\varepsilon)z/2+\phi]}a_s^{\dagger}(\Omega-\varepsilon,z)]\,. \tag{5b}$$

The quadrature-phase amplitudes $\bar{\alpha}_1$ and $\bar{\alpha}_2$ contain the spectral information about the squeezing produced by the DPA. If $z=L$, $\bar{\alpha}_1(\varepsilon,L)$ and $\bar{\alpha}_2(\varepsilon,L)$ can be detected by a balanced homodyne detector by changing the phase of the local oscillator as a function of rf frequency ε.

By combining Eqs. (1), (5a), and (5b) we can write the equation of motion for the DPA in terms of the barred quadrature-phase amplitudes,

$$\frac{d\bar{\alpha}_1(\varepsilon,z)}{dz}=-g_0\bar{\alpha}_1(\varepsilon,z)+\frac{1}{2}\Delta k(\varepsilon)\bar{\alpha}_2(\varepsilon,z)\,, \tag{6a}$$

$$\frac{d\bar{\alpha}_2(\varepsilon,z)}{dz}=g_0\bar{\alpha}_2(\varepsilon,z)-\frac{1}{2}\Delta k(\varepsilon)\bar{\alpha}_1(\varepsilon,z)\,. \tag{6b}$$

At phase-matched frequencies, where $\Delta k(\varepsilon)=0$, the $\bar{\alpha}_1$ quadrature is deamplified (squeezed) and the $\bar{\alpha}_2$ quadrature is amplified. At other frequencies, where $\Delta k(\varepsilon)\neq 0$, the phase mismatch degrades the squeezing by mixing part of the amplified quadrature with the squeezed quadrature. The solutions to Eqs. (6a) and (6b) are given by

$$\bar{\alpha}_1(\varepsilon,z)=\mathrm{Re}\,[\mu(\varepsilon,z)+\nu(\varepsilon,z)]\bar{\alpha}_1(\varepsilon,0)-\mathrm{Im}\,[\mu(\varepsilon,z)-\nu(\varepsilon,z)]\bar{\alpha}_2(\varepsilon,0)\,, \tag{7a}$$

$$\bar{\alpha}_2(\varepsilon,z)=\mathrm{Im}\,[\mu(\varepsilon,z)+\nu(\varepsilon,z)]\bar{\alpha}_1(\varepsilon,0)+\mathrm{Re}\,[\mu(\varepsilon,z)-\nu(\varepsilon,z)]\bar{\alpha}_2(\varepsilon,0)\,, \tag{7b}$$

where

$$\mu(\varepsilon,z)=\cosh g(\varepsilon)z-i\frac{\Delta k(\varepsilon)}{2g(\varepsilon)}\sinh g(\varepsilon)z\,, \tag{8a}$$

$$\nu(\varepsilon,z)=-\frac{g_0}{g(\varepsilon)}\sinh g(\varepsilon)z \tag{8b}$$

when $g_0^2>[\Delta k(\varepsilon)/2]^2$, and

$$\mu(\varepsilon,z)=\cos K(\varepsilon)z-i\frac{\Delta k(\varepsilon)}{2K(\varepsilon)}\sin K(\varepsilon)z\,, \tag{9a}$$

$$\nu(\varepsilon,z)=-\frac{g_0}{K(\varepsilon)}\sin K(\varepsilon)z \tag{9b}$$

when $g_0^2<[\Delta k(\varepsilon)/2]^2$. Here

$$g(\varepsilon)=iK(\varepsilon)=[g_0^2-(\Delta k(\varepsilon)/2)^2]^{1/2}\,. \tag{10}$$

Spectral information about the squeezing produced by the DPA is contained in the spectral-density matrix[3-5] $\bar{S}_{mn}(\varepsilon)$ of the output quadrature-phase amplitudes $\bar{\alpha}_1(\varepsilon,L)$ and $\bar{\alpha}_2(\varepsilon,L)$:

$$<\Delta\bar{\alpha}_m^{\dagger}(\varepsilon',L)\Delta\bar{\alpha}_n(\varepsilon,L)>_{sym}=\pi\bar{S}_{mn}(\varepsilon)\delta(\varepsilon-\varepsilon')\,,\quad m,n=1,2\,. \tag{11}$$

Here, for any operator θ, $\Delta\theta=\theta-<\theta>$, and sym denotes a symmetrized product. Using the continuum commutation relation

$$[a(\omega,z),a^{\dagger}(\omega',z)]=2\pi\delta(\omega-\omega')\,, \tag{12}$$

one can show that for a vacuum input

$$<\Delta\bar{\alpha}_m^{\dagger}(\varepsilon',0)\Delta\bar{\alpha}_n(\varepsilon,0)>_{sym}=\frac{\pi}{2}\delta_{mn}\delta(\varepsilon-\varepsilon')\,. \tag{13}$$

Although the barred spectral-density matrix $\bar{S}_{mn}(\varepsilon)$ contains all the spectral information about squeezing, it does not give directly the maximum and minimum spectra at each ε. This is obtained by diagonalizing the spectral-density matrix by applying a suitable frequency- and position-dependent rotation $\theta(\varepsilon,L)$ to the output quadrature-phase amplitudes $\bar{\alpha}_1(\varepsilon,L)$ and $\bar{\alpha}_2(\varepsilon,L)$. We define $\tilde{\alpha}_1(\varepsilon,L)$ and $\tilde{\alpha}_2(\varepsilon,L)$ by

$$\tilde{\alpha}_1(\varepsilon,L)=\bar{\alpha}_1(\varepsilon,L)\cos\theta+\bar{\alpha}_2(\varepsilon,L)\sin\theta\,, \tag{14a}$$

$$\tilde{\alpha}_2(\varepsilon,L)=-\bar{\alpha}_1(\varepsilon,L)\sin\theta+\bar{\alpha}_2(\varepsilon,L)\cos\theta\,, \tag{14b}$$

and the new spectral-density matrix $\tilde{S}_{mn}(\varepsilon)$ by

$$<\Delta\tilde{\alpha}_m^{\dagger}(\varepsilon',L)\Delta\tilde{\alpha}_n(\varepsilon,L)>_{sym}=\pi\tilde{S}_{mn}(\varepsilon)\delta(\varepsilon-\varepsilon')\,. \tag{15}$$

Using Eqs. (7a) and (7b), we find that the elements of the rotated spectral-density matrix $\tilde{S}_{mn}(\varepsilon)$ are given by

$$\tilde{S}_{11}(\varepsilon)=\frac{1}{2}\{|\mu(\varepsilon,L)|^2+2\mathrm{Re}\,[\mu(\varepsilon,L)\nu(\varepsilon,L)\,e^{-2i\theta}]+|\nu(\varepsilon,L)|^2\}\,, \tag{16a}$$

$$\tilde{S}_{12}(\varepsilon)=\tilde{S}_{21}(\varepsilon)=\mathrm{Im}\,[\mu(\varepsilon,L)\nu(\varepsilon,L)\,e^{-2i\theta}]\,, \tag{16b}$$

$$\tilde{S}_{22}(\varepsilon)=\frac{1}{2}\{|\mu(\varepsilon,L)|^2-2\mathrm{Re}\,[\mu(\varepsilon,L)\nu(\varepsilon,L)\,e^{-2i\theta}]+|\nu(\varepsilon,L)|^2\}\,. \tag{16c}$$

We diagonalize the spectral-density matrix by choosing θ to satisfy

$$\mu(\varepsilon,L)\nu(\varepsilon,L)\,e^{-2i\theta}=-|\mu(\varepsilon,L)|\,|\nu(\varepsilon,L)|\,. \tag{17}$$

The matrix element $\tilde{S}_{11}(\varepsilon)$ gives the spectrum of the differenced photocurrent from a

balanced homodyne detector when the phase of the local oscillator is chosen to yield the maximum squeezing at rf frequency ε. The elements of the spectral-density matrix resulting from this choice are

$$\tilde{S}_{11}(\varepsilon)=\frac{1}{2}[|\mu(\varepsilon,L)|-|\nu(\varepsilon,L)|]^2, \tag{18a}$$

$$\tilde{S}_{22}(\varepsilon)=\frac{1}{2}[|\mu(\varepsilon,L)|+|\nu(\varepsilon,L)|]^2. \tag{18b}$$

Equations (17), (18a), and (18b) are formally equivalent to results obtained recently by Potasek and Yurke for four-wave mixing in an optical fiber.[6]

The frequency dependence of the phase mismatch $\Delta k(\varepsilon)$—and thus the index of refraction—must be specified before we can study the squeezing spectrum. Since the index of refraction varies only a small amount over the phase-matched bandwidth, we can expand it in a Taylor series about Ω,

$$n(\Omega\pm\varepsilon)=n(\Omega)\pm n^{(1)}(\Omega)\varepsilon+\frac{1}{2}n^{(2)}(\Omega)\varepsilon^2+\cdots, \quad \varepsilon\ll\Omega \tag{19}$$

where $n^{(j)}(\Omega)$ denotes the j^{th} derivative of n evaluated at Ω. One normally assumes phase matching at degeneracy, i.e., $n(2\Omega)=n(\Omega)$. Here we will not make such an assumption, but will assume $n(2\Omega)=n(\Omega+\varepsilon_0)$, where $\varepsilon_0\ll\Omega$. Equation (3) then becomes

$$\Delta k(\varepsilon)=\frac{1}{c}[2\Omega n(\Omega+\varepsilon_0)-(\Omega+\varepsilon)n(\Omega+\varepsilon)-(\Omega-\varepsilon)n(\Omega-\varepsilon)]. \tag{20}$$

Substituting Eq. (19) into Eq. (20), we find to fourth order in ε/Ω,

$$\Delta k(\varepsilon)=\frac{\Omega}{c}[\Delta-p\,(\varepsilon/\Omega)^2-q\,(\varepsilon/\Omega)^4], \tag{21a}$$

where the dimensionless parameters Δ, p, and q are given by

$$\Delta = 2[n(\Omega+\varepsilon_0) - n(\Omega)]\,, \tag{21b}$$

$$p = 2\Omega n^{(1)}(\Omega) + \Omega^2 n^{(2)}(\Omega)\,, \tag{21c}$$

$$q = \frac{1}{12}[4\Omega^3 n^{(3)}(\Omega) + \Omega^4 n^{(4)}(\Omega)]\,. \tag{21d}$$

Phase-matching occurs at frequency $\Omega+\varepsilon_m$ where $\Delta k(\varepsilon_m)=0$; setting Eq. (21a) equal to zero and solving for ε_m, we find

$$\varepsilon_m = 2\pi f_m = \Omega\left\{-\frac{p}{2q}\left[1 \pm \left[1 + \frac{4\Delta q}{p^2}\right]^{1/2}\right]\right\}^{1/2}. \tag{22}$$

We wish to investigate the case where $\Delta=0$ and $p=0$ simultaneously, so we must find a frequency Ω_0 such that $n(2\Omega_0)=n(\Omega_0)$ and $p(\Omega_0)=0$; then $\Delta k(\varepsilon) \propto (\varepsilon/\Omega)^4$ varies from zero only slowly as long as $\varepsilon \ll \Omega$. For example, using a modified Sellmeier equation for the ordinary refractive index in lithium niobate[7] and assuming that phase matching is possible at any frequency, we find that $p=0$ at $\lambda_0 = 2\pi c/\Omega_0 \simeq 1.9025\,\mu\text{m}$; we also find that $p>0$ for $\lambda<\lambda_0$, $p<0$ for $\lambda>\lambda_0$, and $q<0$ for all wavelengths in the neighborhood of λ_0. In the following we will assume $g_0 = 1.0\,\text{m}^{-1}$, and $L = 1.0\,\text{m}$. Figure 1 is a plot of the squeezed spectral density S (where $S = 2\tilde{S}_{11}$, so that $S=1$ is the vacuum level) as a function of $f = \varepsilon/2\pi$ for relatively large values of p. The solid line is for $\lambda = 1.935\,\mu\text{m}$, where $p = -3.208\times10^{-3}$ and $q = -4.883\times10^{-2}$. The short-dashed line is for $\lambda = 1.875\,\mu\text{m}$, where $p = 2.76\times10^{-3}$ and $q = -4.545\times10^{-2}$. The bandwidth over which squeezing occurs at these frequencies can be improved by taking Δ to be nonzero; the result is a nonzero phase-matching frequency, as is seen from Eq. (22). The medium-dashed line in Fig. 1 shows the broadened squeezing band for $\lambda = 1.935\,\mu\text{m}$ obtained by taking $f_0 = \varepsilon_0/2\pi = -1$ GHz, resulting in $\Delta = -7.86\times10^{-7}$ and, from Eq. (22), a new phase-matching frequency $f_m = 2.42$ THz. The long-dashed line in Fig. 1 shows the broadened squeezing band for

$\lambda = 1.875\,\mu m$ obtained by taking $f_0 = 1$ GHz, resulting in $\Delta = 7.38\times10^{-7}$ and a new phase-matching frequency $f_m = 2.62$ THz.

Squeezing over much greater bandwidths is obtained near λ_0, where p is small. The solid line in Fig. 2 shows S as a function of f for $\lambda = \lambda_0$, where $p = 0$, $q = -4.7\times10^{-2}$, and $\Delta = 0$. In practice, p can be small, but not identically zero. The short-dashed line in Fig. 2 is for $\lambda = 1.8971\,\mu m$, where $p = 5.39\times10^{-4}$, $q = -4.67\times10^{-2}$, and $\Delta = 0$. Because p and q are of opposite sign, Eq. (22) yields *two* phase-matching frequencies: one at $f_m = 0$ and another at $f_m = 16.99$ THz. The long-dashed line in Fig. 2 is for $\lambda = 1.8971\,\mu m$ and $f_0 = 1$ GHz, where $\Delta = 7.55\times10^{-7}$. Again we have phase matching at two frequencies, $f_m = 6.39$ THz and $f_m = 15.75$ THz, resulting in squeezing of roughly 80% or better over a bandwidth of 17 THz.

Similar results are obtained for four-wave mixing in an optical fiber.[6,8] To derive the spatial equation of motion for four-wave mixing, we proceed as in Ref. 3; we propagate the field through a slab of ideal (dispersionless) nonlinear medium, and then introduce dispersion via the beam splitter method of Ref. 3. Because the signal and the pump occupy the same band, we need not treat the signal and the pump separately as we did with the DPA. The positive frequency part of the magnetic field operator in an ideal nonlinear medium is given by

$$B_0^{(+)} = \int_\beta \frac{d\omega}{2\pi} B_0(\omega,\xi)\, e^{i(k_0\xi - \omega t)}, \qquad k_0 = \omega n_0/c\,, \tag{23a}$$

where

$$B_0(\omega,\xi) = A_0 e^{i(\gamma z + \theta)} 2\pi\delta(\omega - \Omega) + \left[\frac{2\pi n_0 \hbar\omega}{c\sigma}\right] b_0(\omega,\xi)\,. \tag{23b}$$

Here A_0 (θ) is the amplitude (phase) of the classical pump,

$$\gamma = \frac{24\pi\Omega\chi^{(3)}A_0^2}{n_0^3 c} = \frac{48\pi^2\Omega\chi^{(3)}}{n_0^2 c^2 \sigma} P_p \tag{24}$$

is the nonlinear phase shift due to the interaction of the pump with itself, i.e., the optical Kerr effect, and P_p is the pump power. The integral [Eq. (23a)] runs over a bandwidth β about Ω that contains all relevant signal frequencies. The Heisenberg equations of motion for a lossless, dispersionless nonlinear medium are simply an operator version of Maxwell's equations, supplemented by a constitutive relation.[9] As with the DPA, the two important Maxwell equations are $c^{-1}\partial D_0^{(+)}/\partial t = -\partial B_0^{(+)}/\partial \xi$ and $\partial E_0^{(+)}/\partial \xi = -c^{-1}\partial B_0^{(+)}/\partial t$. Once again we write a constitutive relation for the electric field in terms of the displacement field rather than the usual relation for the displacement field in terms of the electric field. The resulting constitutive relation is

$$E_0^{(+)} = D_0^{(+)}/n_0^2 - (12\pi\chi^{(3)}/n_0^8)[D_0^{(+)}]^2 D_0^{(-)} . \tag{25}$$

By plugging the Fourier expansion [Eqs. (23a,b)] into the Maxwell equations and the constitutive relation and by keeping only the highest order terms in γ, we find the spatial propagation equation

$$\frac{db_0(\Omega+\varepsilon,z)}{dz} = 2i\gamma b_0(\Omega+\varepsilon,z) + i\gamma e^{2i(\gamma z+\theta)} b_0^\dagger(\Omega-\varepsilon,z) . \tag{26}$$

If we then use the beam splitter method to introduce dispersion, we find

$$\frac{db_s(\Omega+\varepsilon,z)}{dz} = 2i\gamma b_s(\Omega+\varepsilon,z) + i\gamma e^{2i(\gamma z+\theta)} e^{i\Delta k_s(\varepsilon)z} b_s^\dagger(\Omega-\varepsilon,z) , \tag{27}$$

where

$$\Delta k_s(\varepsilon) \equiv 2K_p(\Omega) - k(\Omega+\varepsilon) - k(\Omega-\varepsilon) = \frac{1}{c}[2\Omega n(\Omega) - (\Omega+\varepsilon)n(\Omega+\varepsilon) - (\Omega-\varepsilon)n(\Omega-\varepsilon)] . \tag{28}$$

The magnetic field operator in the dispersive medium is then given by Eq. (4) with $a_s(\omega,z)$ replaced by $b_s(\omega,z)$. Introducing $b_s(\Omega+\varepsilon,z)=c_s(\Omega+\varepsilon,z)\exp(2i\gamma z)$, we find

$$\frac{dc_s(\Omega+\varepsilon,z)}{dz}=-\gamma e^{i[\Delta k_{eff}(\varepsilon)z+2\phi_s]}c_s^{\dagger}(\Omega-\varepsilon,z)\,, \tag{29}$$

where $\phi_s=\theta-\pi/4$ and

$$\Delta k_{\text{eff}}(\varepsilon)=\Delta k_s(\varepsilon)-2\gamma\,. \tag{30}$$

Equation (29) has the same form as the equation for the DPA, Eq. (1); the solution of Eq. (29) follows from Eqs. (7), (8), and (9) if $\Delta k_{\text{eff}}(\varepsilon)$ is substituted for $\Delta k(\varepsilon)$, γ for g_0, and ϕ_s for ϕ. The solution so obtained is different from that of the nonlinear Schrödinger equation only in the absence of odd-order dispersion terms that have been shown by Potasek and Yurke[6] to have no effect on the squeezing. Using Eq. (20), we expand $\Delta k_{\text{eff}}(\varepsilon)$ in a Taylor series:

$$\Delta k_{\text{eff}}(\varepsilon)=\frac{\Omega}{c}[\Delta_s-p_s(\varepsilon/\Omega)^2-q_s(\varepsilon/\Omega)^4]\,, \tag{31a}$$

where

$$\Delta_s=-\frac{2\gamma c}{\Omega}\,. \tag{31b}$$

Here p_s and q_s are given by Eqs. (21c) and (21d), respectively. Equations (29) and (31a) are the four-wave-mixing analogs of Eqs. (1) and (21a) for parametric amplification; in this sense, four-wave mixing and parametric amplification are equivalent processes for generating squeezed-state light.

Maximum squeezing occurs not when $\Delta k_s(\varepsilon)=0$, but when $\Delta k_{\text{eff}}(\varepsilon)=0$; we find the "phase-matching" frequencies f_s by substituting p_s for p, q_s for q, and Δ_s for Δ in Eq.

(22). If q_s and Δ_s are both negative—as they tend to be for optical fibers—then only one real solution f_s will exist regardless of the sign of p_s. If Δ_s could be made positive—as is possible with the DPA—then for $p_s>0$ one would obtain two real solutions f_{s1} and f_{s2}. For $p_s<0$ there are no real solutions when $\Delta_s>0$. It is the possibility of obtaining two phase-matching frequencies that distinguishes parametric amplification from four-wave mixing in an optical fiber. As we saw in Fig. 2, two phase matching frequencies result in squeezing over a very wide band. This is not possible with four-wave mixing.

In our example, we have assumed that one could phase match lithium niobate at or near $\lambda_0 = 1.9025\,\mu m$, a wavelength somewhat into the infrared. We are not proposing lithium niobate as a candidate material for the generation of broadband squeezed-state light, but use it merely as an illustrative example. Whether or not suitable materials can be found is a problem we have not addressed; the point we wish to make is that *if* one can find a nonlinear material in which it is possible to phase match at a frequency Ω at which $p(\Omega) \sim 0$, one can then obtain squeezing over a large bandwidth.

REFERENCES

1. L.-A. Wu, H. J. Kimble, J. L. Hall, and H. Wu, Phys. Rev. Lett. **57**, 2520 (1986).

2. R. E. Slusher, P. Grangier, A. LaPorta, B. Yurke, and M. J. Potasek, Phys. Rev. Lett. **59**, 2566 (1987).

3. C. M. Caves and D. D. Crouch, J. Opt. Soc. Am. B **4**, 1535 (1987); see also Chapter 2 of this thesis.

4. C. M. Caves and B. L. Schumaker, Phys. Rev. A **31**, 3068 (1985).

5. B. Yurke, Phys. Rev. A **32**, 300 (1985).

6. M. J. Potasek and B. Yurke, Phys. Rev. A **35**, 3974 (1987).

7. D. S. Smith, H. D. Riccius, and R. P. Edwin, Opt. Commun. **17**, 332 (1976).

8. P. D. Drummond and S. J. Carter, J. Opt. Soc. Am. B **4**, 1565 (1987).

9. M. Hillery and L. D. Mlodinow, Phys. Rev. A **30**, 1860 (1984).

FIGURE CAPTIONS

Fig. 1. Spectral-density S as a function of detuning f for degenerate parametric amplification in lithium niobate; $S=1$ is the vacuum level. Solid line: $\lambda=1.935\,\mu m$, $f_0=0$. Short-dashed line: $\lambda=1.875\,\mu m$, $f_0=0$. Medium-dashed line: $\lambda=1.935\,\mu m$, $f_0=-1$ GHz. Long-dashed line: $\lambda=1.875\,\mu m$, $f_0=1$ GHz.

Fig. 2. Broadened squeezing spectra near $\lambda_0=1.9025\,\mu m$, where the dispersion parameter $p=0$. Solid line: $\lambda=\lambda_0$, $f_0=0$. Short-dashed line: $\lambda=1.8971\,\mu m$, $f_0=0$. Long-dashed line: $\lambda=1.8971\,\mu m$, $f_0=1$ GHz.

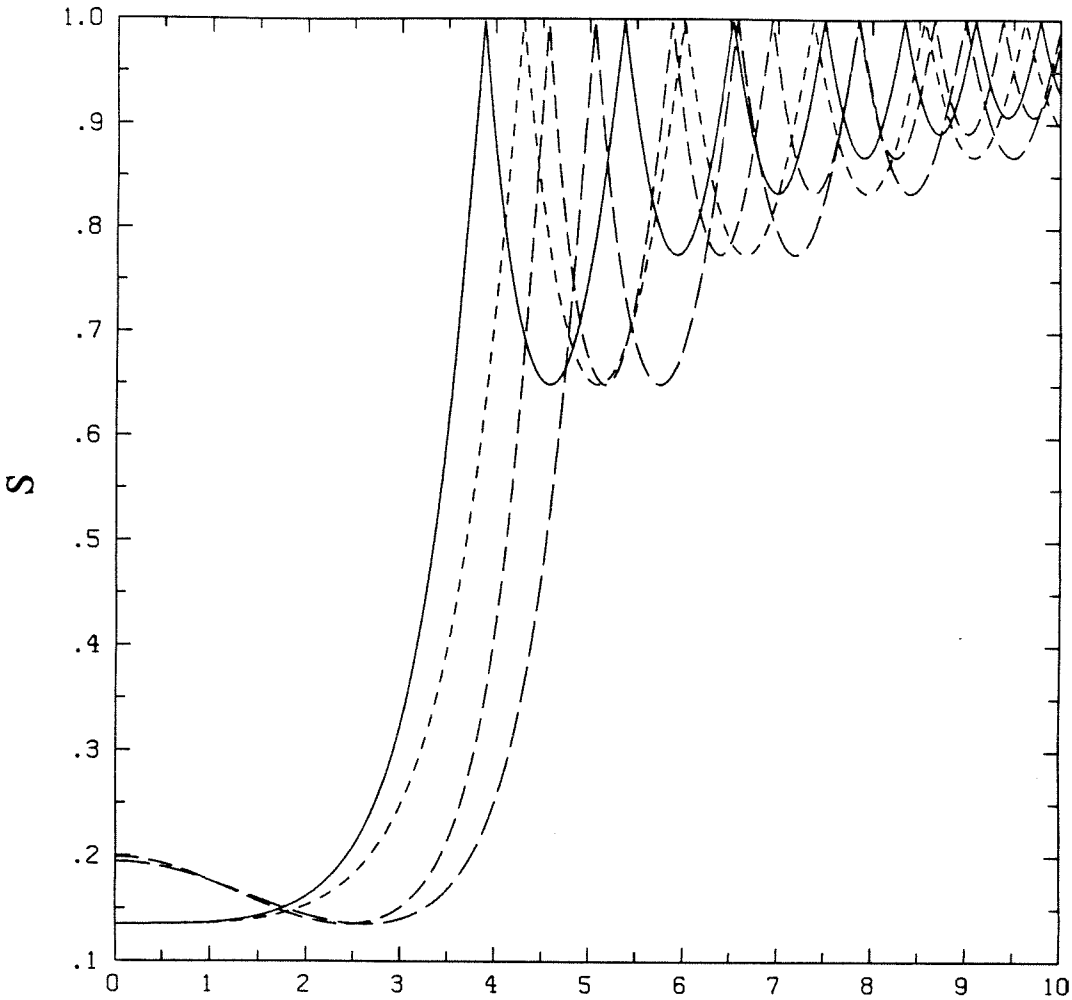

Figure 1

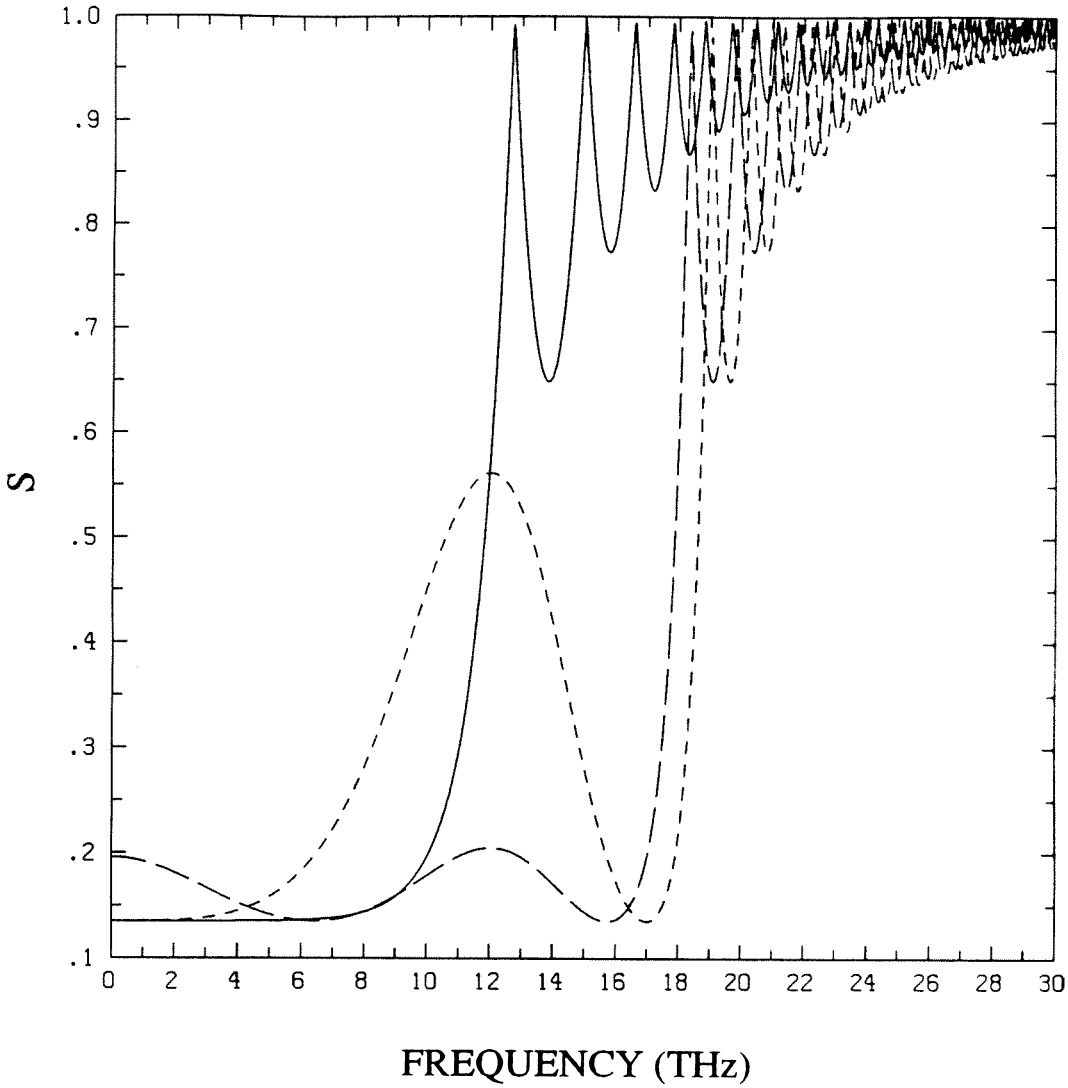
1.0
.9
.8
.7
.6
.5
.4
.3
.2
.1
S
0
2
4
6
8
10
12
14
16
18
20
22
24
26
28
30
FREQUENCY (THz)

Figure 2

CHAPTER 4

Limitations to Squeezing in a Parametric Amplifier due to Pump Quantum Fluctuations

by David D. Crouch and Samuel L. Braunstein

Part of a paper submitted to Physical Review A.

ABSTRACT

We perform discrete mode calculations for a parametric amplifier with a quantum pump, and discuss some of the limitations on calculations of this sort in quantum optics. We calculate corrections to the squeezing due to pump quantum fluctuations to order $1/\bar{N}^2$, for a pump initially in a coherent state with average photon number $\bar{N}$. We find that the limit to the variance of the squeezed quadrature due to the quantum nature of the pump goes as $\bar{N}^{-1/2}$.

1. INTRODUCTION

The parametric amplifier[1,2] (PA) is a basic device in quantum optics and quantum electronics. It couples a pump field at frequency ω_p to signal modes at frequencies near $\omega=\omega_p/2$. In this chapter we are mainly interested in the application of the PA for generating squeezed states,[3–5] i.e., quantum states for which one of a pair of canonically conjugate variables has its quantum noise (uncertainty) reduced below the vacuum level (zero point noise). The main purpose of this chapter is to show that the ability of a PA to produce squeezed-state light is limited by the initial phase noise in the pump.

When the signal modes are initially in vacuum states, only the pump's phase can determine which quadrature will be squeezed. If the pump's phase fluctuates, then the quadrature chosen will have a slight admixture[6] of its conjugate quadrature—the noisy quadrature. This argument is treated more carefully in Section 2 for the case of phase noise in a classical pump. Calculations of the corrections to semiclassical order (to order $1/\bar{N}$ in the matrix elements, where $\bar{N}$ is the average photon number of the pump) have been previously performed for both the one-[7] and the two-mode[8] PA.

Hillery and Zubairy[7] studied the one-mode PA with an interaction Hamiltonian

$$\hat{H}_{\text{int}}=i\frac{\hbar\kappa}{2}(\hat{a}^{\dagger 2}\hat{a}_p-\hat{a}^2\hat{a}_p^{\dagger}) \tag{1.1}$$

(up to a phase rotation of the variables), where $\hat{a}$ and $\hat{a}_p$ are the annihilation operators for the signal and pump modes, respectively, and κ is a coupling constant which is proportional to the second order nonlinear susceptibility $\chi^{(2)}$ of the medium in which the interaction is taking place. They used a path-integral technique[9] to obtain corrections at the semiclassical order. They did not claim to get the full semiclassical correction,[10] and the dominant terms they obtained for the fluctuation in the squeezed quadrature were

$$<\Delta\hat{x}_2^2> \approx \frac{e^{-2u}}{4} + \frac{e^{2u}}{64\bar{N}}, \tag{1.2}$$

where $\hat{x}_2 = -i(\hat{a} - \hat{a}^\dagger)/2$ is the quadrature (analogous to the position operator) which is squeezed by the interaction in Eq. (1.1), and $u = \bar{N}^{1/2}\kappa t$ is a dimensionless time. This yields a minimum variance, and hence a limit to the squeezing, of

$$<\Delta\hat{x}_2^2>_{\min} \approx \frac{1}{8\bar{N}^{1/2}}, \tag{1.3}$$

which is just what the argument of phase noise in the classical pump gives (see Section 2).

Scharf and Walls[8] studied the two-mode PA whose interaction Hamiltonian is (again up to a rotation of the variables' phases)

$$\hat{H}_{\text{int}} = i\hbar\kappa(\hat{a}_1^\dagger \hat{a}_2^\dagger \hat{a}_p - \hat{a}_1 \hat{a}_2 \hat{a}_p^\dagger), \tag{1.4}$$

where $\hat{a}_1$ and $\hat{a}_2$ are the annihilation operators for the two signal modes. They used an asymptotic method developed by Scharf[11–13] to arrive at the dominant correction to the variance of the Hermitian variable

$$\hat{y}_2 \equiv -\frac{i}{2}(\hat{a}_+ - \hat{a}_+^\dagger), \tag{1.5}$$

as

$$<\Delta\hat{y}_2^2> \approx \frac{e^{-2u}}{4} + \frac{e^{6u}}{1920\bar{N}}, \tag{1.6}$$

where $\hat{a}_+ \equiv (\hat{a}_1 + \hat{a}_2)/\sqrt{2}$. They concluded that the minimum variance obtainable by the two-mode PA would be

$$\langle \Delta \hat{y}_2^2 \rangle_{\min} \approx \frac{1}{6(10\bar{N})^{1/4}} . \tag{1.7}$$

How can we compare these calculations? If one rewrites Eq. (1.4) in terms of the variables

$$\hat{a}_+ \equiv \frac{1}{\sqrt{2}}(\hat{a}_1 + \hat{a}_2) , \tag{1.8a}$$

$$\hat{a}_- \equiv \frac{1}{\sqrt{2}}(\hat{a}_1 - \hat{a}_2) , \tag{1.8b}$$

then the interaction Hamiltonian may be written[14]

$$\hat{H}_{\text{int}} = i\frac{\hbar\kappa}{2}(\hat{a}_+^{\dagger 2}\hat{a}_p - \hat{a}_+^2\hat{a}_p^\dagger) - i\frac{\hbar\kappa}{2}(\hat{a}_-^{\dagger 2}\hat{a}_p - \hat{a}_-^2\hat{a}_p^\dagger) . \tag{1.9}$$

If the pump is now treated classically, then the $\hat{a}_+$ and $\hat{a}_-$ modes become completely independent, each described by the one-mode PA Hamiltonian Eq. (1.1). Thus we might expect the same correction to the squeezing due to a quantum pump as found by Hillery and Zubairy [see Eq. (1.2)]. In fact, since the pump is allowed to be quantum mechanical, the $\hat{a}_+$ and $\hat{a}_-$ modes can interact with each other by modifying their common pump. Thus these modes cannot completely decouple. Even so Scharf and Walls' results of Eqs. (1.6) and (1.7) are surprising; for a pump with $\bar{N} = 10^9$ there is a large discrepancy

$$\frac{\langle \Delta \hat{y}_2^2 \rangle_{\min}}{\langle \Delta \hat{x}_2^2 \rangle_{\min}} = \frac{4}{3}\left[\frac{\bar{N}}{10}\right]^{1/4} = \frac{400}{3} . \tag{1.10}$$

The purpose of this chapter is to resolve the apparent discrepancy between these two calculations, first noted by Caves and Crouch.[15]

This chapter is divided into four sections. Section 2 justifies our use of discrete mode calculations for a traveling-wave device, which in principle should be given a full continuum treatment, and also reviews the argument for the contribution of phase noise in a classical pump. In Section 3, we use the positive-P distribution[16] to derive Fokker-Planck equations for one- and two-mode parametric amplifiers. Standard methods of stochastic calculus[17] are then used to derive Ito stochastic differential equations (SDEs) from the Fokker-Planck equations. An approximate solution of the SDEs is obtained by iteration, and the full semiclassical correction is then calculated analytically.

We have found that Hillery and Zubairy have in fact calculated the exact semi-classical corrections to the parametric approximation for the one-mode PA, and that the dominant corrections for the one- and two-mode calculations are the same, and agree with the dominant correction obtained by Caves and Crouch[15] from a *continuum* calculation.

2. DISCUSSION

The conventional approach to problems in quantum optics typically makes use of a mode expansion to describe the electromagnetic field. Using this approach, one can derive from an appropriate Hamiltonian *temporal* differential equations for the modal creation and annihilation operators, the spatial dependence being carried by the mode functions. Such an approach is suitable for cavity devices in which one has well defined standing-wave modes (the eigenmodes of the cavity), but not for a traveling-wave device in which such modes are non-existent. One would like to derive *spatial* differential equations governing the evolution of the field operators through the medium, in analogy with classical nonlinear optics; the conventional approach is clearly unsuited to this purpose. Tucker and Walls[18] and Lane *et al.*[19] recognized these

problems with the conventional approach and developed a continuum wave-packet formalism in an attempt to deal with them.

In this section we briefly describe a discrete mode expansion of the electromagnetic field in terms of *wave-packet* modes that enable us to derive *spatial* equations of motion for PAs. We assume that the wave packets are short compared to the nonlinear medium through which they propagate, so that they "fit" inside the medium, allowing us to ignore boundary effects. Physically, the individual wave packet propagates from free space through the entrance boundary on a time scale short compared to the time it will spend inside the nonlinear medium; in this way the interaction is "turned on." This method is preferable to the technique often used in the conventional approach in which the interaction is suddenly turned on throughout all space, either at time $t=0$ or at some time in the remote past. We also present a heuristic argument for the dominant effect of pump quantum fluctuations on the variance of the squeezed quadrature in a PA.

We will give a brief outline of the derivation of the discrete wave-packet mode equations of motion for the PA; details will be given elsewhere. The discrete mode expansions of the signal and pump magnetic field operators in a dispersionless medium are given by

$$\hat{B}_{os}^{(+)}(z,t)=\sum_{n=-M}^{M}\sum_{k=-\infty}^{\infty}\left[\frac{2\pi n_0\hbar\omega_n}{c\sigma T_s}\right]^{1/2}\hat{a}_{nk}(z)\,e^{-i\omega_n[(t-n_0z/c)-kT_s]}f[(t-n_0z/c)-kT_s]\,, \quad (2.1a)$$

$$\hat{B}_{op}^{(+)}(z,t)=i\sum_{k=-\infty}^{\infty}\left[\frac{2\pi n_0\hbar\Omega_p}{c\sigma T_p}\right]^{1/2}\hat{b}_k(z)\,e^{-i\Omega_p[(t-n_0z/c)-kT_p]}f[(t-n_0z/c)-kT_p]\,, \quad (2.1b)$$

where

$$[\hat{a}_{nk}(z),\hat{a}_{n'k'}(z)]=[\hat{b}_k(z),\hat{b}_{k'}(z)]=0\,, \quad (2.2a)$$

$$[\hat{a}_{nk}(z),\hat{a}^{\dagger}_{n'k'}(z)]=\delta_{nn'}\delta_{kk'}, \tag{2.2b}$$

$$[\hat{b}_{k}(z),\hat{b}^{\dagger}_{k'}(z)]=\delta_{kk'}, \tag{2.2c}$$

and

$$f_j(t)=\frac{\sin\pi t/T_j}{\pi t/T_j}, \quad j=s,p \tag{2.3}$$

is the wave-packet envelope function. Here n_0 is the index of refraction of the dispersionless medium, $\Omega_p=2\Omega$ is the pump frequency, and σ is a cross-sectional area we use to account crudely for the transverse structure of the field. The discrete-mode expansions described by Eqs. (2.1a) and (2.1b) are obtained from a continuum description by dividing the signal and pump bandwidths into ''bins'' of width $\Delta\omega_s$ and $\Delta\omega_p$, respectively, with signal center frequency $\omega_n=\Omega+n\Delta\omega$ and pump center frequency $\Omega_p=2\Omega$.[20] Here we have assumed that the pump can be described by a single frequency bin. Each signal (pump) bin corresponds to a train of wave packets in the time domain, each of duration $T_s=2\pi/\Delta\omega_s$ ($T_p=2\pi/\Delta\omega_p$) with envelope given by Eq. (2.3).

By substituting Eqs. (2.1a) and (2.1b) into Maxwell's equations, we obtain the *spatial* equations of motion

$$\frac{d\hat{a}_{nk}(z)}{dz}=\kappa'\sum_{k'=-\infty}^{\infty}e^{i\Omega_p(k'T_p-kT_s)}\frac{\sin[\pi(kT_s-k'T_p)/T_p]}{\pi(kT_s-k'T_p)/T_p}\hat{b}_{k'}(z)\hat{a}^{\dagger}_{-nk}(z), \tag{2.4a}$$

$$\frac{d\hat{b}_{k}(z)}{dz}=-\frac{\kappa'}{2}\sum_{n=-M}^{M}\sum_{k'=-\infty}^{\infty}e^{i\Omega_p(k'T_s-kT_p)}\frac{\sin[\pi(k'T_s-kT_p)/T_p]}{\pi(k'T_s-kT_p)/T_p}\hat{a}_{nk'}(z)\hat{a}_{-nk'}(z), \tag{2.4b}$$

where the coupling constant κ' is given by

$$\kappa'=\frac{4\pi\Omega\chi^{(2)}}{n_0^2c}\left(\frac{2\pi n_0\hbar\Omega_p}{c\sigma T_p}\right)^{1/2}. \tag{2.5}$$

Here we have assumed that $\Delta\omega_p \ll \Delta\omega_s$ (or $T_p \gg T_s$) to avoid coupling among energy non-conserving modes. By restricting our observations to the region of spacetime near $t - n_0 z/c = 0$, we can discard all wave packets (both signal and pump) with $k \neq 0$, since $f_j(kT_j) = \delta_{k,0}$. With $\hat{a}_{n0}(z) \equiv \hat{a}_n(z)$ and $\hat{b}_0(z) \equiv \hat{a}_p(z)$, we find

$$\frac{d\hat{a}_n(z)}{dz} = \kappa' \hat{a}_p(z) \hat{a}_{-n}^{\dagger}(z), \tag{2.6a}$$

$$\frac{d\hat{a}_p(z)}{dz} = -\frac{\kappa'}{2} \sum_{n=-M}^{M} \hat{a}_n(z) \hat{a}_{-n}(z). \tag{2.6b}$$

Assuming that the wave packets are narrow compared to the scale of variation set by κ', we can replace z by ct/n_0 and obtain the *temporal* equations of motion

$$\frac{d\hat{a}_n(t)}{dt} = \kappa \hat{a}_p(t) \hat{a}_{-n}^{\dagger}(t), \tag{2.7a}$$

$$\frac{d\hat{a}_p(t)}{dt} = -\frac{\kappa}{2} \sum_{n=-M}^{M} \hat{a}_n(t) \hat{a}_{-n}(t), \tag{2.7b}$$

where $\kappa = c\kappa'/n_0$. Equations (2.7a) and (2.7b) are identical to the Heisenberg equations of motion that are derived from the multimode interaction Hamiltonian

$$H = i\frac{\hbar\kappa}{2} \sum_{n=-M}^{M} [\hat{a}_p(t)\hat{a}_n^{\dagger}(t)\hat{a}_{-n}^{\dagger}(t) - \hat{a}_p^{\dagger}(t)\hat{a}_n(t)\hat{a}_{-n}(t)] \tag{2.8}$$

when the conventional approach is used.

The Hamiltonian Eq. (2.8) correctly describes the interaction of a discrete pump mode with $2M+1$ discrete signal modes, but it does not provide a completely accurate description of traveling-wave parametric amplification, since it ignores the interaction of the pump wave packet $k = 0$ with signal wave packets other than $k = 0$. Ignoring as it

does interactions with these wave packets, the Hamiltonian cannot correctly describe nonlinear effects such as pump depletion; it does, however, correctly describe the effect of the initial pump quantum fluctuations on the signal modes. We will show, first by a heuristic argument and then by the results of detailed calculations using the Hamiltonian Eq. (2.8), that the initial pump quantum fluctuations are responsible for the dominant correction to the squeezing due to the quantum nature of the pump. We also calculate higher-order corrections. By the argument just given, the exact form of these corrections cannot be related to the physical parameters of a traveling-wave PA; these corrections *are* of physical interest, however, in showing how nonlinear effects affect the squeezing, and of mathematical interest in demonstrating the computational tools we have developed to calculate them.

The wave-packet approach gives us a new and more realistic way to deal with traveling-wave problems in quantum optics; it also leads one to realize that the conventional Hamiltonian approach can lead to misleading results when used blindly. We will, however, ignore distinctions between the conventional and the wave-packet approaches through much of this chapter. The point we wish to make is that the wave-packet modes are an appropriate set of modes for describing the spatial evolution of quantized electromagnetic fields in traveling-wave devices without resorting to continuum calculations.

We will now give a heuristic argument for the effect of pump quantum fluctuations on the squeezing produced by a PA. Our treatment of parametric amplification has thus far treated the pump quantum mechanically. Under certain circumstances, one can treat the pump classically, in what is known as the parametric approximation; in this approximation, one replaces the pump operator by a c-number $\alpha_p = \bar{N}^{1/2} e^{i\phi_r}$. The interaction Hamiltonian for a one-mode PA, where we ignore all modes in Eq. (2.8)

except for $n=0$, is

$$H_p = i\frac{\hbar\kappa\bar{N}^{1/2}}{2}[\hat{a}^{\dagger 2}(t)e^{i\phi_p} - \hat{a}^2(t)e^{-i\phi_p}], \tag{2.9}$$

where $\hat{a}_0(t)\equiv\hat{a}(t)$; two resulting equations of motion are

$$\frac{d\hat{a}(t)}{dt} = \kappa\bar{N}^{1/2}e^{i\phi_p}\hat{a}^{\dagger}(t), \tag{2.10a}$$

$$\frac{d\hat{a}^{\dagger}(t)}{dt} = \kappa\bar{N}^{1/2}e^{-i\phi_p}\hat{a}(t). \tag{2.10b}$$

We define *two* sets of quadrature-phase amplitudes,[14]

$$\hat{x}_1(t) = \frac{1}{2}[\hat{a}(t)+\hat{a}^{\dagger}(t)], \tag{2.11a}$$

$$\hat{x}_2(t) = -\frac{i}{2}[\hat{a}(t)-\hat{a}^{\dagger}(t)], \tag{2.11b}$$

and

$$\hat{x}_1'(t) = \frac{1}{2}[\hat{a}(t)e^{-i\phi_p/2}+\hat{a}^{\dagger}(t)e^{i\phi_p/2}], \tag{2.12a}$$

$$\hat{x}_2'(t) = -\frac{i}{2}[\hat{a}(t)e^{-i\phi_p/2}-\hat{a}^{\dagger}(t)e^{i\phi_p/2}], \tag{2.12b}$$

the two sets being identical when $\phi_p=0$. The two sets of quadrature-phase amplitudes are related by the rotation

$$\hat{x}_1(t) = \hat{x}_1'(t)\cos(\phi_p/2) - \hat{x}_2'(t)\sin(\phi_p/2), \tag{2.13a}$$

$$\hat{x}_2(t) = \hat{x}_2'(t)\cos(\phi_p/2) + \hat{x}_1'(t)\sin(\phi_p/2), \tag{2.13b}$$

pictured in Fig. 1 for $\phi_p/2=\Delta\phi$. By substituting Eqs. (2.12a) and (2.12b) in Eqs. (2.10a)

and (2.10b), we see that the quadrature-phase amplitudes $\hat{x}_1'(t)$ and $\hat{x}_2'(t)$ decouple the equations of motion:

$$\frac{d\hat{x}_1'(t)}{dt} = \kappa \bar{N}^{1/2} \hat{x}_1'(t) \quad \Longrightarrow \quad \hat{x}_1'(u) = \hat{x}_1'(0)\, e^{u} , \tag{2.14a}$$

$$\frac{d\hat{x}_2'(t)}{dt} = -\kappa \bar{N}^{1/2} \hat{x}_2'(t) \quad \Longrightarrow \quad \hat{x}_2'(u) = \hat{x}_2'(0)\, e^{-u} , \tag{2.14b}$$

where $u = \kappa \bar{N}^{1/2} t$ is a dimensionless time. For a vacuum input, one easily finds that

$$<\Delta \hat{x}_1'^2(u)> = \frac{1}{4} e^{2u} , \tag{2.15a}$$

$$<\Delta \hat{x}_2'^2(u)> = \frac{1}{4} e^{-2u} ; \tag{2.15b}$$

the $\hat{x}_2'$ quadrature exhibits maximum squeezing when the pump's phase is ϕ_p. The corresponding noise in the quadrature-phase amplitudes $\hat{x}_1$ and $\hat{x}_2$, from Eqs. (2.13a), (2.13b), (2.15a), and (2.15b) is described by

$$<\Delta \hat{x}_1^2(u)> = \frac{1}{4} e^{2u} \cos^2(\phi_p/2) + \frac{1}{4} e^{-2u} \sin^2(\phi_p/2) , \tag{2.16a}$$

$$<\Delta \hat{x}_2^2(u)> = \frac{1}{4} e^{-2u} \cos^2(\phi_p/2) + \frac{1}{4} e^{2u} \sin^2(\phi_p/2) . \tag{2.16b}$$

Suppose we allow the pump's phase to fluctuate. For the quantized pump in a coherent state $|\bar{N}^{1/2}>$ with mean photon number $\bar{N}$, the phase fluctuations are characterized by

$$<\Delta \phi_p^2> = <\phi_p^2> = \frac{1}{4\bar{N}} , \tag{2.17}$$

since we may choose without loss of generality $<\phi_p> = 0$. Because $\bar{N}$ is large, $<\Delta \phi_p^2>$

will be small; we can thus approximate $\cos^2(\phi_p/2)$ by 1, $\sin^2(\phi_p/2)$ by $<\phi_p^2/4> = 1/16\bar{N}$, and the variance of the $\hat{x}_2$ quadrature by

$$<\Delta\hat{x}_2^2(u)> \simeq \frac{1}{4}e^{-2u} + \frac{1}{64\bar{N}}e^{2u} . \tag{2.18}$$

The pump can be considered classical and the parametric approximation valid when the correction term is small, that is, when

$$\bar{N} \gg \frac{1}{16}\exp(4\bar{N}^{1/2}\kappa t) , \tag{2.19}$$

where we have used the definition of u. The second term of Eq. (2.18) is the dominant correction to the variance of the squeezed quadrature due to pump quantum fluctuations. Because of the quantum nature of the pump, phase fluctuations are unavoidable; Fig. 1 illustrates their effect. The solid ellipse represents squeezing with a classical pump (i.e. the parametric approximation) with a well defined phase $\phi_p = 0$. When $\phi_p \neq 0$, the ellipse is rotated by an angle $\phi_p/2$ as demonstrated by Eqs. (2.13a,b). Pump phase fluctuations cause the orientation of the ellipse to fluctuate about $\phi_p = 0$ with the characteristic angle $\Delta\phi = <\phi_p^2/4> = 1/4\bar{N}^{1/2}$, as represented by the dotted ellipse in Fig. 1, feeding noise from the amplified quadrature into the squeezed quadrature. One also sees why amplitude fluctuations are unimportant. Amplitude fluctuations merely produce fluctuations in the gain (or rate of squeezing); they do not couple noise in the amplified quadrature into the squeezed quadrature.

The above argument is for a one-mode PA, but it is easily extended to any number of modes; the same argument has been given for a continuum-mode PA,[15] yielding the same dominant correction as given by Eq. (2.18), but given $\bar{N}$ in terms of the pump power by identification of an appropriate bandwidth defined by phase mismatching. In

the parametric approximation, the signal modes interact in pairs at frequencies $\Omega+n\Delta\omega$ and $\Omega-n\Delta\omega$; there are no interactions among different pairs in this approximation, and each pair can thus be considered separately. The correction that we have been discussing is due to fluctuations in the initial state of the pump, and has nothing to do with back-action from the signal modes—pump depletion being one example of such back action—which would depend on the number of signal modes. The initial fluctuations act on each pair of modes in the same manner as described in Eq. (2.18) for the one-mode PA, yielding *for each pair of modes* a correction identical to that of Eq. (2.18). This correction is then independent of the number of signal modes, justifying our one-mode treatment.

The arguments given above are not rigorous; we have cited quantum mechanics as the ultimate source of pump phase fluctuations, yet we have treated their effect on squeezing classically. What we have given is a plausibility argument for and a physical picture of the dominant effect due to such fluctuations. The validity of our arguments will be confirmed by our detailed calculations showing the correction terms in Eq. (2.18) to be the dominant effect of pump quantum fluctuations on the squeezing, independent of the number of signal modes.

3. STOCHASTIC DIFFERENTIAL EQUATIONS

A. The one-mode PA

The dynamic evolution of a one-mode PA is described by von Neumann's equation in the interaction picture

$$\frac{\partial\hat{\rho}_I(t)}{\partial t}=\frac{i}{\hbar}[\hat{\rho}_I(t),\hat{H}_{\text{int}}(t)]\,, \tag{3.1}$$

where the interaction Hamiltonian $\hat{H}_{int}(t)$ is given by Eq. (1.1). All operators are now in the interaction picture. We will assume that initially the signal mode is in the vacuum state, and the pump is in a coherent state of real amplitude α_0:

$$\hat{\rho}(0)=\hat{\rho}_I(0)=|0,\alpha_0><0,\alpha_0| \ . \tag{3.2}$$

To solve Eq. (3.1), it is convenient to project the density operator $\hat{\rho}_I(t)$ onto a suitable set of basis states. The positive-P representation[16] is an off-diagonal representation obtained from an expansion on a coherent state basis:

$$\hat{\rho}_I(t)=\iiiint P(\alpha,\alpha_p,\beta,\beta_p,t)\,\hat{\Lambda}(\alpha,\alpha_p,\beta,\beta_p)\,d^2\alpha\,d^2\alpha_p\,d^2\beta\,d^2\beta_p \ , \tag{3.3}$$

where the operator $\hat{\Lambda}$ is given by

$$\hat{\Lambda}(\alpha,\alpha_p,\beta,\beta_p)\equiv \frac{|\alpha,\alpha_p><\beta^*,\beta_p^*|}{<\beta^*,\beta_p^*|\alpha,\alpha_p>}$$

$$=e^{-(\alpha\beta+\alpha_r\beta_r)}e^{\alpha\hat{a}^\dagger+\alpha_r\hat{a}_r^\dagger}|0,0><0,0|e^{\beta\hat{a}+\beta_r\hat{a}_r} \ . \tag{3.3a}$$

Using Eq. (3.3a), one obtains the operator identities

$$\hat{a}\hat{\Lambda}=\alpha\hat{\Lambda} \ , \qquad \hat{\Lambda}\hat{a}^\dagger=\beta\hat{\Lambda} \ ,$$

$$\hat{a}_p\hat{\Lambda}=\alpha_p\hat{\Lambda} \ , \quad \hat{\Lambda}\hat{a}_p^\dagger=\beta_p\hat{\Lambda} \ , \tag{3.4a}$$

and

$$\hat{a}^\dagger\hat{\Lambda}=\left(\frac{\partial}{\partial\alpha}+\beta\right)\hat{\Lambda} \ , \qquad \hat{\Lambda}\hat{a}=\left(\alpha+\frac{\partial}{\partial\beta}\right)\hat{\Lambda} \ ,$$

$$\hat{a}_p^\dagger\hat{\Lambda}=\left(\frac{\partial}{\partial\alpha_p}+\beta_p\right)\hat{\Lambda} \ , \quad \hat{\Lambda}\hat{a}_p=\left(\alpha_p+\frac{\partial}{\partial\beta_p}\right)\hat{\Lambda} \ . \tag{3.4b}$$

Substituting Eqs. (3.3) into Eq. (3.1), using the operator identities in Eqs. (3.4), and integrating by parts yields the Fokker-Planck equation

$$\frac{\partial P}{\partial \tau} = \left[-\alpha_p \beta \frac{\partial}{\partial \alpha} - \alpha \beta_p \frac{\partial}{\partial \beta} + \frac{\alpha^2}{2} \frac{\partial}{\partial \alpha_p} + \frac{\beta^2}{2} \frac{\partial}{\partial \beta_p} + \frac{\alpha_p}{2} \frac{\partial^2}{\partial \alpha^2} + \frac{\beta_p}{2} \frac{\partial^2}{\partial \beta^2} \right] P \,, \tag{3.5}$$

where $\tau = \kappa t$ and $P \equiv P(\alpha, \alpha_p, \beta, \beta_p, \tau)$.

In its present form, Eq. (3.5) is a complex eight dimensional Fokker-Planck equation. The analyticity of $\hat{\Lambda} \equiv \hat{\Lambda}(\alpha, \alpha_p, \beta, \beta_p)$, however, allows us some freedom of choice in interpreting the derivatives:

$$\frac{\partial \hat{\Lambda}}{\partial \alpha} = \frac{\partial \hat{\Lambda}}{\partial \alpha_x} = -i \frac{\partial \hat{\Lambda}}{\partial \alpha_y} \,, \tag{3.6a}$$

$$\frac{\partial \hat{\Lambda}}{\partial \beta} = \frac{\partial \hat{\Lambda}}{\partial \beta_x} = -i \frac{\partial \hat{\Lambda}}{\partial \beta_y} \,, \tag{3.6b}$$

$$\frac{\partial \hat{\Lambda}}{\partial \alpha_p} = \frac{\partial \hat{\Lambda}}{\partial \alpha_{px}} = -i \frac{\partial \hat{\Lambda}}{\partial \alpha_{py}} \,, \tag{3.6c}$$

$$\frac{\partial \hat{\Lambda}}{\partial \beta_p} = \frac{\partial \hat{\Lambda}}{\partial \beta_{px}} = -i \frac{\partial \hat{\Lambda}}{\partial \beta_{py}} \,. \tag{3.6d}$$

Here "x" and "y" denote real and imaginary parts of a complex number. By properly interpreting the derivatives in Eq. (3.5), we obtain a real Fokker-Planck equation with positive-semidefinite diffusion. A detailed derivation of the diffusion matrices for both one- and two-mode PAs is given in the Appendix. Using the standard methods of stochastic calculus,[17] this eight dimensional Fokker-Planck equation yields a set of eight real, first order Ito stochastic differential equations (SDEs). When written in complex notation, the resulting SDEs are

$$d\alpha = \alpha_p \beta \, d\tau + \sqrt{\alpha_p} \, dW_1 \,, \tag{3.7a}$$

$$d\beta = \alpha\beta_p \, d\tau + \sqrt{\beta_p} \, dW_2 , \tag{3.7b}$$

$$d\alpha_p = -\frac{1}{2}\alpha^2 d\tau , \tag{3.7c}$$

$$d\beta_p = -\frac{1}{2}\beta^2 d\tau , \tag{3.7d}$$

where, in the Ito calculus,

$$dW_1^2 = dW_2^2 = d\tau . \tag{3.7e}$$

The Wiener increments dW_1 and dW_2 are real and independent.

Although we cannot solve Eqs. (3.7) analytically, an approximate solution is possible in the case of a nearly classical pump. We assume that the stochastic pump mode variables α_p and β_p consist of a mean amplitude α_0 (chosen to be real) plus fluctuations $\Delta\alpha$ and $\Delta\beta$:

$$\alpha_p \equiv \alpha_0 + \Delta\alpha , \tag{3.8a}$$

$$\beta_p \equiv \alpha_0 + \Delta\beta . \tag{3.8b}$$

We define new variables x_1, p_1, x_2, and p_2 by

$$x_1 = \frac{1}{2}(\alpha + \beta) , \qquad x_2 = -\frac{i}{2}(\alpha - \beta) , \tag{3.9a}$$

$$p_1 = \frac{1}{2}(\Delta\alpha + \Delta\beta) , \quad p_2 = -\frac{i}{2}(\Delta\alpha - \Delta\beta) . \tag{3.9b}$$

It is convenient to change variables once again. We define the variables z_1 and z_2 by

$$z_1 = x_1 e^{-\mu} , \tag{3.10a}$$

$$z_2 = x_2 e^{u} \ . \tag{3.10b}$$

The resulting SDEs are

$$dz_1 = \frac{1}{\alpha_0}(z_1 p_1 + z_2 p_2 e^{-2u})\,du + \frac{1}{2}e^{-u}\left[\left[1+\frac{p_1+ip_2}{\alpha_0}\right]^{1/2} dV_1 + \left[1+\frac{p_1-ip_2}{\alpha_0}\right]^{1/2} dV_2\right] , \tag{3.11a}$$

$$dz_2 = \frac{1}{\alpha_0}(z_1 p_2 e^{2u} - z_2 p_1)\,du - \frac{i}{2}e^{u}\left[\left[1+\frac{p_1+ip_2}{\alpha_0}\right]^{1/2} dV_1 - \left[1+\frac{p_1-ip_2}{\alpha_0}\right]^{1/2} dV_2\right] , \tag{3.11b}$$

$$dp_1 = \frac{1}{2\alpha_0}(z_2^2 e^{-2u} - z_1^2 e^{2u})\,du \ , \tag{3.11c}$$

$$dp_2 = -\frac{1}{\alpha_0} z_1 z_2\,du \ , \tag{3.11d}$$

where $u = \alpha_0 \tau$, $dV_1 = \sqrt{\alpha_0}\,dW_1$, and $dV_2 = \sqrt{\alpha_0}\,dW_2$.

We use an iterative procedure to obtain an approximate solution of Eqs. (3.11). The square roots are expanded in a Taylor series:

$$\left[1+\frac{p_1 \pm ip_2}{\alpha_0}\right]^{1/2} = 1 + \frac{1}{\alpha_0}\frac{p_1 \pm ip_2}{2} - \frac{1}{\alpha_0^2}\frac{(p_1 \pm ip_2)^2}{8} + \cdots \ . \tag{3.12}$$

Substituting Eq. (3.12) into Eqs. (3.11) and integrating formally, we find

$$z_1(u) = z_1(0) + \frac{1}{\alpha_0}\int_0^u [z_1(x)p_1(x) + z_2(x)p_2(x)e^{-2x}]\,dx$$

$$+ \frac{1}{\sqrt{2}}\int_0^u e^{-x}\left\{dV + \frac{1}{\alpha_0}\left[\frac{1}{2}p_1(x)dV + \frac{i}{2}p_2(x)dW\right] + \cdots\right\} , \tag{3.13a}$$

$$z_2(u)=z_2(0)+\frac{1}{\alpha_0}\int_0^u [z_1(x)p_2(x)e^{2x}-z_2(x)p_1(x)]\,dx$$

$$-\frac{i}{\sqrt{2}}\int_0^u e^x\left\{dW+\frac{1}{\alpha_0}\left[\frac{1}{2}p_1(x)dW+\frac{i}{2}p_2(x)dV\right]+\cdots\right\}, \tag{3.13b}$$

$$p_1(u)=p_1(0)+\frac{1}{2\alpha_0}\int_0^u [z_2^2(x)e^{-2x}-z_1^2(x)e^{2x}]\,dx\ , \tag{3.13c}$$

$$p_2(u)=p_2(0)-\frac{1}{\alpha_0}\int_0^u z_1(x)z_2(x)\,dx\ . \tag{3.13d}$$

Here we have defined two new independent Wiener increments

$$dV(x)=\frac{dV_1(x)+dV_2(x)}{\sqrt{2}}\ , \tag{3.14a}$$

$$dW(x)=\frac{dV_1(x)-dV_2(x)}{\sqrt{2}}\ . \tag{3.14b}$$

The new Wiener increments defined in Eqs. (3.14) correspond to a rotation of the old Wiener increments, dV_1 and dV_2, and hence retain the same correlation matrix.[17]

We can ignore the initial values $z_1(0)=x_1(0)$, $z_2(0)=x_2(0)$, $p_1(0)$ and $p_2(0)$ in subsequent calculations because all moments involving these quantities are zero. To see this, we observe that the P-function gives normally ordered averages for all moments α^n and β^n, and all normally ordered averages are initially zero for the case studied here. By extension, all moments involving the initial values $x_1(0)$, $x_2(0)$, $p_1(0)$, and $p_2(0)$ are zero.

The formal solution [Eqs. (3.13)] yields an approximate solution, valid for short interaction times and large pump amplitude, when the stochastic variables are expanded in a perturbation series in the reciprocal of the pump amplitude:

$$\theta=\sum_{n=0}^{\infty}\alpha_0^{-n}\theta^{(n)}\ . \tag{3.15}$$

By substituting the expansion Eq. (3.15) into the formal solution Eqs. (3.13) and equating equal powers of α_0^{-n}, we obtain an approximate solution to the set of SDEs: (i) to zeroth order,

$$z_1^{(0)}(u)=\frac{1}{\sqrt{2}}\int_0^u e^{-x}\,dV\,, \tag{3.16a}$$

$$z_2^{(0)}(u)=-\frac{i}{\sqrt{2}}\int_0^u e^{x}\,dW\,, \tag{3.16b}$$

$$p_1^{(0)}(u)=p_2^{(0)}(u)=0\,, \tag{3.16c}$$

(ii) to first order,

$$z_1^{(1)}(u)=z_2^{(1)}(u)=0\,, \tag{3.17a}$$

$$p_1^{(1)}(u)=\frac{1}{2}\int_0^u [z_2^{(0)2}(x)e^{-2x}-z_1^{(0)2}(x)e^{2x}]\,dx\,, \tag{3.17b}$$

$$p_2^{(1)}(u)=-\int_0^u z_1^{(0)}(x)z_2^{(0)}(x)\,dx\,, \tag{3.17c}$$

and (iii) to second order,

$$z_1^{(2)}(u)=\int_0^u [z_1^{(0)}(x)p_1^{(1)}(x)+z_2^{(0)}(x)p_2^{(1)}(x)e^{-2x}]\,dx$$

$$+\frac{1}{2\sqrt{2}}\int_0^u e^{-x}[p_1^{(1)}(x)\,dV+ip_2^{(1)}(x)\,dW]\,, \tag{3.18a}$$

$$z_2^{(2)}(u)=\int_0^u [z_1^{(0)}(x)p_2^{(1)}(x)e^{2x}-z_2^{(0)}(x)p_1^{(1)}(x)]\,dx$$

$$-\frac{i}{2\sqrt{2}}\int_0^u e^{x}[p_1^{(1)}(x)\,dW+ip_2^{(1)}(x)\,dV]\,, \tag{3.18b}$$

$$p_1^{(2)}(u)=p_2^{(2)}(u)=0\,. \tag{3.18c}$$

The SDEs corresponding to the zeroth order solutions $z_1^{(0)}(u)$ and $z_2^{(0)}(u)$ are

$$dz_1^{(0)} = \frac{1}{\sqrt{2}} e^{-u}\, dV \,, \tag{3.19a}$$

$$dz_2^{(0)} = -\frac{i}{\sqrt{2}} e^{u}\, dW \,. \tag{3.19b}$$

We define the new variables

$$A_1(u) = z_1^{(0)}(u)\, e^{u} \,, \tag{3.20a}$$

$$A_2(u) = i z_2^{(0)}(u)\, e^{-u} \,, \tag{3.20b}$$

with the resulting SDEs

$$dA_1 = A_1\, du + \frac{1}{\sqrt{2}}\, dV \,, \tag{3.21a}$$

$$dA_2 = -A_2\, du + \frac{1}{\sqrt{2}}\, dW \,. \tag{3.21b}$$

Equations (3.21) describe two independent Ornstein-Uhlenbeck processes, each with zero mean. Thus $z_1^{(0)}(u)$ and $z_2^{(0)}(u)$, apart from the exponential factors e^{u} and e^{-u}, respectively, are themselves Ornstein-Uhlenbeck processes. They are Gaussian variables; all higher order moments can be expressed in terms of second order moments. With this in mind, we can formulate a pair of rules to guide us through the remaining calculations: (i) a rule for quadratic moments,

$$\langle z_1^{(0)}(u) z_1^{(0)}(w) \rangle_{av} = \frac{1}{4}(1 - e^{-2w}) \quad u \geq w \,, \tag{3.22a}$$

$$\langle z_2^{(0)}(u) z_2^{(0)}(w) \rangle_{av} = -\frac{1}{4}(e^{2w} - 1) \quad u \geq w \,, \tag{3.22b}$$

$$<z_1^{(0)}(u)z_2^{(0)}(w)>_{av}=0\,, \tag{3.22c}$$

and (ii) a rule for quartic moments,

$$\begin{aligned}<z_1^{(0)}(u)z_1^{(0)}(v)z_1^{(0)}(w)z_1^{(0)}(z)>_{av}&=<z_1^{(0)}(u)z_1^{(0)}(v)>_{av}<z_1^{(0)}(w)z_1^{(0)}(z)>_{av}\\&+<z_1^{(0)}(u)z_1^{(0)}(w)>_{av}<z_1^{(0)}(v)z_1^{(0)}(z)>_{av}\\&+<z_1^{(0)}(u)z_1^{(0)}(z)>_{av}<z_1^{(0)}(v)z_1^{(0)}(w)>_{av}\,,\end{aligned} \tag{3.23a}$$

$$\begin{aligned}<z_2^{(0)}(u)z_2^{(0)}(v)z_2^{(0)}(w)z_2^{(0)}(z)>_{av}&=<z_2^{(0)}(u)z_2^{(0)}(v)>_{av}<z_2^{(0)}(w)z_2^{(0)}(z)>_{av}\\&+<z_2^{(0)}(u)z_2^{(0)}(w)>_{av}<z_2^{(0)}(v)z_2^{(0)}(z)>_{av}\\&+<z_2^{(0)}(u)z_2^{(0)}(z)>_{av}<z_2^{(0)}(v)z_2^{(0)}(w)>_{av}\,,\end{aligned} \tag{3.23b}$$

where $<\ >_{av}$ denotes an average in the positive-P representation.

The squeezing in the signal mode is easily calculated by the repeated application of (i) and (ii). The quadrature-phase amplitudes are defined by

$$\hat{x}_1=\frac{1}{2}(\hat{a}+\hat{a}^\dagger)\,,\qquad \hat{x}_2=-\frac{i}{2}(\hat{a}-\hat{a}^\dagger)\,, \tag{3.24a}$$

$$\hat{P}_1=\frac{1}{2}(\hat{a}_p+\hat{a}_p^\dagger)\,,\qquad \hat{P}_2=-\frac{i}{2}(\hat{a}_p-\hat{a}_p^\dagger)\,, \tag{3.24b}$$

where $\hat{x}_1$ and $\hat{x}_2$ are signal mode quadrature-phase amplitudes, and $\hat{P}_1$ and $\hat{P}_2$ are pump mode quadrature-phase amplitudes. The expectation values of the signal-mode quadrature-phase amplitudes $\hat{x}_1$ and $\hat{x}_2$ are zero when the signal is initially vacuum. We then find that the uncertainties in $\hat{x}_1$ and $\hat{x}_2$ are

$$<\Delta\hat{x}_1^2>=\frac{1}{4}+<x_1^2(u)>_{av}=\frac{1}{4}+<z_1^2(u)>_{av}e^{2u}\,, \tag{3.25a}$$

$$<\Delta\hat{x}_2^2> = \frac{1}{4} + <x_2^2(u)>_{av} = \frac{1}{4} + <z_2^2(u)>_{av} e^{-2u} . \tag{3.25b}$$

We see from Eqs. (3.25) that x_1 and x_2 are the c-number equivalents of the quadrature-phase amplitudes $\hat{x}_1$ and $\hat{x}_2$, respectively. To second order in α_0^{-1}, the uncertainties are

$$<\Delta\hat{x}_1^2> = \frac{1}{4} + <z_1^{(0)2}(u)>_{av} e^{2u} + \frac{1}{\alpha_0^2} <2z_1^{(0)}(u) z_1^{(2)}(u)>_{av} e^{2u} , \tag{3.26a}$$

$$<\Delta\hat{x}_2^2> = \frac{1}{4} + <z_2^{(0)2}(u)>_{av} e^{-2u} + \frac{1}{\alpha_0^2} <2z_2^{(0)}(u) z_2^{(2)}(u)>_{av} e^{-2u} . \tag{3.26b}$$

Application of (i) yields the ideal squeezing:

$$<\Delta\hat{x}_1^2>_{ideal} = \frac{1}{4} + <z_1^{(0)2}(u)>_{av} e^{2u} = \frac{1}{4} e^{2u} , \tag{3.27a}$$

$$<\Delta\hat{x}_2^2>_{ideal} = \frac{1}{4} + <z_2^{(0)2}(u)>_{av} e^{-2u} = \frac{1}{4} e^{-2u} . \tag{3.27b}$$

Repeated applications of (i) and (ii) yield the quadrature variances correct to semiclassical order $\alpha_0^{-2} = \bar{N}^{-1}$:

$$<\Delta\hat{x}_1^2> = \frac{1}{4} e^{2u} + \frac{1}{8\bar{N}} \left[u^2 e^{2u} + u(e^{2u}+1) - (3\sinh^2 u + 2)\sinh u\, e^{u} - \sinh^2 u \right] , \tag{3.28a}$$

$$<\Delta\hat{x}_2^2> = \frac{1}{4} e^{-2u} + \frac{1}{8\bar{N}} \left[u^2 e^{-2u} - u(e^{-2u}+1) + (3\sinh^2 u + 2)\sinh u\, e^{-u} - \sinh^2 u \right] , \tag{3.28b}$$

which are exactly the results obtained by Hillery and Zubairy.[7] The variance of the squeezed quadrature, including the dominant correction for at best moderate squeezing only, is

$$<\Delta\hat{x}_2^2> = \frac{1}{4} e^{-2u} + \frac{1}{64\bar{N}} e^{2u} , \tag{3.29}$$

which agrees with Eq. (2.18), validating our heuristic picture of the effects of pump fluctuations on squeezing.

B. The two-mode PA

The analysis of the two-mode PA is similar to that of the one-mode PA. The equation of motion is again von Neumann's equation in the interaction representation, Eq. (3.1), with the two-mode interaction Hamiltonian given by Eq. (1.4). Initially, we assume the signal modes are in vacuum states, and the pump mode is in a coherent state:

$$\hat{\rho}(0)=\hat{\rho}_I(0)=|0,0,\alpha_0\rangle\langle 0,0,\alpha_0| \ . \tag{3.30}$$

The positive-P representation for the density operator is

$$\hat{\rho}_I(t)=\iiiint\!\!\iint P(\alpha_1,\alpha_2,\alpha_p,\beta_1,\beta_2,\beta_p,t)\,\hat{\Lambda}(\alpha_1,\alpha_2,\alpha_p,\beta_1,\beta_2,\beta_p)$$

$$\times d^2\alpha_1\, d^2\alpha_2\, d^2\alpha_p\, d^2\beta_1\, d^2\beta_2\, d^2\beta_p \ , \tag{3.31}$$

where the operator $\hat{\Lambda}(\alpha_1,\alpha_2,\alpha_p,\beta_1,\beta_2,\beta_p)$ is given by

$$\hat{\Lambda}(\alpha_1,\alpha_2,\alpha_p,\beta_1,\beta_2,\beta_p)\equiv \frac{|\alpha_1,\alpha_2,\alpha_p\rangle\langle\beta_1^*,\beta_2^*,\beta_p^*|}{\langle\beta_1^*,\beta_2^*,\beta_p^*|\alpha_1,\alpha_2,\alpha_p\rangle}$$

$$=e^{-(\alpha_1\beta_1+\alpha_2\beta_2+\alpha_p\beta_p)}e^{\alpha_1\hat{a}_1^{\dagger}+\alpha_2\hat{a}_2^{\dagger}+\alpha_p\hat{a}_p^{\dagger}}|0,0,0\rangle\langle 0,0,0|e^{\beta_1\hat{a}_1+\beta_2\hat{a}_2+\beta_p\hat{a}_p} \ . \tag{3.31a}$$

Substituting Eqs. (3.31) into Eq. (3.1), using the two-mode version of the operator identities in Eqs. (3.4), and integrating by parts, we find the Fokker-Planck equation for the

two-mode PA:

$$\frac{\partial P}{\partial \tau} = \Bigg[-\beta_2\alpha_p \frac{\partial}{\partial \alpha_1} - \alpha_2\beta_p \frac{\partial}{\partial \beta_1} - \beta_1\alpha_p \frac{\partial}{\partial \alpha_2} - \alpha_1\beta_p \frac{\partial}{\partial \beta_2}$$

$$+\alpha_1\alpha_2 \frac{\partial}{\partial \alpha_p} + \beta_1\beta_2 \frac{\partial}{\partial \beta_p} + \alpha_p \frac{\partial^2}{\partial \alpha_1 \partial \alpha_2} + \beta_p \frac{\partial^2}{\partial \beta_1 \partial \beta_2} \Bigg] P \,, \tag{3.32}$$

where $\tau = \kappa t$ and $P \equiv P(\alpha_1, \alpha_2, \alpha_p, \beta_1, \beta_2, \beta_p, \tau)$.

Proceeding as in the one-mode case (see Appendix for details), we can derive a set of Ito SDEs from the Fokker-Planck equation, Eq. (3.32):

$$d\alpha_1 = \beta_2\alpha_p \, d\tau + \sqrt{\alpha_p} \, dW_1 \,, \tag{3.33a)}$$

$$d\alpha_2 = \beta_1\alpha_p \, d\tau + \sqrt{\alpha_p} \, dW_1^* \,, \tag{3.33b}$$

$$d\beta_1 = \alpha_2\beta_p \, d\tau + \sqrt{\beta_p} \, dW_2 \,, \tag{3.33c}$$

$$d\beta_2 = \alpha_1\beta_p \, d\tau + \sqrt{\beta_p} \, dW_2^* \,, \tag{3.33d}$$

$$d\alpha_p = -\alpha_1\alpha_2 \, d\tau \,, \tag{3.33e}$$

$$d\beta_p = -\beta_1\beta_2 \, d\tau \,. \tag{3.33f}$$

The complex Wiener increments dW_1 and dW_2 are defined by

$$dW_1 = \frac{dW_{1x} + i dW_{1y}}{\sqrt{2}} \,, \tag{3.34a}$$

$$dW_2 = \frac{dW_{2x} + i dW_{2y}}{\sqrt{2}} \,, \tag{3.34b}$$

where dW_{1x}, dW_{1y}, dW_{2x}, and dW_{2y} are independent, real Wiener increments, and, in the

Ito calculus,

$$dW_{1s}^2 = dW_{2s}^2 = d\tau \qquad s = x, y \ . \tag{3.34c}$$

The complex pump amplitudes α_p and β_p are again assumed to consist of a large, real mean value α_0 plus small fluctuations, as in Eqs. (3.8). We define the new variables X_1, Y_1, X_2, Y_2, P_1, and P_2 by

$$X_1 = \frac{1}{2}(\alpha_1 + \beta_2), \quad X_2 = -\frac{i}{2}(\alpha_1 - \beta_2), \tag{3.35a}$$

$$Y_1 = \frac{1}{2}(\alpha_2 + \beta_1), \quad Y_2 = -\frac{i}{2}(\alpha_2 - \beta_1), \tag{3.35b}$$

$$P_1 = \frac{1}{2}(\Delta\alpha + \Delta\beta), \quad P_2 = -\frac{i}{2}(\Delta\alpha - \Delta\beta). \tag{3.35c}$$

It is convenient to change variables one more time:

$$U_1 = X_1 e^{-u}, \quad U_2 = X_2 e^{u}, \tag{3.36a}$$

$$Z_1 = Y_1 e^{-u}, \quad Z_2 = Y_2 e^{u}. \tag{3.36b}$$

The resulting SDEs are

$$dU_1 = \frac{1}{\alpha_0}(U_1 P_1 + U_2 P_2 e^{-2u})\,du + \frac{1}{2}e^{-u}\left[\left(1 + \frac{P_1 + iP_2}{\alpha_0}\right)^{1/2} dV_1 + \left(1 + \frac{P_1 - iP_2}{\alpha_0}\right)^{1/2} dV_2^*\right], \tag{3.37a}$$

$$dZ_1=\frac{1}{\alpha_0}(Z_1P_1+Z_2P_2e^{-2u})\,du+\frac{1}{2}e^{-u}\left[\left(1+\frac{P_1+iP_2}{\alpha_0}\right)^{1/2}dV_1^*+\left(1+\frac{P_1-iP_2}{\alpha_0}\right)^{1/2}dV_2\right],$$

(3.37b)

$$dU_2=\frac{1}{\alpha_0}(U_1P_2e^{2u}-U_2P_1)\,du-\frac{i}{2}e^{u}\left[\left(1+\frac{P_1+iP_2}{\alpha_0}\right)^{1/2}dV_1-\left(1+\frac{P_1-iP_2}{\alpha_0}\right)^{1/2}dV_2^*\right],$$

(3.37c)

$$dZ_2=\frac{1}{\alpha_0}(Z_1P_2e^{2u}-Z_2P_1)\,du-\frac{i}{2}e^{u}\left[\left(1+\frac{P_1+iP_2}{\alpha_0}\right)^{1/2}dV_1^*-\left(1+\frac{P_1-iP_2}{\alpha_0}\right)^{1/2}dV_2\right],$$

(3.37d)

$$dP_1=\frac{1}{\alpha_0}(U_2Z_2e^{-2u}-U_1Z_1e^{2u})\,du\,,\tag{3.37e}$$

$$dP_2=-\frac{1}{\alpha_0}(U_1Z_2+U_2Z_1)\,du\,,\tag{3.37f}$$

where $u=\alpha_0\tau$, $dV_1=\sqrt{\alpha_0}\,dW_1$ and $dV_2=\sqrt{\alpha_0}\,dW_2$.

We can obtain an approximate solution to Eqs. (3.37) just as we did in the one-mode case; we formally integrate Eqs. (3.37), expand the square roots, and substitute the expansion Eq. (3.15). We have found the approximate solution up to second order in α_0^{-1}: (i) to zeroth order,

$$U_1^{(0)}(u)=\frac{1}{2}\int_0^u e^{-x}(dS_1+idS_2)\,,\tag{3.38a}$$

$$Z_1^{(0)}(u)=U_1^{(0)*}(u)\,,\tag{3.38b}$$

$$U_2^{(0)}(u)=\frac{1}{2}\int_0^u e^{x}(dS_3-idS_4)\,,\tag{3.38c}$$

$$Z_2^{(0)}(u) = -U_2^{(0)*}(u)\,, \tag{3.38d}$$

$$P_1^{(0)}(u) = P_2^{(0)}(u) = 0\,, \tag{3.38e}$$

(ii) to first order,

$$U_1^{(1)}(u) = Z_1^{(1)}(u) = 0\,, \tag{3.39a}$$

$$U_2^{(1)}(u) = Z_2^{(1)}(u) = 0\,, \tag{3.39b}$$

$$P_1^{(1)}(u) = \int_0^u [U_2^{(0)}(x) Z_2^{(0)}(x) e^{-2x} - U_1^{(0)}(x) Z_1^{(0)}(x) e^{2x}]\, dx\,, \tag{3.39c}$$

$$P_2^{(1)}(u) = -\int_0^u [U_1^{(0)}(x) Z_2^{(0)}(x) + U_2^{(0)}(x) Z_1^{(0)}(x)]\, dx\,, \tag{3.39d}$$

and (iii) to second order,

$$U_1^{(2)}(u) = \int_0^u [U_1^{(0)}(x) P_1^{(1)}(x) + U_2^{(0)}(x) P_2^{(1)}(x) e^{-2x}]\, dx$$

$$+ \frac{1}{4}\int_0^u e^{-x} [P_1^{(1)}(x)(dS_1 + idS_2) - P_2^{(1)}(x)(dS_3 - idS_4)]\,, \tag{3.40a}$$

$$Z_1^{(2)}(u) = \int_0^u [Z_1^{(0)}(x) P_1^{(1)}(x) + Z_2^{(0)} P_2^{(1)}(x) e^{-2x}]\, dx$$

$$+ \frac{1}{4}\int_0^u e^{-x} [P_1^{(1)}(x)(dS_1 - idS_2) + P_2^{(1)}(x)(dS_3 + idS_4)]\,, \tag{3.40b}$$

$$U_2^{(2)}(u) = \int_0^u [U_1^{(0)}(x) P_2^{(1)}(x) e^{2x} - U_2^{(0)}(x) P_1^{(1)}(x)]\, dx$$

$$+ \frac{1}{4}\int_0^u e^{x} [P_1^{(1)}(x)(dS_3 - idS_4) + P_2^{(1)}(x)(dS_1 + idS_2)]\,, \tag{3.40c}$$

$$Z_2^{(2)}(u)=\int_0^u [Z_1^{(0)}(x)P_2^{(1)}(x)e^{2x}-Z_2^{(0)}(x)P_1^{(1)}(x)]\,dx$$

$$-\frac{1}{4}\int_0^u e^x[P_1^{(1)}(x)(dS_3+idS_4)-P_2^{(1)}(x)(dS_1-idS_2)]\,, \tag{3.40d}$$

$$P_1^{(2)}(u)=P_2^{(2)}(u)=0\,. \tag{3.40e}$$

Notice that in Eqs. (3.38) and Eqs. (3.40) we have replaced the complex noise increments by the real Wiener increments dS_1, dS_2, dS_3, and dS_4, where, using Eqs. (3.34),

$$dS_1=\frac{dW_{1x}+dW_{2x}}{\sqrt{2}}\,,\quad dS_2=\frac{dW_{1y}-dW_{2y}}{\sqrt{2}}\,, \tag{3.41a}$$

$$dS_3=\frac{dW_{1y}+dW_{2y}}{\sqrt{2}}\,,\quad dS_4=\frac{dW_{1x}-dW_{2x}}{\sqrt{2}}\,. \tag{3.41b}$$

Also note that, as in the one-mode case, we have dropped all contributions arising from the initial conditions.

By comparing Eqs. (3.38) with Eqs. (3.16), we see that the zeroth-order solutions $U_1^{(0)}(u)$, $Z_1^{(0)}(u)$, $U_2^{(0)}(u)$, and $Z_2^{(0)}(u)$ have real and imaginary parts that are Gaussian variables. Let

$$U_1^{(0)}(u)=Z_1^{(0)*}(u)=Q_1(u)+iQ_2(u)\,, \tag{3.42a}$$

$$U_2^{(0)}(u)=-Z_2^{(0)*}(u)=Q_3(u)+iQ_4(u)\,, \tag{3.42b}$$

where $Q_1(u)$, $Q_2(u)$, $Q_3(u)$, and $Q_4(u)$ are *independent* Gaussian variables with zero mean. We can use Eqs. (3.42) to generalize the one-mode rules [Eqs. (3.22) and Eqs. (3.23)] to the two-mode case: (i) a rule for quadratic moments,

$$<Q_1(u)Q_1(w)>_{av}=<Q_2(u)Q_2(w)>_{av}=\frac{1}{8}(1-e^{-2w})\quad u\geq w\,, \tag{3.43a}$$

$$<Q_3(u)Q_3(w)>_{av}=<Q_4(u)Q_4(w)>_{av}=\frac{1}{8}(e^{2w}-1) \qquad u \geq w\ , \tag{3.43b}$$

$$<Q_i(u)Q_j(u)>_{av}=0 \qquad i \neq j\ , \tag{3.43c}$$

and (ii) a rule for quartic moments,

$$\begin{aligned}<Q_1(u)Q_1(v)Q_1(w)Q_1(z)>_{av}=&<Q_1(u)Q_1(v)>_{av}<Q_1(w)Q_1(z)>_{av}\\&+<Q_1(u)Q_1(w)>_{av}<Q_1(v)Q_1(z)>_{av}\\&+<Q_1(u)Q_1(z)>_{av}<Q_1(v)Q_1(w)>_{av}\ ,\end{aligned} \tag{3.44a}$$

$$<Q_2(u)Q_2(v)Q_2(w)Q_2(z)>_{av}=<Q_1(u)Q_1(v)Q_1(w)Q_1(z)>_{av}\ , \tag{3.44b}$$

$$\begin{aligned}<Q_3(u)Q_3(v)Q_3(w)Q_3(z)>_{av}=&<Q_3(u)Q_3(v)>_{av}<Q_3(w)Q_3(z)>_{av}\\&+<Q_3(u)Q_3(w)>_{av}<Q_3(v)Q_3(z)>_{av}\\&+<Q_3(u)Q_3(z)>_{av}<Q_3(v)Q_3(w)>_{av}\ ,\end{aligned} \tag{3.44c}$$

$$<Q_4(u)Q_4(v)Q_4(w)Q_4(z)>_{av}=<Q_3(u)Q_3(v)Q_3(w)Q_3(z)>_{av}\ . \tag{3.44d}$$

We can calculate the two-mode squeezing by repeated application of (i) and (ii). The two-mode quadrature-phase amplitudes are defined by

$$\hat{X}_1=\frac{1}{2}(\hat{a}_1+\hat{a}_2^{\dagger})\ , \qquad \hat{X}_2=-\frac{i}{2}(\hat{a}_1-\hat{a}_2^{\dagger})\ , \tag{3.45a}$$

$$\hat{P}_1=\frac{1}{2}(\hat{a}_p+\hat{a}_p^{\dagger})\ , \qquad \hat{P}_2=-\frac{i}{2}(\hat{a}_p-\hat{a}_p^{\dagger})\ . \tag{3.45b}$$

The two-mode signal quadrature-phase amplitudes are *not* Hermitian operators. The mean-square uncertainties in the two-mode quadrature-phase amplitudes are given by[14]

$$<|\Delta\hat{X}_1|^2> \equiv \frac{1}{2}<\hat{X}_1^{\dagger}\hat{X}_1+\hat{X}_1\hat{X}_1^{\dagger}> - <\hat{X}_1><\hat{X}_1^{\dagger}>, \tag{3.46a}$$

$$<|\Delta\hat{X}_2|^2> \equiv \frac{1}{2}<\hat{X}_2^{\dagger}\hat{X}_2+\hat{X}_2\hat{X}_2^{\dagger}> - <\hat{X}_2><\hat{X}_2^{\dagger}>, \tag{3.46b}$$

or, in terms of the stochastic c-numbers, by

$$<|\Delta\hat{X}_1|^2> = \frac{1}{4} + <X_1Y_1>_{av} - <X_1>_{av}<Y_1>_{av}, \tag{3.47a}$$

$$<|\Delta\hat{X}_2|^2> = \frac{1}{4} + <X_2Y_2>_{av} - <X_2>_{av}<Y_2>_{av}. \tag{3.47b}$$

From Eqs. (3.47) we see that X_1 and Y_1 are the c-number equivalents of the operators $\hat{X}_1$ and its Hermitian conjugate $\hat{X}_1^{\dagger}$, respectively, and X_2 and Y_2 are the c-number equivalents of the operators $\hat{X}_2$ and its Hermitian conjugate $\hat{X}_2^{\dagger}$. Substituting Eq. (3.15), Eqs. (3.38), Eqs. (3.39), and Eqs. (3.40) into Eqs. (3.47), we have to second order in α_0^{-1}

$$<|\Delta\hat{X}_1|^2> = \frac{1}{4} + <U_1^{(0)}(u)Z_1^{(0)}(u)>_{av} e^{2u} + <U_1^{(0)}(u)Z_1^{(2)}(u)+U_1^{(2)}(u)Z_1^{(0)}(u)>_{av} e^{2u}, \tag{3.48a}$$

$$<|\Delta\hat{X}_2|^2> = \frac{1}{4} + <U_2^{(0)}(u)Z_2^{(0)}(u)>_{av} e^{-2u} + \frac{1}{\alpha_0^2}<U_2^{(0)}(u)Z_2^{(2)}(u)+U_2^{(2)}(u)Z_2^{(0)}(u)>_{av} e^{-2u}, \tag{3.48b}$$

since the expectation values of X_1, Y_1, X_2, and Y_2 are zero.

Repeated application of the two-mode rules (i) and (ii) yields the mean-squared

uncertainties correct to semiclassical order $\alpha_0^{-2}=\bar{N}^{-1}$:

$$<|\Delta\hat{X}_1|^2>=\frac{1}{4}e^{2u}+\frac{1}{8\bar{N}}\left[u^2e^{2u}+u(\frac{3}{2}e^{2u}+1)-(4\sinh^2u+\frac{5}{2})\sinh u\ e^{u}-\frac{3}{2}\sinh^2u\right],$$

(3.49a)

$$<|\Delta\hat{X}_2|^2>=\frac{1}{4}e^{-2u}+\frac{1}{8\bar{N}}\left[u^2e^{-2u}-u(\frac{3}{2}e^{-2u}+1)+(4\sinh^2u+\frac{5}{2})\sinh u\ e^{-u}-\frac{3}{2}\sinh^2u\right],$$

(3.49b)

which are slightly different from the one-mode result, Eqs. (3.28). When the dominant correction only is kept, the uncertainty in the squeezed quadrature is

$$<|\Delta\hat{X}_2|^2>\cong\frac{1}{4}e^{-2u}+\frac{1}{64\bar{N}}e^{2u}, \tag{3.50}$$

which is the same as the dominant correction found for the one-mode case, Eq.(3.29), in contrast to the result obtained by Scharf and Walls,[8] Eq. (1.6).

4. CONCLUSION

We have calculated, for the one- and two-mode PA, the explicit corrections for squeezing to order $\bar{N}^{-1}$, due to a quantum pump in a coherent state with an average photon number of $\bar{N}$. We found that the pump's phase noise is responsible for the dominant contribution to the limitations on squeezing for any number of signal modes. We also briefly discuss when traveling-wave calculations can be treated by Hamiltonian methods in the most direct way. This was done by discretizing the continuum problem.

APPENDIX: DETAILED DERIVATION OF THE STOCHASTIC DIFFERENTIAL EQUATIONS

We will first consider the one-mode PA. Equations (3.6) allow us to choose the derivatives in Eq. (3.5) so that a Fokker-Planck equation with real drift and positive-semidefinite diffusion result:

$$\frac{\partial}{\partial \xi} = \frac{\partial}{\partial \xi_x} = -i\frac{\partial}{\partial \xi_y}, \tag{A.1}$$

where ξ represents any of the complex variables α, β, α_p, or β_p, and "x" and "y" denote the real and imaginary parts of the complex number ξ. For the drift terms, we have

$$-\alpha_p \beta \frac{\partial}{\partial \alpha} = -\mathrm{Re}(\alpha_p \beta)\frac{\partial}{\partial \alpha_x} - \mathrm{Im}(\alpha_p \beta)\frac{\partial}{\partial \alpha_y}, \tag{A.2a}$$

$$-\alpha \beta_p \frac{\partial}{\partial \beta} = -\mathrm{Re}(\alpha \beta_p)\frac{\partial}{\partial \beta_x} - \mathrm{Im}(\alpha \beta_p)\frac{\partial}{\partial \beta_y}, \tag{A.2b}$$

$$\frac{\alpha^2}{2}\frac{\partial}{\partial \alpha_p} = \mathrm{Re}\left[\frac{\alpha^2}{2}\right]\frac{\partial}{\partial \alpha_{px}} + \mathrm{Im}\left[\frac{\alpha^2}{2}\right]\frac{\partial}{\partial \alpha_{py}}, \tag{A.2c}$$

$$\frac{\beta^2}{2}\frac{\partial}{\partial \beta_p} = \mathrm{Re}\left[\frac{\beta^2}{2}\right]\frac{\partial}{\partial \beta_{px}} + \mathrm{Im}\left[\frac{\beta^2}{2}\right]\frac{\partial}{\partial \beta_{py}}. \tag{A.2d}$$

The corresponding drift coefficients are

$$A_1 = \mathrm{Re}(\alpha_p \beta), \qquad A_2 = \mathrm{Im}(\alpha_p \beta), \tag{A.3a}$$

$$A_3 = -\mathrm{Re}\left[\frac{\alpha^2}{2}\right], \qquad A_4 = -\mathrm{Im}\left[\frac{\alpha^2}{2}\right], \tag{A.3b}$$

$$A_5 = \mathrm{Re}(\alpha \beta_p), \qquad A_6 = \mathrm{Im}(\alpha \beta_p), \tag{A.3c}$$

$$A_7 = -\mathrm{Re}\left[\frac{\beta^2}{2}\right], \qquad A_8 = -\mathrm{Im}\left[\frac{\beta^2}{2}\right], \tag{A.3d}$$

where the subscript 1 corresponds to α_x, 2 to α_y, 3 to α_{px}, 4 to α_{py}, 5 to β_x, 6 to β_y, 7 to β_{px}, and 8 to β_{py}.

To simplify the derivation of the diffusion matrix, we let $\alpha_p = (x+iy)^2$ and $\beta_p = (u+iv)^2$.[21] Using Eq. (A.1), we find

$$\alpha_p \frac{\partial^2}{\partial \alpha^2} = (x+iy)^2 \frac{\partial^2}{\partial \alpha^2} = x^2 \frac{\partial^2}{\partial \alpha_x^2} + 2xy \frac{\partial^2}{\partial \alpha_x \alpha_y} + y^2 \frac{\partial^2}{\partial \alpha_y^2}, \tag{A.4a}$$

$$\beta_p \frac{\partial^2}{\partial \beta^2} = (u+iv)^2 \frac{\partial^2}{\partial \beta^2} = u^2 \frac{\partial^2}{\partial \beta_x^2} + 2uv \frac{\partial^2}{\partial \beta_x \partial \beta_y} + v^2 \frac{\partial^2}{\partial \beta_y^2}. \tag{A.4b}$$

The resulting nonzero elements of the one-mode diffusion matrix are

$$D_{11} = x^2, \quad D_{21} = xy, \tag{A.5a}$$

$$D_{21} = xy, \quad D_{22} = y^2, \tag{A.5b}$$

$$D_{55} = u^2, \quad D_{56} = uv, \tag{A.5c}$$

$$D_{65} = uv, \quad D_{66} = v^2, \tag{A.5d}$$

where we have used the same subscript convention as in Eqs. (A.3). In matrix form,

Eqs. (A.5) become

$$\mathbf{D}=\begin{bmatrix} x^2 & xy & 0 & 0 & 0 & 0 & 0 & 0 \\ xy & y^2 & 0 & 0 & 0 & 0 & 0 & 0 \\ 0 & 0 & 0 & 0 & 0 & 0 & 0 & 0 \\ 0 & 0 & 0 & 0 & 0 & 0 & 0 & 0 \\ 0 & 0 & 0 & 0 & u^2 & uv & 0 & 0 \\ 0 & 0 & 0 & 0 & uv & v^2 & 0 & 0 \\ 0 & 0 & 0 & 0 & 0 & 0 & 0 & 0 \\ 0 & 0 & 0 & 0 & 0 & 0 & 0 & 0 \end{bmatrix} . \tag{A.6}$$

The diffusion matrix **D** can be written as the product of a matrix **B** with its transpose $\mathbf{B}^T$:

$$\mathbf{D}=\mathbf{B}\mathbf{B}^T . \tag{A.7}$$

We can easily show that

$$\mathbf{B}=\frac{1}{\sqrt{2}}\begin{bmatrix} x & x & 0 & 0 & 0 & 0 & 0 & 0 \\ y & y & 0 & 0 & 0 & 0 & 0 & 0 \\ 0 & 0 & 0 & 0 & 0 & 0 & 0 & 0 \\ 0 & 0 & 0 & 0 & 0 & 0 & 0 & 0 \\ 0 & 0 & 0 & 0 & u & u & 0 & 0 \\ 0 & 0 & 0 & 0 & v & v & 0 & 0 \\ 0 & 0 & 0 & 0 & 0 & 0 & 0 & 0 \\ 0 & 0 & 0 & 0 & 0 & 0 & 0 & 0 \end{bmatrix} . \tag{A.8}$$

The Fokker-Planck equation corresponding to the drift coefficients in Eqs. (A.3) and the diffusion matrix Eq. (A.6) has the form

$$\frac{\partial P}{\partial \tau}=\left[-\sum_{i=1}^{N}\frac{\partial}{\partial x_i}A_i+\frac{1}{2}\sum_{i,j=1}^{N}\frac{\partial^2}{\partial x_i \partial x_j}[\mathbf{B}\mathbf{B}^T]_{ij}\right] P . \tag{A.9}$$

Using the Ito calculus, we can derive a set of SDEs from the Fokker-Planck equation Eq. (A.9):

$$dx_i = A_i\, d\tau + \sum_{j=1}^{N} \mathrm{B}_{ij}\, dW_j , \qquad i,j=1,\ldots,N , \tag{A.10}$$

where dW_j is a Wiener increment, and, in the Ito calculus,

$$dW_i\, dW_j = \delta_{ij}\, d\tau, \quad i,j = 1,...,N\ . \tag{A.10a}$$

For the one-mode PA, $x_1 = \alpha_x$, $x_2 = \alpha_y$, etc., $dW_1 = dW_{\alpha_x}$, $dW_2 = dW_{\alpha_y}$, etc., and $N = 8$. Substituting Eqs. (A.3) and Eq. (A.8) into Eq. (A.10) and recalling that $x = \mathrm{Re}\sqrt{\alpha_p}$, $y = \mathrm{Im}\sqrt{\alpha_p}$, $u = \mathrm{Re}\sqrt{\beta_p}$, and $v = \mathrm{Im}\sqrt{\beta_p}$, we find the Ito SDEs for the one-mode PA:

$$d\alpha_x = \mathrm{Re}(\alpha_p \beta)\, d\tau + \mathrm{Re}\sqrt{\alpha_p}\, \frac{dW_{\alpha_x} + dW_{\alpha_y}}{\sqrt{2}}\ , \tag{A.11a}$$

$$d\alpha_y = \mathrm{Im}(\alpha_p \beta)\, d\tau + \mathrm{Im}\sqrt{\alpha_p}\, \frac{dW_{\alpha_x} + dW_{\alpha_y}}{\sqrt{2}}\ , \tag{A.11b}$$

$$d\beta_x = \mathrm{Re}(\alpha\beta_p)\, d\tau + \mathrm{Re}\sqrt{\beta_p}\, \frac{dW_{\beta_x} + dW_{\beta_y}}{\sqrt{2}}\ , \tag{A.11c}$$

$$d\beta_y = \mathrm{Im}(\alpha\beta_p)\, d\tau + \mathrm{Im}\sqrt{\beta_p}\, \frac{dW_{\beta_x} + dW_{\beta_y}}{\sqrt{2}}\ , \tag{A.11d}$$

$$d\alpha_{px} = -\mathrm{Re}\left[\frac{\alpha^2}{2}\right] d\tau\ , \tag{A.11e}$$

$$d\alpha_{py} = -\mathrm{Im}\left[\frac{\alpha^2}{2}\right] d\tau\ , \tag{A.11f}$$

$$d\beta_{px} = -\mathrm{Re}\left[\frac{\beta^2}{2}\right] d\tau\ , \tag{A.11g}$$

$$d\beta_{py} = -\mathrm{Im}\left[\frac{\beta^2}{2}\right] d\tau\ . \tag{A.11h}$$

By defining the new Wiener increments

$$dW_1 = \frac{dW_{\alpha_x} + dW_{\alpha_y}}{\sqrt{2}}\ , \tag{A.12a}$$

$$dW_2 = \frac{dW_{\beta_x} + dW_{\beta_y}}{\sqrt{2}}, \tag{A.12b}$$

and writing Eqs. (A.11) in complex form ($d\alpha = d\alpha_x + id\alpha_y$, etc.), we obtain the complex SDEs Eqs. (3.7).

The derivation for the two-mode PA proceeds in a similar fashion. We can use the two-mode equivalents of Eqs. (3.6) to show that Eq. (A.1) applies in the two-mode case as well. Applying Eq. (A.1) to the drift terms of Eq. (3.32) results in

$$-\beta_2\alpha_p \frac{\partial}{\partial\alpha_1} = -\mathrm{Re}(\beta_2\alpha_p)\frac{\partial}{\partial\alpha_{1x}} - \mathrm{Im}(\beta_2\alpha_p)\frac{\partial}{\partial\alpha_{1y}}, \tag{A.13a}$$

$$-\alpha_2\beta_p \frac{\partial}{\partial\beta_1} = -\mathrm{Re}(\alpha_2\beta_p)\frac{\partial}{\partial\beta_{1x}} - \mathrm{Im}(\alpha_2\beta_p)\frac{\partial}{\partial\beta_{1y}}, \tag{A.13b}$$

$$-\beta_1\alpha_p \frac{\partial}{\partial\alpha_2} = -\mathrm{Re}(\beta_1\alpha_p)\frac{\partial}{\partial\alpha_{2x}} - \mathrm{Im}(\beta_1\alpha_p)\frac{\partial}{\partial\alpha_{2y}}, \tag{A.13c}$$

$$-\alpha_1\beta_p \frac{\partial}{\partial\beta_2} = -\mathrm{Re}(\alpha_1\beta_p)\frac{\partial}{\partial\beta_{2x}} - \mathrm{Im}(\alpha_1\beta_p)\frac{\partial}{\partial\beta_{2y}}, \tag{A.13d}$$

$$\alpha_1\alpha_2 \frac{\partial}{\partial\alpha_p} = \mathrm{Re}(\alpha_1\alpha_2)\frac{\partial}{\partial\alpha_{px}} + \mathrm{Im}(\alpha_1\alpha_2)\frac{\partial}{\partial\alpha_{py}}, \tag{A.13e}$$

$$\beta_1\beta_2 \frac{\partial}{\partial\beta_p} = \mathrm{Re}(\beta_1\beta_2)\frac{\partial}{\partial\beta_{px}} + \mathrm{Im}(\beta_1\beta_2)\frac{\partial}{\partial\beta_{py}}. \tag{A.13f}$$

The corresponding drift coefficients are

$$A_1 = \mathrm{Re}(\beta_2\alpha_p), \quad A_2 = \mathrm{Im}(\beta_2\alpha_p), \tag{A.14a}$$

$$A_3 = \mathrm{Re}(\beta_1\alpha_p), \quad A_4 = \mathrm{Im}(\beta_1\alpha_p), \tag{A.14b}$$

$$A_5 = \mathrm{Re}(\alpha_2\beta_p), \quad A_6 = \mathrm{Im}(\alpha_2\beta_p), \tag{A.14c}$$

$$A_7 = \mathrm{Re}(\alpha_1 \beta_p), \quad A_8 = \mathrm{Im}(\alpha_1 \beta_p), \tag{A.14d}$$

$$A_9 = -\mathrm{Re}(\alpha_1 \alpha_2), \quad A_{10} = -\mathrm{Im}(\alpha_1 \alpha_2), \tag{A.14e}$$

$$A_{11} = -\mathrm{Re}(\beta_1 \beta_2), \quad A_{12} = -\mathrm{Im}(\beta_1 \beta_2), \tag{A.14f}$$

where the subscript 1 corresponds to α_{1x}, 2 to α_{1y}, 3 to α_{2x}, 4 to α_{2y}, 5 to β_{1x}, 6 to β_{1y}, 7 to β_{2x}, 8 to β_{2y}, 9 to α_{px}, 10 to α_{py}, 11 to β_{px}, and 12 to β_{py}.

As in the one-mode case, we let $\alpha_p = (x + iy)^2$ and $\beta_p = (u + iv)^2$. We choose the derivatives so that

$$\alpha_p \frac{\partial^2}{\partial \alpha_1 \partial \alpha_2} = \frac{1}{4}\left[(x^2 + y^2)\left(\frac{\partial^2}{\partial \alpha_{1x}^2} + \frac{\partial^2}{\partial \alpha_{1y}^2} + \frac{\partial^2}{\partial \alpha_{2x}^2} + \frac{\partial^2}{\partial \alpha_{2y}^2} \right) \right.$$

$$\left. + 2(x^2 - y^2)\left(\frac{\partial^2}{\partial \alpha_{1x} \partial \alpha_{2x}} - \frac{\partial^2}{\partial \alpha_{1y} \partial \alpha_{2y}} \right) + 4xy\left(\frac{\partial^2}{\partial \alpha_{1x} \partial \alpha_{2y}} + \frac{\partial^2}{\partial \alpha_{1y} \partial \alpha_{2x}} \right) \right], \tag{A.15a}$$

$$\beta_p \frac{\partial^2}{\partial \beta_1 \partial \beta_2} = \frac{1}{4}\left[(u^2 + v^2)\left(\frac{\partial^2}{\partial \beta_{1x}^2} + \frac{\partial^2}{\partial \beta_{1y}^2} + \frac{\partial^2}{\partial \beta_{2x}^2} + \frac{\partial^2}{\partial \beta_{2y}^2} \right) \right.$$

$$\left. + 2(u^2 - v^2)\left(\frac{\partial^2}{\partial \beta_{1x} \partial \beta_{2x}} - \frac{\partial^2}{\partial \beta_{1y} \partial \beta_{2y}} \right) + 4uv\left(\frac{\partial^2}{\partial \beta_{1x} \partial \beta_{2x}} + \frac{\partial^2}{\partial \beta_{1y} \partial \beta_{2x}} \right) \right]. \tag{A.15b}$$

The resulting nonzero elements of the two-mode diffusion matrix are

$$D_{11} = D_{22} = D_{33} = D_{44} = \frac{1}{2}(x^2 + y^2), \tag{A.16a}$$

$$D_{13} = -D_{24} = \frac{1}{2}(x^2 - y^2), \tag{A.16b}$$

$$D_{14}=D_{23}=xy\ , \tag{A.16c}$$

$$D_{55}=D_{66}=D_{77}=D_{88}=\frac{1}{2}(u^2+v^2)\ , \tag{A.16d}$$

$$D_{57}=-D_{68}=\frac{1}{2}(u^2-v^2)\ , \tag{A.16e}$$

$$D_{58}=D_{67}=uv\ , \tag{A.16f}$$

where the remaining nonzero elements are obtained from the symmetry relation $D_{ij}=D_{ji}$, and the subscripts follow the same convention defined in Eqs. (A.14). In matrix form, Eq. (A.16) becomes

$$\mathbf{D}=\frac{1}{2}\begin{bmatrix} x^2+y^2 & 0 & x^2-y^2 & 2xy & 0 & 0 & 0 & 0 \\ 0 & x^2+y^2 & 2xy & y^2-x^2 & 0 & 0 & 0 & 0 \\ x^2-y^2 & 2xy & x^2+y^2 & 0 & 0 & 0 & 0 & 0 \\ 2xy & y^2-x^2 & 0 & x^2+y^2 & 0 & 0 & 0 & 0 \\ 0 & 0 & 0 & 0 & u^2+v^2 & 0 & u^2-v^2 & 2uv \\ 0 & 0 & 0 & 0 & 0 & u^2+v^2 & 2uv & v^2-u^2 \\ 0 & 0 & 0 & 0 & u^2-v^2 & 2uv & u^2+v^2 & 0 \\ 0 & 0 & 0 & 0 & 2uv & v^2-u^2 & 0 & u^2+v^2 \end{bmatrix}. \tag{A.17}$$

Here we have suppressed the rows and columns of $\mathbf{D}$ corresponding to α_p and β_p since all elements of these rows and columns are zero. The diffusion matrix $\mathbf{D}$ can be written as a product of a matrix $\mathbf{B}$ and its transpose:

$$\mathbf{D}=\mathbf{B}\mathbf{B}^{\mathrm{T}}\ . \tag{A.18}$$

We find that

$$\mathbf{B}=\frac{1}{2}\begin{bmatrix} -y & -y & x & x & 0 & 0 & 0 & 0 \\ x & x & y & y & 0 & 0 & 0 & 0 \\ y & y & x & x & 0 & 0 & 0 & 0 \\ -x & -x & y & y & 0 & 0 & 0 & 0 \\ 0 & 0 & 0 & 0 & -v & -v & u & u \\ 0 & 0 & 0 & 0 & u & u & v & v \\ 0 & 0 & 0 & 0 & v & v & u & u \\ 0 & 0 & 0 & 0 & -u & -u & v & v \end{bmatrix}. \tag{A.19}$$

The Fokker-Planck equation corresponding to the drift coefficients Eqs. (A.14) and the diffusion matrix Eq. (A.17) is of the form Eq. (A.9), with the corresponding SDEs of the form Eq. (A.10). In the two-mode case, $N=12$. Substituting Eq. (A.14) and Eq. (A.19) into Eq. (A.10), and recalling that $x=\mathrm{Re}\sqrt{\alpha_p}$, $y=\mathrm{Im}\sqrt{\alpha_p}$, $u=\mathrm{Re}\sqrt{\beta_p}$, and $v=\mathrm{Im}\sqrt{\beta_p}$, we find the SDEs for the two-mode PA:

$$d\alpha_{1x}=\mathrm{Re}(\beta_2\alpha_p)\,d\tau+\frac{1}{\sqrt{2}}(\mathrm{Re}\sqrt{\alpha_p}\,dW_{1x}-\mathrm{Im}\sqrt{\alpha_p}\,dW_{1y}), \tag{A.20a}$$

$$d\alpha_{1y}=\mathrm{Im}(\beta_2\alpha_p)\,d\tau+\frac{1}{\sqrt{2}}(\mathrm{Im}\sqrt{\alpha_p}\,dW_{1x}+\mathrm{Re}\sqrt{\alpha_p}\,dW_{1y}), \tag{A.20b}$$

$$d\alpha_{2x}=\mathrm{Re}(\beta_1\alpha_p)\,d\tau+\frac{1}{\sqrt{2}}(\mathrm{Re}\sqrt{\alpha_p}\,dW_{1x}+\mathrm{Im}\sqrt{\alpha_p}\,dW_{1y}), \tag{A.20c}$$

$$d\alpha_{2y}=\mathrm{Im}(\beta_1\alpha_p)\,d\tau+\frac{1}{\sqrt{2}}(\mathrm{Im}\sqrt{\alpha_p}\,dW_{1x}-\mathrm{Re}\sqrt{\alpha_p}\,dW_{1y}), \tag{A.20d}$$

$$d\beta_{1x}=\mathrm{Re}(\alpha_2\beta_p)\,d\tau+\frac{1}{\sqrt{2}}(\mathrm{Re}\sqrt{\beta_p}\,dW_{2x}-\mathrm{Im}\sqrt{\beta_p}\,dW_{2y}), \tag{A.20e}$$

$$d\beta_{1y}=\mathrm{Im}(\alpha_2\beta_p)\,d\tau+\frac{1}{\sqrt{2}}(\mathrm{Im}\sqrt{\beta_p}\,dW_{2x}+\mathrm{Re}\sqrt{\beta_p}\,dW_{2y}), \tag{A.20f}$$

$$d\beta_{2x}=\mathrm{Re}(\alpha_1\beta_p)\,d\tau+\frac{1}{\sqrt{2}}(\mathrm{Re}\sqrt{\beta_p}\,dW_{2x}+\mathrm{Im}\sqrt{\beta_p}\,dW_{2y}), \tag{A.20g}$$

$$d\beta_{2y} = \mathrm{Im}(\alpha_1\beta_p)d\tau + \frac{1}{\sqrt{2}}(\mathrm{Im}\sqrt{\beta_p}\, dW_{2x} - \mathrm{Re}\sqrt{\beta_p}\, dW_{2y}), \tag{A.20h}$$

$$d\alpha_{px} = -\mathrm{Re}(\alpha_1\alpha_2)\, d\tau, \tag{A.20i}$$

$$d\alpha_{py} = -\mathrm{Im}(\alpha_1\alpha_2)\, d\tau, \tag{A.20j}$$

$$d\beta_{px} = -\mathrm{Re}(\beta_1\beta_2)\, d\tau, \tag{A.20k}$$

$$d\beta_{py} = -\mathrm{Im}(\beta_1\beta_2)\, d\tau, \tag{A.20l}$$

where

$$dW_{1x} = \frac{dW_{\alpha_{2x}} + dW_{\alpha_{2y}}}{\sqrt{2}}, \quad dW_{1y} = \frac{dW_{\alpha_{1x}} + dW_{\alpha_{1y}}}{\sqrt{2}}, \tag{A.21a}$$

$$dW_{2x} = \frac{dW_{\beta_{2x}} + dW_{\beta_{2y}}}{\sqrt{2}}, \quad dW_{2y} = \frac{dW_{\beta_{1x}} + dW_{\beta_{1y}}}{\sqrt{2}}. \tag{A.21b}$$

By defining the complex Wiener increments

$$dW_1 = \frac{dW_{1x} + i dW_{1y}}{\sqrt{2}}, \tag{A.22a}$$

$$dW_2 = \frac{dW_{2x} + i dW_{2y}}{\sqrt{2}}, \tag{A.22b}$$

and writing Eqs. (A.20) in complex form, we obtain the complex SDEs Eqs. (3.33).

The choice of derivatives in Eqs. (A.15) is certainly not an obvious one. One might make a more reasonable choice such as

$$\alpha_p \frac{\partial^2}{\partial\alpha_1\alpha_2} = x^2 \frac{\partial^2}{\partial\alpha_{1x}\partial\alpha_{2x}} + xy\left[\frac{\partial^2}{\partial\alpha_{1x}\partial\alpha_{2y}} + \frac{\partial^2}{\partial\alpha_{1y}\partial\alpha_{2x}}\right] + y^2 \frac{\partial^2}{\partial\alpha_{1y}\partial\alpha_{2y}}, \tag{A.23a}$$

$$\beta_p \frac{\partial^2}{\partial\beta_1\partial\beta_2} = u^2 \frac{\partial^2}{\partial\beta_{1x}\partial\beta_{2x}} + uv\left[\frac{\partial^2}{\partial\beta_{1x}\partial\beta_{2y}} + \frac{\partial^2}{\partial\beta_{1y}\partial\beta_{2x}}\right] + v^2 \frac{\partial^2}{\partial\beta_{1y}\partial\beta_{2y}}. \tag{A.23b}$$

A similar choice worked quite well for the one-mode PA. For the two-mode PA, however, this choice leads to a diffusion matrix that is *not* positive-semidefinite, which in turn results in a complex matrix **B**. The resulting SDEs for the "real" and "imaginary" parts of α_1, α_2, β_1, β_2, α_p, and β_p are *complex* rather than real. Writing the SDEs in complex form, however, results in the same set of complex SDEs that one obtains with the original choice of derivatives, Eqs. (3.33). One can then work backwards to find the correct choice of derivatives, i.e., the one that results in a positive-semidefinite diffusion matrix **D** and thus a real matrix **B**.

REFERENCES

1. A. Yariv, *Quantum Electronics* (Wiley, New York, 1975), Chap. 17.
2. R. G. Smith, in *Laser Handbook,* F. T. Arrechi and E. O. Shulz-Dubois, eds. (North Holland, Amsterdam, 1972), Vol. I, p. 837.
3. H. Takahashi, Adv. Commun. Syst. **1**, 227 (1965), especially Sec. VI.
4. E. Y. C. Lu, Lett. Nuovo Cimento **3**, 585 (1972).
5. D. Stoler, Phys. Rev. Lett. **33**, 1397 (1974).
6. K. Wódkiewicz and M. S. Zubairy, Phys. Rev. A **27**, 2003 (1983).
7. M. Hillery and M. S. Zubairy, Phys. Rev. A **29**, 1275 (1984).
8. G. Scharf and D. F. Walls, Opt. Commun. **50**, 245 (1984).
9. M. Hillery and M. S. Zubairy, Phys. Rev. A **26**, 451 (1982).
10. M. S. Zubairy, private communication.
11. G. Scharf, Annals of Physics **83**, 71 (1974).
12. G. Scharf and R. Weiss, Helvetica Physica Acta **47**, 505 (1974).
13. G. Scharf, Helvetica Physica Acta **48**, 329 (1975); **50**, 253 (1977).
14. C. M. Caves and B. L. Schumaker, Phys. Rev. A **31**, 3068 (1985).
15. C. M. Caves and D. D. Crouch, J. Opt. Soc. Am. B **4**, 1535 (1987); see also Chapter 2 of this thesis.
16. P. D. Drummond and C. W. Gardiner, J. Phys. A **13**, 2353 (1980).
17. C. W. Gardiner, *Handbook of Stochastic Methods* (Springer-Verlag, Berlin, 1983); L. Arnold, *Stochastic Differential Equations* (Wiley, New York, 1973).

18. J. Tucker and D. F. Walls, Phys. Rev. **178**;, 2036 (1969).

19. A. Lane, P. Tombesi, H. J. Carmichael, and D. F. Walls, Opt. Commun **48**, 155 (1983).

20. C. M. Caves and B. L. Schumaker, in *Quantum Optics IV,* J. D. Harvey and D. F. Walls, eds., Springer Proceedings in Physics (Springer-Verlag, New York, 1986).

21. H. J. Carmichael and M. Wolinsky, in *Quantum Optics IV,* J. D. Harvey and D. F. Walls, eds., Springer Proceedings in Physics (Springer-Verlag, New York, 1986).

FIGURE CAPTION

Fig. 1. The effect of pump phase fluctuations on squeezing. The ellipse with solid lines represents ideal squeezing, in which the pump has a well defined phase. Phase fluctuations in the pump cause the orientation of the ellipse to fluctuate about $\phi_p = 0$, with the characteristic angle $\Delta\phi = 1/(4\bar{N}^{1/2})$, feeding noise from the amplified quadrature into the squeezed quadrature.

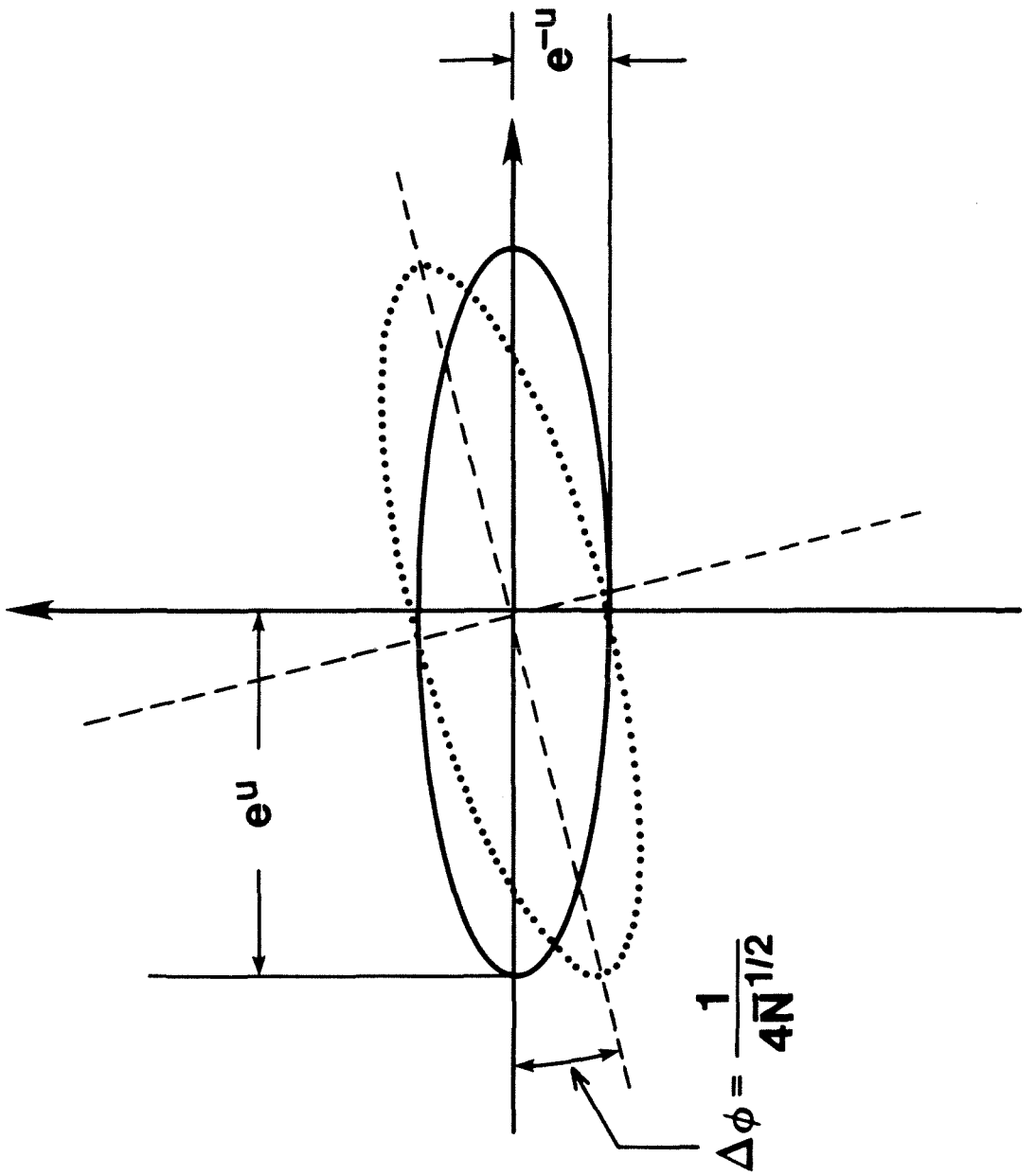

Figure 1

CHAPTER 5

The Spectral Consequences of Internal Squeezing in a Laser Oscillator

by Amnon Yariv and David D. Crouch

An expanded version of a paper submitted to Optics Letters

ABSTRACT

We study the effects of squeezing the intracavity noise in a laser oscillator. In particular, we find that by squeezing the in-phase quadrature of the noise (squeezed amplitude fluctuations), the phase fluctuations are reduced, resulting in a reduction in laser linewidth.

We are witnessing a nascent interest in the possible effect of squeezing[1] on laser oscillators. The few treatments published to date use a quantum theoretical approach to look at phase diffusion but do not consider the all-important amplitude-phase coupling which dominates the phase noise of semiconductor lasers.[2,3]

In this chapter, we solve the classical noise problem of a realistic laser model by making a bold—and possibly unrealizable—assumption, that the in-phase and quadrature Langevin sources which are responsible for the "noisiness" of the laser can be squeezed. We proceed to show that the effect of such squeezing is to reduce the phase noise, including the linewidth, of the laser but, due to amplitude-phase coupling, not to eliminate them altogether. Intensity fluctuations, on the other hand, are fully squeezed.

The method we use is that of Ref. (3), which we will repeat in part for completeness. We start with Maxwell's equations

$$\nabla\times\vec{E}=-\frac{\partial\vec{B}}{\partial t}\,, \tag{1}$$

$$\nabla\times\vec{H}=\sigma\vec{E}+\varepsilon\frac{\partial\vec{E}}{\partial t}+\frac{\partial}{\partial t}[\vec{P}+\vec{p}]\,, \tag{2}$$

where σ is the conductivity of the medium used to account for distributed losses and output coupling, ε is the nonresonant dielectric constant, $\vec{P}$ is the component of the polarization due to stimulated emission, and $\vec{p}$ represents a Langevin noise source due to spontaneous emission. Solving Eqs. (1) and (2) for $\vec{E}(\vec{r},t)$ yields the wave equation

$$\nabla^2\vec{E}-\mu\sigma\frac{\partial\vec{E}}{\partial t}-\mu\varepsilon\frac{\partial^2\vec{E}}{\partial t^2}=\mu\left[\frac{\partial^2\vec{P}}{\partial t^2}+\frac{\partial^2\vec{p}}{\partial t^2}\right]\,, \tag{3}$$

where we have assumed that $\nabla(\nabla\cdot\vec{E})\sim 0$. We then expand the electric field and the polarization in terms of orthogonal cavity modes:

$$\vec{E}(\vec{r},t)=\mathrm{Re}\left[\sum_m E_m(t)\vec{e}_m(\vec{r})\right], \tag{4a}$$

$$\vec{P}(\vec{r},t)=\mathrm{Re}\left[\sum_m P_m(t)\vec{e}_m(\vec{r})\right], \tag{4b}$$

$$\vec{p}(\vec{r},t)=\mathrm{Re}\left[\sum_m p_m(t)\vec{e}_m(\vec{r})\right], \tag{4c}$$

where the spatial mode functions satisfy the homogeneous wave equation

$$\nabla^2\vec{e}_m(\vec{r})+\omega_m^2\mu\varepsilon\vec{e}_m(\vec{r})=0 \tag{5}$$

and the orthogonality relation

$$\int_{\text{cavity}}\vec{e}_n(\vec{r})\cdot\vec{e}_m^*(\vec{r})\,dv=V\delta_{nm}\,. \tag{6}$$

Here V is the cavity volume and ω_m is the passive cavity resonance frequency. By substituting Eqs. (4) into Eq. (3), using the orthogonality relation [Eq. (6)], and assuming that only one mode oscillates, we find the equation of motion for a single-mode laser

$$\ddot{E}(t)+\frac{1}{\tau_p}\dot{E}(t)+\omega_0^2E(t)=-\frac{1}{\varepsilon}[\ddot{P}(t)+\ddot{p}(t)], \tag{7}$$

where τ_p and ω_0 are the photon lifetime and resonant frequency, respectively, of the passive resonator.

We can relate the polarization $P(t)$ to the electric field $E(t)$ by the relation

$$P(t)=\varepsilon_0[\chi^{(1)}+\chi^{(3)}\overline{E^2(t)}]E(t) \tag{8}$$

where $\chi^{(1)}$ and $\chi^{(3)}$ are the *complex* linear and nonlinear susceptibilities of the laser medium, respectively, due to the population inversion; the imaginary part of $\chi^{(3)}$, $\chi_i^{(3)}$,

represents gain saturation, and the real part of $\chi^{(3)}$, $\chi_r^{(3)}$, represents an intensity-dependent index of refraction.[3] We take

$$E(t)=[A_0+\delta(t)]\,e^{i[\omega t+\phi(t)]}, \tag{9}$$

where A_0 is real and $\delta(t)$ and $\phi(t)$ with zero means represent amplitude and phase quantum fluctuations, respectively, caused by $p(t)$. The linearized van der Pol equations resulting from a substitution of Eqs. (8) and (9) in Eq. (7) are[3]

$$\dot{\delta}(t)+\omega_1\delta(t)=\frac{\Delta_i(t)}{2\omega}, \tag{10a}$$

and

$$A_0\dot{\phi}(t)+\frac{3\omega\chi_r^{(3)}A_0^2}{2n^2}\delta(t)=-\frac{\Delta_r(t)}{2\omega}, \tag{10b}$$

where $\omega_1\equiv-3\chi_i^{(3)}A_0^2\omega/2n^2$ and

$$-\frac{\ddot{p}(t)}{\varepsilon}=[\Delta_r(t)+i\Delta_i(t)]\,e^{i[\omega t+\phi(t)]}, \tag{11}$$

so that $\Delta_r(t)$ and $\Delta_i(t)$ are the in-phase and quadrature noise (Langevin) sources.

Our main ensatz will be to assume that as a result of squeezing the intracavity noise, the ''powers'' of Δ_r and Δ_i are no longer equal. The equality of these powers is at the heart of all present laser theories and the consequences of our departure from this equality are of fundamental importance. We thus take

$$<\Delta_i(t_1)\Delta_i(t_2)>=Qe^{-2s}\,D(t_1-t_2), \tag{12}$$

$$<\Delta_r(t_1)\Delta_r(t_2)>=Qe^{2s}\,D(t_1-t_2), \tag{13}$$

$$<\Delta_i(t_1)\Delta_r(t_2)>=0\,, \tag{14}$$

where s is the squeezing parameter ($s=0$ is the non-squeezed case), $Q=4\hbar\omega_0^3\eta/\varepsilon V\tau_p$ (V is the volume of the resonator, and η the inversion factor), and $D(t)$ is the Dirac delta function.

The solution of Eqs. (10) using Eqs. (12), (13), and (14) follows the method of Ref. (3) leading, respectively, to the following results for the spectral density of the frequency fluctuations, the laser field spectrum, the laser linewidth, and the spectral density of the power fluctuations:

$$W_{\Delta\omega}(\Omega)=\frac{\eta}{\pi\tau_p^2}\left[\frac{\hbar\omega}{P_0}\right]\left[e^{2s}+\frac{\alpha^2 e^{-2s}}{1+(\Omega/\omega_1)^2}\right]\,, \tag{15}$$

$$W(\Omega)=\frac{A_0^2}{2\pi}\frac{\Delta\omega_s/2}{(\Omega-\omega)^2+(\Delta\omega_s/2)^2}\,, \tag{16}$$

$$(\Delta\nu)_{\text{laser}}\equiv\frac{\Delta\omega_s}{2\pi}=\frac{\hbar\omega\eta}{2\pi\tau_p^2P_0}(e^{2s}+\alpha^2e^{-2s})\,, \tag{17}$$

$$W_{\Delta P}(\Omega)=\frac{4}{\pi}\frac{\hbar\omega\eta P_0}{\tau_p^2}\frac{e^{-2s}}{\Omega^2+\omega_1^2}\,, \tag{18}$$

where $P_0=\varepsilon A_0^2V/\tau_p$ is the mean output power of the laser oscillator and $\alpha\equiv\chi_r^{(3)}/\chi_i^{(3)}$ is the amplitude-phase coupling constant.[3]

The laser linewidth is proportional to the factor $\exp(2s)+\alpha^2\exp(-2s)$. The first term $\exp(2s)$ represents an amplification of the direct phase diffusion term while the term $\alpha^2\exp(-2s)$ is due to a deamplification (squeezing) of the amplitude-phase coupling. It thus follows that because of the coupling the phase noise cannot be squeezed out completely unless $\alpha=0$, and the minimum value of the noise factor is $[\exp(2s)+\alpha^2\exp(-2s)]_{\min}=2\alpha$ and obtains with $s=\ln\sqrt{\alpha}$, resulting in a minimum laser

linewidth of

$$\Delta\nu_{\min} \equiv \frac{\Delta\omega_{\min}}{2\pi} = \frac{\hbar\omega\eta\alpha}{\pi\tau_p^2 P_0} . \tag{19}$$

We can, however, squeeze the power fluctuation spectrum, Eq. (18), which depends only on the factor $\exp(-2s)$. Figure 1 is a plot of the normalized laser field spectrum $R(\nu') \equiv (\pi\Delta\omega_{\min}/A_0^2)W(2\pi\nu')$, normalized in the sense that $R(0)=1$ when $s=\ln\sqrt{\alpha}$. Here $\nu' \equiv \Omega/2\pi$. Using typical parameters for a GaAs semiconductor laser, we have $\nu=\omega/2\pi=3.53\times10^{14}$ Hz, $\eta=3$, $\tau_p=5\times10^{-12}$ s, $P_0=0.5$ mW, and $\alpha=4$. The solid line is for $s=0$, when the intracavity noise is unsqueezed and is equally distributed between the two quadratures $\Delta_r(t)$ and $\Delta_i(t)$. The dashed line is for $s=\ln\sqrt{4}$, which results in the minimum laser linewidth $\Delta\nu_{\min}$.

Our conclusions follow directly from the assumed form of Eqs. (12), (13), and (14). These take their inspiration from the form of the squeezing of the quadrature field components of the field operators in quantum optics.[1,4] To the extent that the laser noise can be attributed to the transitions induced by the resonator vacuum (zero point) field, the form of Eqs. (12), (13), and (14) is plausible if the laser vacuum field is squeezed, although the issue of whether the vacuum field accounts for all or one half of the spontaneous emission is not yet resolved.[5]

Recent proposals for reducing laser fluctuations involve injecting a squeezed vacuum field into a laser to inhibit phase diffusion,[6] injecting a sub-Poissonian current into a semiconductor laser to reduce amplitude fluctuations,[7] and pumping the laser with an incoherent source in a squeezed vacuum state.[8] The first two techniques are directly applicable to semiconductor lasers as such lasers are limited by quantum, rather than technical noise. It is possible that a direct squeezing using a nonlinear element inside the laser resonator might more closely approximate the assumed form of Eqs.

(12) and (13). One such method might employ the amplified and doubled output of the laser to pump a degenerate parametric amplifier crystal within the laser resonator. Such an arrangement is known[9] to lead to squeezing in configurations which do not include the gain medium. An important basic issue then is what happens to the cavity vacuum fluctuations in the presence of gain *and* squeezing.

REFERENCES

1. D.F. Walls, Nature **306**, 141 (1983), and references therein.

2. C. H. Henry, IEEE J. Quant. Electron. **QE–18**, 259 (1982).

3. K. Vahala and A. Yariv, IEEE J. Quant. Electron. **QE–19**, 1096 (1983).

4. C. M. Caves, Phys. Rev. D **26**, 1817 (1982); B. Yurke, Phys. Rev. A **32**, 300 (1985); C. M. Caves and B. L. Schumaker, Phys. Rev. A **31**, 3068.

5. I. R. Senitzky, Phys. Rev. Lett. **31**, 955 (1973); P. W. Milonni, J. R. Ackerhalt, and W. A. Smith, Phys. Rev. **31**, 958 (1973); P. W. Milonni and W. A. Smith, Phys. Rev. A **11**, 814 (1975); J. Dalibard, J. Dupont-Roc, and C. Cohen-Tannodji, J. Phys. (Paris) **43**, 1617 (1982).

6. J. Gea-Banacloche, Phys. Rev. Lett. **59**, 543 (1987).

7. Y. Yamamoto, S. Machida, and O. Nilsson, Phys. Rev. A **34**, 4025 (1986); S. Machida, Y. Yamamoto, and Y. Itaya, Phys. Rev. Lett. **58**, 1000 (1987); S. Machida and Y. Yamamoto, Phys. Rev. Lett. **60**, 792 (1988).

8. M. A. M. Marte and D. F. Walls, Phys. Rev. A **37**, 1235 (1988).

9. L. -A. Wu, H. J. Kimble, J. L. Hall, and H. Wu, Phys. Rev. Lett. **57**, 2520 (1986).

FIGURE CAPTION

Figure 1. Normalized laser field spectrum R as a function of detuning from line center $\nu' - \nu$. The solid line is the field spectrum when the intracavity noise is unsqueezed, i.e., $s = 0$. The dashed line is the field spectrum when the intracavity noise *is* squeezed, with $s = \ln\sqrt{4}$.

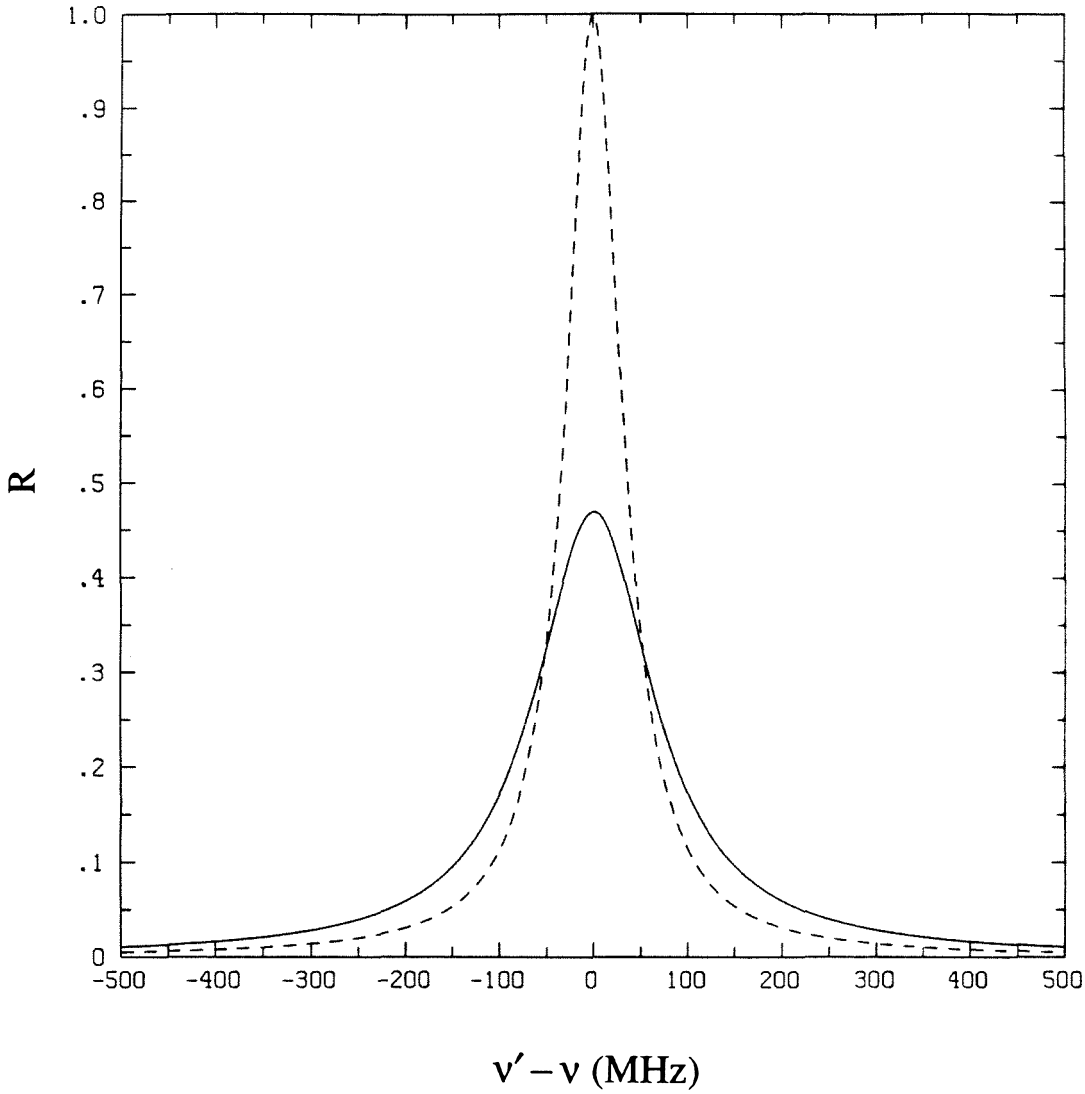

Figure 1